Improving solubility and supersaturation of poorly soluble drugs using solid dispersions based on natural polymers and mixtures thereof

Dissertation

zur

Erlangung des Doktorgrades (Dr. rer. nat.)

der

Mathematisch-Naturwissenschaftlichen Fakultät

der

Rheinischen Friedrich-Wilhelms-Universität Bonn

vorgelegt von

Dnyaneshwar Nandkumar Kapote

aus

Nashik, Indien

Bonn 2021

Angefertigt mit Genehmigung der Mathematisch-Naturwissenschaftlichen

Fakultät der Rheinischen Friedrich-Wilhelms-Universität Bonn

Promotionskommission:

Erstgutachter: Prof. Dr. Karl-Gerhard Wagner

Zweitgutachter: Prof. Dr. Alf Lamprecht

Fachnaher Gutachterin: Prof. Dr. Diana Imhof

Fachfremder Gutachter: Prof. Dr. Valentin Stein

Tag der Promotion: 03.05.2021

Erscheinungsjahr: 2021

Significant portions of Chapter 4 were published in an article entitled, Influence of shellac on the improvement of solubility and supersaturation of loratadine amorphous solid dispersion using a new grade of HPMC in Journal of Drug Delivery Science and Technology. Chapter 5 refers to the article entitled, Shellac- a natural carrier for colon targeting of indomethacin using Hot melt extrusion, is submitted to Drug Development and Industrial Pharmacy.

Acknowledgments

It is my great honor and privilege to be the student of institute of pharmacy, University of Bonn, which is one of the renowned institutions in research. It has been an enriching and rewarding experience for me working on the Ph.D. It enabled me to not only explore my potential but also satisfy my curiosity to simply understanding your research topic and applying it in experiments. I learn it is important to stay calm, when result is contrary to expectation. During the past few years, at different stages of the thesis, I met many people who shared their valuable feedback. I am indebted to their time, care and ceaseless efforts.

First of all, I would like to express my gratitude and humble bow to my Ph.D. supervisor Prof. Dr. Karl Gerhard Wagner, who accepted me as his doctoral student and gave me the opportunity to work on such an interesting topic. I consider myself fortunate to work under his mentorship, which was very exciting and insightful too. I think he has been phenomenal in my life be in scientific input or on the personal front. His pieces of advice, steady support, promptness and, precious time for discussion of research work helped me. His rich experience and expertise offered me the research lens to be analytical and change my viewpoint towards science becoming an independent researcher. I appreciate from bottom of my heart his friendly interaction and guidance throughout my Ph.D. Thank you for all your support and giving me opportunity to be with you in Bonn.

I am very thankful to many of my colleagues with whom I shared research work, bench, office. To mention a few like Mariane, Ozan Hirlak, Anna Krome, Fabian, Alvaro, Bashar, Mert, Rafael, Marius, Alex, Maryam and our working group who were friendly, supportive and helped whenever needed, especially for facing cultural challenges during initial period. I thank enough Mrs. Martina Gerlitz, for welcoming me warmly on my arrival in Bonn and her useful suggestion regarding material order from India. Alex Ramich for his welcome and for some enjoyable non-technical chats that were mesmerising.

I would also like to thank the University of Bonn and DAAD for providing me the Ph.D funding. Destiny has driven me all the way to Bonn from Pune, a tiny and peaceful town in India. Bonn has very special place in my life that helped me to grow scientifically and met my soulmate too. Thank you, Bonn, for being so generous and endearing River Rhine for nostalgic memories, making it especially pleasant and fascinating place to enjoy!

Surely, words fall short to describe how much I am indebted to my father, Nandkumar, you taught me never to give up, however tough the challenges maybe, but, conquer it with positive attitude. My mother Ashwini has been an inspiration in my life. Your sacrifices, love, constant prayers and showers of your blessings strengthened me. My wife Vandana: your support and confidence in my abilities encouraged me to carry out my research work with full enthusiasm. My sister Tejashree: your caring nature and funny jokes kept me cheerful. In addition, I thank all my Indian friends in India and Germany Kushal Patel, Dr. Somnath Pokhare, Pranav Joshi, Rohit Deshmukh, Shefali and Harish Patel for their short visits, delicious Indian cooking and delightful conversations, adding some value to non-scientific discussions. Finally, big thank you to all who were part of this enlightening journey supporting me directly or indirectly in past few years.

Dnyaneshwar

I like to dedicate this thesis to my family and my Ph.D. supervisor for all their unconditional love and support in the past few years of Ph.D. journey.

"You are the creator of your own destiny"

Swami Vivekananda

TABLE OF CONTENTS

Abbreviations

API	active pharmaceutical ingredient
ASD	amorphous solid dispersion
A15	Affinisol HPMC HME 15 LV
α-G HSP	Alpha glycosyl hesperidin
A	Amorphous
ATR-IR	Attenuated total reflectance infrared spectroscopy
BCS	Biopharmaceutical classification system
C	Crystalline
DC	Directly compressible
DSC	Differential scanning calorimetry
Eudragit FS 100	Aminomethacrylate copolymer
FDA	United states food and drug administration
GRAS	Generally recognized as safe
HME	Hot-melt extrusion
HPLC	High-performance liquid chromatography
HPMC	Hydroxypropyl methyl cellulose
HPC-SSL	Low-viscosity hydroxypropyl cellulose
HPMC-AS	Hydroxypropyl methyl cellulose acetate succinate
HSM	Hot stage microscopy
IND	Indomethacin
ITZ	Itraconazole
LOR	Loratadine

M	Molecularly dispersed
NCE	New chemical entity
PEG	Polyethylene glycol
PLM	polarized light microscopy
PVP-VA 64	polyvinyl pyrrolidone vinyl acetate copolymer
PVA	Polyvinyl alcohol
SD	Spray drying
SDD	Solid dispersion
SSB® 55 Pharma	Shellac
SR	Sustained release
TOPEM	multi frequency temperature modulated differential scanning calorimetry
T_g	glass transition temperature
XPS	x-ray photon electron spectroscopy
XRPD	x-ray powder diffraction
QbD	Quality by design

1 Introduction

The oral drug administration remains one of the most popular routes for delivering drugs in recent decades. Over the years with the advent of high throughput screening and combinatorial chemistry, the number of new chemical entities (NCEs) having poor aqueous solubility has increased. It has been estimated that more than 40% of the marketed APIs and even 70% of the NCEs are poorly soluble compounds [1,2]. Hence, the enhancement of the solubility for these poorly water-soluble drugs for oral delivery now presents one of the most frequent and main challenges for the formulation scientists in the pharmaceutical industry [3].

There are various strategies to improve this solubility limited bioavailability of poorly soluble drugs. Among this amorphous solid dispersion has evolved as potential lead technology to overcome this challenge. The polymeric carrier for preparing amorphous solid dispersion needs to be selected appropriately. There are several commonly used synthetic polymers for ASDs preparation like povidone, copovidone, soluplus, polyvinyl acetate and few semi-synthetic hydroxyl methyl cellulose, hydroxyl propyl methyl cellulose acetate succinate and hydroxyl propyl cellulose (Table 1). Despite the continuous interest in amorphous solid dispersions, the number of different polymeric carriers that have been used during the past 40 years is still rather limited [1]. The main reasons for this limitation might be several requirements which need to be fulfilled. These requirements include the selection of adequate polymers which ultimately influences dissolution characteristics of the dispersed drug and the use of a water-soluble polymer which results in a fast release of the drug from the matrix [4]. A novel polymer is considered as new chemical entity e.g soluplus which was launched in 2010 by BASF after 30 years in pharmaceutical polymer industry for HME application. Thus, we propose natural /renewable polymeric excipients as a new concept to increase the chemical space of available synthetic polymers for preparing amorphous solid dispersions.

The new grade of isomalt which was used earlier in the food industry now have been used in pharma industry as well. The new grade of hydroxyl propyl methyl cellulose (HPMC) with low glass transition temperature and, low melt viscosity allowing melt

extrusion at lower temperatures have been launched by Dupont [5]. Polyvinyl alcohol (Parteck MXP) which has been developed and marketed by Merck is suitable for hot-melt extrusion process [6].

Natural polymers are obtained from abundant renewable sources. Natural excipients as a matrix in ASDs screening have been neglected even though they offer clear advantages such as the ecologically beneficial exploitation of renewable sources and the fact that they are GRAS listed compared to synthetic polymers. Thus, they need less justification for usage in dosage form development compared to synthetic polymers making it one of the most attractive features for using an ASDs matrix. There is a need to extend the chemical space of polymers in an attempt to tailor the physicochemical properties for polymer mixtures containing natural polymers alone or in a combination with synthetic and natural polymers, possessing optimized solubility for a given active ingredient. It is important to understand the interaction between API and polymer to tailor/predict the solubilization potential of the respective polymer mixtures. Therefore, an extension to natural polymers needs to be done as they are the only group of polymers left to investigate as solid dispersions carrier matrix that is easily sourceable with already a broad usage in the food industry.

The natural polymers possess a wide variety of physicochemical properties, which offer an attractive means to study. The processing of these natural polymers depends on the method of preparing solid dispersion and their mixing as binary/ternary system is governed by their miscibility, solubility in the organic solvent, low glass transition temperature and low melt viscosity for easy handling during the implementation of temperature and shear rate during melt extrusion. Thus, there is definitely a need to explore natural polymers per se monographed in Pharmacopoeias or non-compendial literature in combination with synthetic/semi-synthetic polymers as a new matrix for ASDs to achieve enhanced solubility and dissolution rate for poorly soluble APIs.

1.1 Classification of solid dispersions

The term solid dispersion was coined by Chiou and Riegelmann as the dispersions of one or more APIs in an "inert carrier or matrix at the solid-state prepared by solvent, melting or solvent-melting methods" [4]. The molecular arrangement governs the dissolution and stability properties of solid dispersions. There is a need to classify them based on solid-state properties in eutectics, amorphous precipitates, solid solutions and glass dispersions as shown in Table 1, rather than according to their method of preparation [7].

The first type of solid dispersion is based on eutectics. It mainly consists of two crystalline compounds (A and B), which are completely miscible in the liquid state and limited miscible in the solid-state. Therefore, they co-crystallize at their eutectic composition and temperature. It is observed that a deviation from this eutectic composition will lead to crystallization of one of the two components before the other (i.e., primary crystals A/B). In general, eutectic solid dispersions of a poorly soluble API and an inert, readily water-soluble carrier, leads to a rapidly dissolved carrier in an aqueous medium and very fine crystals of the API will be released [8]. The resulting increased surface area of the API might lead to an enhanced dissolution rate and thereby improved bioavailability, a quasi in situ nanoionization. Madgulkar et al. reported promising improvement in dissolution rate of Clotrimazole from a tablet formulation containing a solid dispersion using mannitol (drug to sugar ratio: 1:3) with an enhanced dissolution rate compared to plain drug and directly compressed tablet of Clotrimazole (DC tablet). They attribute this dissolution rate enhancement to attraction of water molecules by the carrier [9].

Amorphous precipitates are another type of solid dispersion where the amorphous API is distributed randomly within a crystalline carrier. Therefore, the crystalline state is a rigid structure where the atoms or molecules are organized in a lattice structure. This rigid three-dimensional structure of a crystalline carrier makes it difficult to incorporate larger clusters of amorphous APIs which is rarely described in pharmaceutical formulations [10].

Table 1: Classification of solid dispersions modified from [7,11]

Type of solid dispersion		API	Carrier	Phases	XRPD profile	Physical stability	Solubility enhancement
Eutectics		C	C	2	Sharp peaks	High	Moderate
Amorphous precipitates in crystalline matrix		A	C	2	Sharp peaks similar to the carrier	Low	High
Solid solutions	Continuous solutions	M	C	1	Halo pattern	Low	High
	Discontinuous solutions (Limited miscibility/ solubility)	M	C	1 or 2	Sharp peak	Low	High
	Substitutional crystalline solution (Molecular diameter differs less than 15%)	M	C	1	Sharp peak	High	High
	Interstitial crystalline solution (Molecular diameter of the API should be less than 59% of the molecular diameter of the carrier molecule)	M	C	1	Sharp peak	High	High
Glass dispersions	Glass suspension	A or C	A	2	Halo pattern	Low	High
	Glass solution	M	A	1	Halo pattern	High	High

A solid solution (Table 1) can be defined as the dissolved state of the API in a crystalline carrier matrix. Solid dispersion in this group can further be classified into a continuous solid solution and a discontinuous solid solution. In case of continuous solid solution both the API and the carrier are miscible in all portions, whereas within discontinuous solid solutions the API and the carrier show limited solid solubility. The latter is expected for most pharmaceutical binary systems. In a discontinuous solid solution, the API can be dissolved in the carrier in two ways first in which the carrier molecule in the crystalline lattice is substituted by an API molecule, and a substitutional crystalline solution is obtained. A requirement for the formation of this kind of solid solution is that the solute (API) molecule does not differ by more than 15 % in size from that of the solvent (carrier) molecule. The second type of a discontinuous solid solution is an interstitial crystalline solid solution, where the API is dissolved within the carrier by occupying the interstitial spaces between the solvent molecules in the crystal lattice. For these systems, the size and volume of the solute molecules are critical. Solvent (API) molecule diameters should not be larger than ~0.59 times the solvent molecule diameter and the volume should not exceed 20 % of the solvent volume [12].

The glass suspensions are divided into two types: amorphous carrier and a crystalline API, or an amorphous API in a crystalline carrier. A glass suspension of first type is a two-phase system where the API remains in its favorite (crystalline) state, which leads to very stable formulations. As example, Srinarong et al. incorporated around 20% and 30% of crystalline Fenofibrate in solid dispersions containing amorphous Inutec SP1 or Inulin 2.3 kDa [13].

In the case of the second type of glass suspension, the API is transformed into an amorphous state without being molecularly dispersed within the polymer matrix. This leads to amorphous API clusters that are incorporated in the polymer. Due to nuclei formation and nuclei growth of the amorphous API, which favors a fast recrystallization, this type of solid dispersion is metastable. It must be noted that small amorphous drug clusters may prevent the formulation from recrystallization and the solid glass suspension might be kinetically stable by immobilizing the API in its supersaturated state in a highly viscous polymer [14].

It is known that in case of solid dispersions, water acts as a plasticizer thus lowering the glass transition temperature and leading to a limited stability. Thus, moisture absorption needs to be avoided. Shibata et al prepared SDs of three APIs (dipyridamole, nifedipine and indomethacin) having a different functional group (amino, carbonyl and hydroxyl groups) with crospovidone using a melt quench cooling technique. When these solid dispersions were stored under conditions of high temperature and moisture (40 °C/ 75%RH/closed and 60 °C/open), differences in the interaction between the hydrogen bond donor of the drugs and the amide carbonyl group of crospovidone were found to be a particularly important factor in contributing to drug recrystallization in SDs [15].

In contrast, in glass solutions the API is molecularly dispersed within an amorphous carrier forming a single-phase system. To obtain this type of solid dispersion, the molecular dispersed drug should be immobilized by interaction with the carrier polymer. The important precondition to enable the formation of a solid glass solution is that the total interaction forces between the drug and the polymer are stronger than self-association forces among the drug molecules themselves. Obaidi et al. produced binary amorphous solid dispersions for griseofulvin and HPMC-AS [16]. These three types of solid dispersions are most important in pharmaceutics, because most of the carriers are amorphous or semi-crystalline in nature.

1.2 Drug release kinetics from solid dispersions

There are a number of potential advantages of solid dispersions that have been reported. One is the improved dissolution rate, hence improved solubility and bioavailability of poorly soluble APIs [17]. The mechanisms, underpinning the drug release from the amorphous solid dispersions, are often concerned but poorly understood. There are mainly two mechanism for the drug release from solid dispersions: carrier or drug controlled.

The carrier-controlled release is governed by the property of the carrier. The carrier might be medium soluble or medium insoluble in the different pH aqueous media. Lee et al prepared amorphous dispersions of 20% indomethacin using medium soluble carriers such as HPMCAS. They observed that the drug release and supersaturation follow a dissolution-controlled mechanism. This might be attributed to the rapid dissolved or dispersed carrier in the dissolution medium, which leads to rapid liberation of the amorphous API and generates a highly supersaturated drug solution. They found that this early surge of drug supersaturation is followed by a rapid decline in concentration of drug of soluble which may be due to precipitation triggered by rapid buildup of supersaturation [18].

In case of a sustained release mechanism, a diffusion-controlled release of medium insoluble carriers was observed. The amorphous solid dispersion containing these medium-insoluble carriers, like ethyl cellulose, lack the initial surge of supersaturation and are sustained for an extended period of time in the absence of any crystallization inhibitor. Sun and Lee concluded that the rate of supersaturation generation is a critical factor imparting the overall kinetic solubility profile. In this study, the dissolution of solid dispersions is more gradual as drug release is controlled by a matrix diffusion-regulated mechanism, which helps to prevent rapid buildup of supersaturation. It avoids the typical ‘Spring and Parachute’ release behavior of amorphous solid dispersions based on soluble carriers and maintains an extended supersaturation. To improve the dissolution profile, it is important to know the release mechanism of solid dispersions [18]. Thus, the focus should not only be on the polymorphic states of the API, but also on the important carrier properties such as solubility, viscosity, ability to maintain supersaturation, crystallization

inhibition and on the ratio of drug-carrier. These key factors affecting the dissolution profile, should be considered [19].

If a drug-dependent release predominates, the rate determining step is the dissolution of the poorly water-soluble API. This drug-controlled dissolution is known for crystalline glass suspensions. Consequently, the dissolution is not dependent on the polymer but is dominated by API solubility properties. In case of glassy solid solutions, a carrier-controlled dissolution is observed. The API particles are molecularly dispersed in the carrier and dissolved into the polymer-rich diffusion layer together with the carrier. Due to the higher surface area of the API particles and the possibility of improved wetting and decreased agglomeration, this may lead to considerable improvements in dissolution, compared to conventional dosage forms.

The release mechanism will depend on whether the drug dissolves in the polymer diffusion layer rapidly or not which will in turn be dependent largely on the solubility of the drug in this layer. The hydrodynamics of the dissolution process may also play a role in determining the mechanism. A more rapid stirring speed may favor drug-controlled dissolution by enhancing the rate of polymer dissolution into the bulk in relation to drug dissolution into the diffusion layer [17]. However, these mechanisms help to understand the different release behaviors of solid dispersions and to figure out the way to enhance dissolution profiles of solid dispersions.[19]

Despite of all these mechanisms, the effect of aging and its impact on stability of solid dispersions needs to be considered. The aging decreases the dissolution rate. In case of the carrier-controlled release system, the effect may be attributed to the properties of polymer (amorphous, semi-crystalline or crystalline) and suitable means of predicting and preventing are reported in the literature. Concerning the drug-controlled release system, the properties of the drug itself must be carefully studied (slow crystallization from solid solutions, changes in the polymorphic form, particle size increase or recrystallization from the amorphous state) [17]. Hence, without a more mechanistic understanding of the drug release from solid dispersions, it would be difficult to select an appropriate polymer carrier (or combination of carrier) for a solid dispersion [18].

1.3 Mechanism of stabilization for solid dispersions

- **Molecular mobility reduction and elevation of Tg for amorphous API**

In general, an amorphous solid dispersion was considered stable, if the storage temperature is 50°C below the glass transition temperature of the system [20]. Nowadays, a lot of investigations revealed different correlations. The importance of molecular mobility and melt viscosity are stronger connected to the inhibition of recrystallization than only the glass transition temperature of the resulting system [21]– [24]. Other studies, however, revealed that a molecular mobility dependent stabilization of the amorphous solid dispersion [23]– [25], the miscibility (for an amorphous API) and the solubility (for a crystalline API) are additional important factors for the stability of such systems [26]. The inhibition of recrystallization of the API can be achieved in two ways, by decreasing the molecular mobility of the system or by increasing the solubility of the API within the polymer matrix which one of the two option is best, depends mainly on the API under investigation [26]– [29].

- **Reduction in free energy of drug (solubility of the drug in the polymer matrix)**

The solubility determination of an API in a polymeric matrix can be estimated theoretically by solubility theories or can be experimentally evaluated [30], [31]. The important theoretical approaches are the Hansen parameter or the Flory-Huggins lattice theory which are based on the assumption that similar solubility parameter values favor mixing. Both theories were originally established for liquid organic systems where a substance is dissolved in infinite dilution [32]– [34]. The Hansen parameters are based on the separation of the cohesive energy density into dipole forces, dispersive forces and hydrogen bonding via employing evaporation enthalpies or group contribution methods. The adaptation for ASD was evaluated by various authors and Hansen parameters or group contribution methods were expanded or adjusted [35]– [37]. Furthermore, the Hansen solubility theory is based on the enthalpy of the system and not on its entropy, which limits the application [38]. The melt viscosity, which might hinder miscibility, is also not taken into account [39]. Another theory is the Flory-Huggins lattice theory with the interaction parameter χ, which is based on the negative free mixing energy that favors miscibility. It takes the molecular mass difference between API and polymer into account

by varying the entropic term for the miscibility [40], [41]. However, the API is still regarded in an infinite solution which is limiting the validation for ASD. In order to adapt this lattice theory to ASD [42], various approaches were published e.g., involving the activation coefficient [43]– [45], molecular dynamics simulations [46], [47], involving the heat capacity in order to determine changes in the Gibbs energy [48] and the validation of temperature dependency [49]– [51]. In conclusion the disadvantage of these theoretical approaches is the low consideration of specific interactions between the API and the polymeric matrix and the missing term for breaking crystal structures. Hence, they are just describing the possible energy exchange based on the deviation in the intermolecular attraction. To sum up, they are only characterizing the miscibility of an amorphous system, but they don't take the dissolution of a crystalline substance into a polymeric matrix into account [41], [50].

The experimental approach in solubility estimation is mainly based on DSC, FT-IR / Raman [52], XRPD [53], HSM [54] and measurements of low molecular weight analog. Moreover, the DSC methods can be separated in melting point depression [55], dissolution endpoint [56] and recrystallization [57] techniques. Usually, the scope is the detection of residual crystals to decide whether the polymer was able to dissolve the whole API content. In case of FT-IR, specific interactions between API and polymer matrix can be evaluated (analysis of characteristic bands). Further techniques, which are rarely used, are XPS [58], solid-state NMR and dielectric spectroscopy [59] to gain knowledge about the specific interactions. In general, measuring techniques should be combined, to obtain an accurate result.

- **Intermolecular interactions**

In general, the interaction between the polymer matrix and the API is often via hydrogen bonding [53], [60]. Due to the chemical structure of most polymers, they normally act as proton acceptor, whereas the API in turn need proton donor sites to favor interactions and consequently mixing with the polymer [52], [61].

Maniruzzaman et al prepared hot melt extrudates of the cationic drugs cetirizine HCl and verapamil HCl with anionic carriers like Eudragit L100 and Eudragit L100-55. They studied drug- polymer interactions using an X-ray photoelectron study (XPS) advanced chemical surface analysis enabled the confirmation of the mechanism of the interaction via H-

bonding between the carboxyl group of the anionic methacrylate co-polymers and the amine group of the active substances as well as the interaction strength. This analysis thus broadened the knowledge about the drug–polymer interactions at the atomic level and helped to compare the results to those obtained by traditional methods with limited surface resolution [47]. Kinoshita et al reported the improvement of oral bioavailability for the development drug TAS-301 with porous calcium silicate FLR using hot melt extrusion. They found that the amorphous phase produced from extrusion was physically stable for around 2 years at ambient temperature. The porous silicate shows a pronounced hydrogen bonding ability between the drug and the silanol groups on the surface of the silicate. The inorganic silicates thus offer a new stabilization effect [62]. In contrast to organic polymers, the inorganic silicates, e.g. Neusilin, show an alternate mechanism of stabilization of amorphous APIs through their salt formation potential**.** Furthermore, a minimum number of monomer units needs to be available to promote miscibility and no change in solubility is observable if additional monomer units are replaced by other functional groups [63]. Comparison to solutions with low molecular weight analog of the polymer revealed similar behavior which demonstrates the "solution" nature of the amorphous state [44]. The majority of intermolecular interaction depends on the drug-polymer miscibility which will increase the physical stability of the amorphous solid dispersion. Even under harsh condition, such as high relative humidity, the ASD might be stable [64]. In some cases, the polymer has ionic groups within its structure and enables ionic interactions with cationic APIs, as it is known from anionic polymethacrylates [58], [65], e.g. Eudragit EPO or polyacrylamide [59]. Khougaz et al investigated the ion dipole interaction between the development drug MK-0591 and different PVP based solid dispersions which were prepared by the solvent method. They proposed the existence of an ion-dipole interaction between the $COO^{-}Na^{+}$ moiety of the drug and the cyclic amide group of PVP [66] Other specific interactions, such as dipole-dipole interactions [59] are less known, which might be due to lack of the appropriate analysis techniques.

1.4 Set of available natural excipients

The natural excipients are obtained through different sources in nature like from plants or insect animals. They have been widely used in the food industry and few are also used in pharma industry and classified as shown in Figure 1

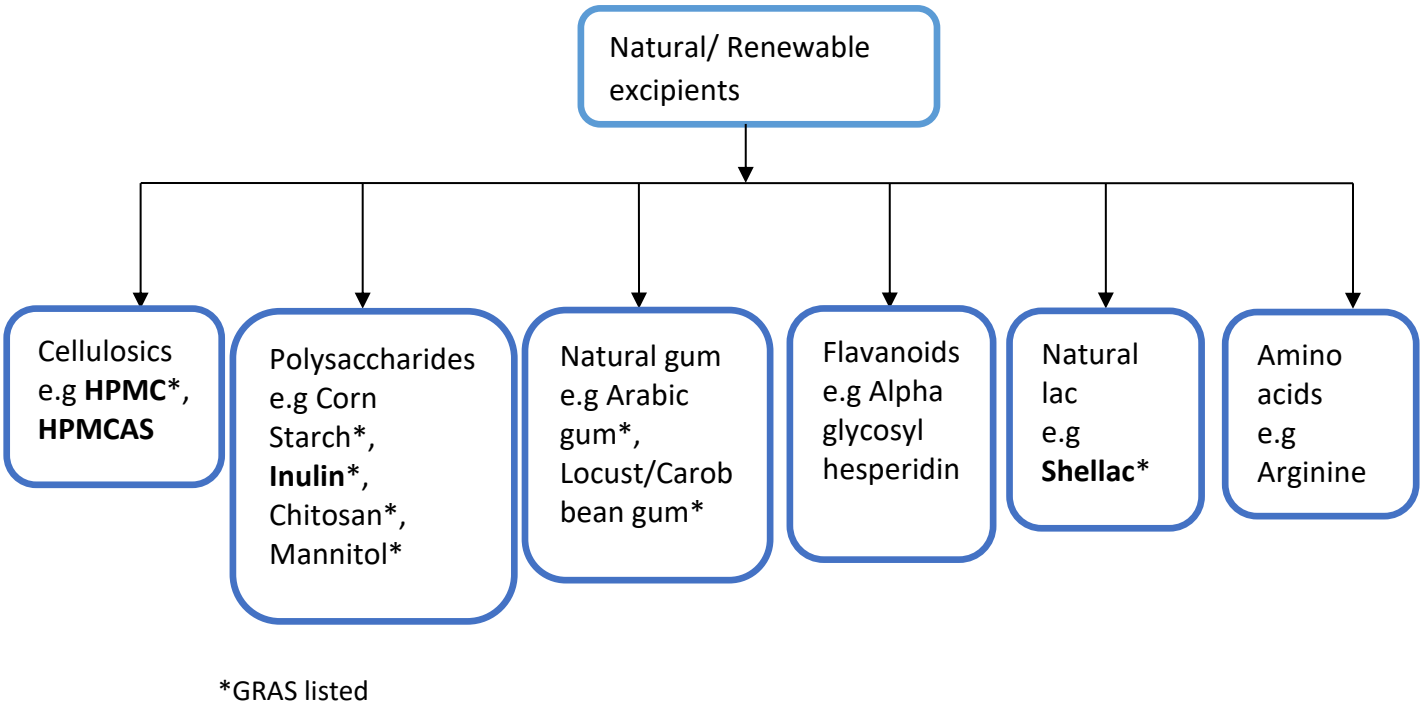

Figure 1: Classification of natural excipients based on their source from nature

The natural excipients listed above are subjected to pre-screening and studied further based on their individual characteristics. Their typical monograph is represented below to demonstrate the currently existing knowledge gap with respect to the use of natural excipients for the application in an ASDs matrix for pharmaceuticals. They have great potential for solubility enhancement of poorly soluble drugs using industrial popular spray drying and hot melt extrusion.

1.5 Monographs

1.5.1 Inulin

Structure:

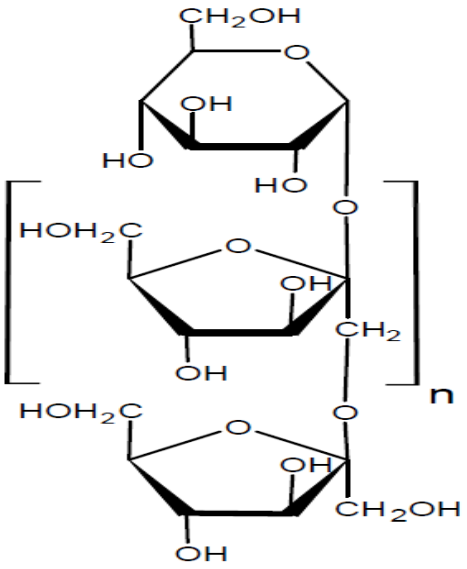

Inulin

Physiochemical properties:

Molecular weight (g/mol)	2600
Tg (°C)	122 ± 0.9
Tm (°C)	NA
Tdeg (°C)	255.9 ± 2.8
Solubility	Slightly soluble in ethanol, acetone and soluble in water
XRPD	Amorphous
H donor and acceptor:	H_D = 13, H_A = 17

Potential Space:

Protein stabilizing agent [67]**,** Pore forming agent [68], ASDs matrix [69], diagnostic tool for glomerular filtration rate [70], colon targeting [71]

How to process:

Inulin can be dissolved into the aqueous solution with the respective drug that might be processed using spray drying, freeze drying and spray freeze drying to manufacture ASDs or the desired protein formulations.

Marketed product: Orafti® GR

1.5.2 Shellac

Structure:

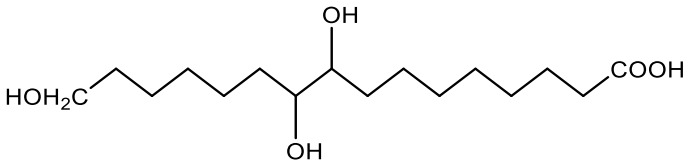

Aleuritic acid

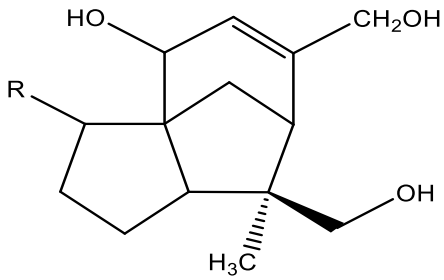

R = COOH- Shellolic acid
CHO- Jalaric acid
CH_2OH - Laksholic acid

Shellac derivatives thereof (SSB 55)

Physiochemical properties:

Molecular weight (g/mol)	1047
Tg (°C)	36.9 ± 0.3
Tm (°C)	NA
Solubility	Insoluble in water, freely soluble in ethanol
XRPD	Amorphous
H donor and acceptor:	$H_D = 8$, $H_A = 11$

Potential Space: ASDs, Colon targeting matrix

How to process:

Shellac starts dissolving at pH 6.8 and completely dissolves at pH 7.3 and above making it interesting to target the colonic site in the body. Shellac can be mixed with hydroxyl methyl propyl cellulose to tailor the release profile at intestinal pH 6.8 and to improve the processability of shellac for ASDs manufacturing using spray drying or HME.

Marketed product: SSB 55®Pharma

1.5.3 Alpha glycosyl hesperidin

Structure:

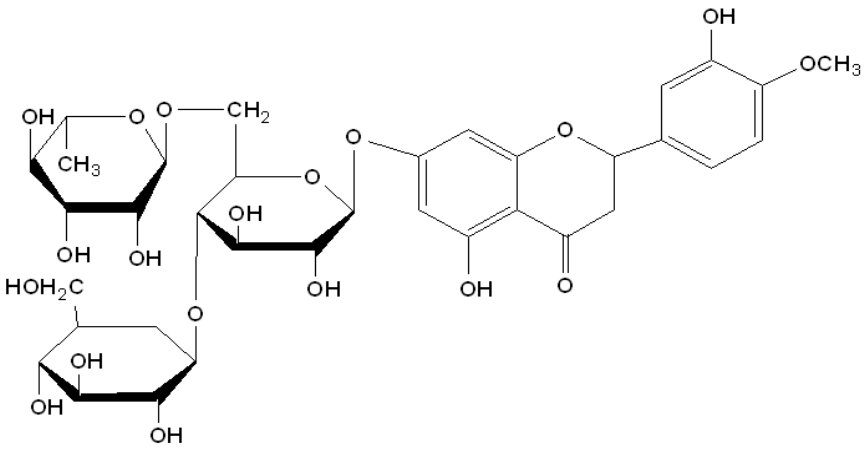

Alpha Glycosyl Hesperidin

Physiochemical properties:

Molecular weight (g/mol)	772.70
Tg (°C)	147.9 ± 0.5
Tm (°C)	NA
Tdeg (°C)	286.6 ± 3.4
Solubility	Slightly soluble in ethanol, acetone and freely soluble in water
XRPD	Amorphous
H donor and acceptor:	$H_D = 8$, $H_A = 15$

Potential Space:

ASDs, micellar solubilization [12], surface active material [73]

How to process:

AGHSP is freely soluble in water. It is interesting to use AGHSP in combination with organic solvents for spray drying and freeze drying to prepare ASDs and to improve the solubility of poorly soluble drugs

Marketed products: αG Hesperidin®

1.5.4 Hydroxy Propyl Methyl Cellulose 15 LV

Structure:

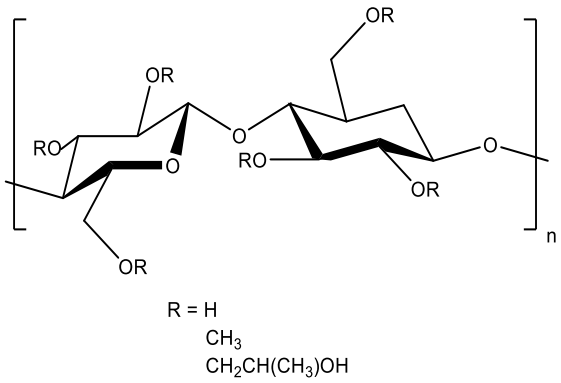

Hydroxy propyl methyl cellulose 15 LV

Physiochemical properties:

Molecular weight (g/mol)	80,000 – 85,000
Tg (°C)	98.8 ± 0.04
Tm (°C)	NA
Tdeg (°C)	213.2 ± 1.8
Solubility	Soluble in cold water forming viscous colloidal solution, clear solution in the mixtures of ethanol and acetone
XRPD	Amorphous
H donor and acceptor:	$H_D = 8$, $H_A = 30$

Potential Space: ASDs for HME, spray drying, Direct compression

How to process:

HPMC can be mixed with several excipients/ drug substances for the manufacturing of ASDs using hot melt extrusion due to its low glass transition temperature allowing the processing at low temperatures. Also, its application in spray drying needs to be explored.

Marketed products: Affinisol® HPMC 15 LV

1.5.5 Hydroxy propyl methyl cellulose acetate succinate

Structure:

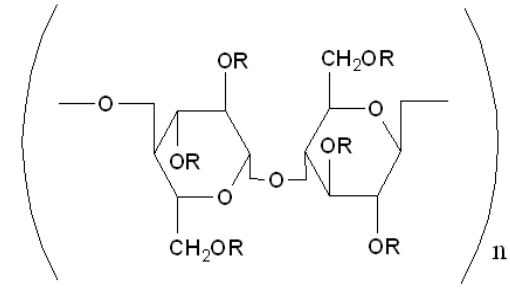

R = −H, −CH3, −CH2CH(CH3)OH, −COCH3, −COCH2CH2COOH, −CH2CH(CH3)OCOCH3, −CH2CH(CH3)OCOCH2CH2COOH

Hydroxy Propyl Methyl Cellulose Acetate Succinate

Physiochemical properties:

Molecular weight (g/mol)	55,000 – 93,000
Tg (°C)	119.9 ± 1.5
Tm (°C)	NA
Tdeg (°C)	251.7 ± 2.8
Solubility	Insoluble in water, forms a clear solution in the mixture of ethanol: acetone (1:1)
XRPD	Amorphous
H donor and acceptor:	$H_D = 6$, $H_A = 9$

Potential Space: ASDs using HME and Spray drying

How to process:

HPMCAS can be mixed with immediate release polymers to tailor the release profile in the gastrointestinal tract and to maintain the supersaturation of ASDs

Marketed products: AQOAT®LG

1.6 Marketed products of ASDs

The number of FDA approved ASDs products has significantly increased within the last few years making it one of the most attractive technologies for improving solubility of poorly soluble drugs and maintaining the supersaturation. Table 1 represents the comprehensive examples of approved ASDs manufactured using different techniques by various pharmaceutical companies. In the following, some examples of these marketed products will be discussed to highlight the applicability of ASDs for bioavailability enhancement.

The ASD product Kaletra® was available as soft gelatin capsule containing the combination of lopinavir (133.3 mg) and ritonavir (33.3 mg). The soft gelatin capsule needed refrigeration and the daily dose of the capsule was recommended to be taken throughout the meal to maximize the bioavailability of lopinavir. Because of the need to optimize the drug delivery and to render the dosage more efficient, the product was reformulated as ASDs using HME. The dose was 200/50 mg and the need of refrigeration was circumvented making it advantageous for patients from the African continent where high temperature, humidity and inadequate access to refrigerator would have limited the application of the initial product. Another advantage of the HME formulation was the maintenance of a consistent drug level across meal conditions, which has reduced extreme high or low blood plasma concentrations [74].

An Itraconazole based ASDs formulation is another interesting example. A mixture of the API and HPMC was dissolved in dichloromethane and methanol as co-solvent and sprayed on inert sugar spheres using the fluid bed layering process. The formulation was then filled into a capsule and available as Sporanox capsule approved in 1992 by FDA [75]. It was noticed that itraconazole bioavailability increased significantly by 55 % of the administered dose absorbed [76]. However, it has been reformulated into a tablet formulation containing HPMC 2910 by HME that utilized Meltrex technology. The dose of the tablet formulation is 200 mg once a day and available under the trade name Onmel®. This approach helped to reduce the twice daily dose to once daily and eliminated the use of organic solvents for the manufacturing of ASDs [77]. It can be observed from Table 2 that most of the ASDs are manufactured using synthetic or semisynthetic polymers and

the potential of natural polymers still needs to be further investigated in ASDs manufacturing. Thus, we set out to explore this potential and to reconsider a new direction for the formulation of ASDs.

Table 2: Marketed Preparations for ASDs formulation [74], [75], [76]

Product /Brand name	API	Polymer used	Dosage form	Manufacturing company and FDA approval	Technology used for ASDs manufacture
Isoptin SR-E	Verapamil	HPC/HPMC	SR-Tablet	Ranbaxy laboratories (1989)	Melt extrusion
Sporanox	Itraconazole	HPMC	Capsule	Janssen(1992)	Fluid bed bead layering
Prograf	Tacromilus	HPMC	Capsule	Astellas (1994)	Spray drying
Rezulin	Troglitazone	HPMC	Tablet	Pfizer(1997)	HME
Kaletra	Liponavir/ Ritonavir	PVPVA	Tablet	AbbVie (2007)	HME
Intelence	Etravirine	HPMC	Tablet	Janssen (2008)	Spray drying
Norvir	Ritonavir	PVPVA-64	Capsule	Abbott(2010)	HME
Modigraf	Tacrolimus	HPMC	Granules	Astellas (2009)	Spray drying
Onmel	Itraconazole	HPMC	Tablet	Merz pharma (2010)	Melt extrusion
Zotress	Everolimus	HPMC	Tablet	Novartis (2010)	Spray drying
Zelboraf	Vermurafenib	HPMCA-AS	Tablet	Genentech (2011)	Co-precipitation
Incivek	Telaprevir	HPMCAS-M	Tablet	Vertex Pharmaceuticals (2011)	Spray drying
Kalydeco	Ivacaftor	HPMCAS	Tablet	Vertex (2012)	Spray drying
Noxafil	Posaconazole	HPMCAS	Delayed release Tablet	Merck(2013)	Melt extrusion
Viekira XR	Dasabuvir/Ombitasvir/ Paritaprevir and Ritonavir	Copovidone Vitamin E TPGS	Tablet	AbbVie (2014)	HME
Envarsus	Tacrolimus	Poloxamer and HPMC	Tablet	Veloxis Pharmaceuticals (2015)	Melt granulation
Epclusa	Sofosbuvir/ Velpatasvir	Copovidone	Tablet	Gilead (2016)	Spray drying
Zepatier	Elbasvir/Grazoprevir	HPMC/ Copovidone	Tablet	Merck (2016)	Spray drying
Mavyret	Glecaprevir/Pibrentasvir	Copovidone	Tablet	AbbVie (2017)	HME
Delstrigo	Doravirine spray drying (+lamivudine, tenovir granulated separately)	HPMCAS	Tablet	MSD (2018)	Spray drying

1.7 Manufacturing process involved in Solid dispersions:

1.7.1 Hot melt method

Hot melt extrusion (HME) has recently attracted increasing attention as promising technology for solubility improvement of poorly soluble drugs. In the HME process the drug and polymer mixture are intensely mixed at a high shear rate induced by the extruder followed by melting and kneading producing the extrudates of different shape used as pellets, granules or implants. The miscibility of drug and polymeric mixture play a crucial role to rationally select the adequate polymer [20]. HME offers various advantages over the traditional approach:

i) Solvent free method reducing the regulatory risk of exceeding the residual solvent limit for the product and reducing the number of processing steps (no drying step required).
ii) Ease of handling highly active pharmaceutical ingredients as it is a closed system.
iii) Uniform mixing of ingredients due to improved shear rate by the rotating screw leading to de-aggregation and thus formation of continuous fine drug particles in the polymer matrix at molecular level.
iv) Ease of scalability to production scale due to the continuous nature of the manufacturing step [77].

However, there are few disadvantages of HME as follows:

i) HME is processed at relatively higher temperature and high thermal stress leads to the thermal degradation of APIs and polymers making it challenging [78].
ii) It is an API consuming process its difficult if limited amount of API is available [79].
iii) It is expensive in terms of time and personal training [80]– [82].

Downstream of HME:

Hot melt extrudates can be down-streamed into small particles using hammer mill or cryogenic milling. The particle size reduction using milling seems a good option to produce fast release ASD containing powders which can be compressed into tablets afterwards. It is reported that milled extrudates are having high bulk density and good flowability compared to spray dried and electro-spun powders. Meanwhile, the other option is to cold cut the extrudate strand reduce particle size by air classifier milling and filling the powder into hard gelatin capsule [83].

The list of marketed products using HME is expanding (Table 2). Huang et al. used Affinisol HPMC HME (100 LV and 4M), a novel grade of a HPMC class polymer that has a low glass transition temperature and melt viscosity compared to other grades of hypromellose. The formulations containing the polymer and carbamazepine (CBZ) were extruded using a 16 mm twin screw extruder, and the effect of temperature, screw speed, and feed rate was investigated. Their studies for non-sink dissolution revealed that CBZ embedded in Affinisol HPMC HME solid dispersions rapidly supersaturated after 15 min, reaching a twofold drug concentration compared to the CBZ equilibrium solubility. Thus, the authors concluded that Affinisol HPMC is an interesting polymer candidate for the HME process aiming at an increased wettability and dissolution [5]. Zecevic and Wagner developed a rationale for solid dispersion preparation of indomethacin with copovidone, Eudragit E 100. They used the microscale hot stage microscope as selection tool for HME and the concept of numeric simulation to improve the understanding and knowledge about the process [2].

1.7.2 **Solvent method**

1.7.2.1 Spray drying

Spray drying is one of the most popular methods used in the pharmaceutical industry for the preparation of solid dispersions of poorly soluble drugs. The liquid solution is atomized into fine droplets and sprayed into the hot chamber containing air or liquid

nitrogen converting these liquid droplets into a dried particulate form in a single step. It provides a control on process variables, resulting in powder with the necessary particle size, shape, residual solvent content, flow property, surface area and release profile for solid dispersion. Drug particles, having very poor aqueous solubility, can be spray dried, but they must be soluble in the desired solvents [21], [22]. Spray drying offers a solubility enhancement for thermolabile drugs in which the solvent evaporation takes at lower temperature with cooling, The API is exposed for shorter period of time preventing thermal degradation of the API. It is also important that the formed amorphous particles are stable until the shelf life of the product for which ternary polymer is added. Spray drying has the advantage of simple scale up, continuous batch manufacturing and [5]. Suryanarayanan et al. investigated the correlation between molecular mobility and physical stability and characterized molecular mobility in amorphous solid dispersions of itraconazole (ITZ) with each polyvinylpyrrolidone (PVP) and hydroxypropyl methylcellulose acetate succinate (HPMC-AS) using spray drying. They found that in amorphous solid dispersions of itraconazole with PVP and HPMC-AS, only HPMC-AS acted as anti-plasticizer of global mobility. Thus, the results suggested that global molecular mobility was correlated to crystallization onset and growth rate indicating the role of cooperative motions in physical instability at storage temperature HPMC-AS was found to be more effective than PVP in inhibiting itraconazole crystallization [85].

1.8 Gap involved in natural and synthetic polymers/excipients

In the formulation development of an amorphous solid dispersion, the excipients form an integral part. The excipient can be either a synthetic polymer or a polymer obtained from a natural source. The synthetic polymers have attracted the attention of various researchers for the use as polymeric carriers for solid dispersions since last 40 years but their use is rather limited. The main reason for this limitation is issues in selecting an appropriate set of polymers which ultimately affects the dissolution properties of the dispersed drug in the polymer matrix. The second reason is the polymer's molecular weight which plays an important role in governing the dissolution rate from the solid

dispersion. An increase in the molecular weight elevates the Tg of the polymer leading to decreased molecular mobility and an increase in stability of the amorphous API. Bolourchian et al. investigated the effect of the molecular weight of PEG 6000, 12000 and 20000 on the dissolution behavior of simvastatin. They prepared a solid dispersion of simvastatin: PEG in ratios 1:1, 1:3, 1:5, 1:7 and 1:9 using solvent method. PEG 12000 showed the highest dissolution rate in 1:7 ratio compared to other PEGs in the same ratio while PEG 20000 showed a decreased dissolution rate due to the high viscosity of the polymer which retarded the release from the solid dispersion [86]. The use of hydrophilic polymer leads to a faster release of the drug molecule from the solid dispersion giving rise to the 'spring and parachute effect' in which there is a rapid increase in solubility followed by improved dissolution rate. But there is difficulty to stabilize this formed supersaturated solution in order to obtain significant absorption followed by satisfactory bioavailability [81]. Liu et al. investigated the solubility improvement of sorafenib up to 50-fold using poly (vinylpyrrolidone-vinyl acetate) (PVP-VA) and sodium lauryl sulfate (SLS) for the tablet formulation which provided a faster initial sorafenib dissolution rate, similar to the 'spring effect' for releasing the drug into solution, but SLS seemed to impair the ability of PVP-VA to act as an efficient 'parachute' in keeping the drug in solution and maintaining the drug supersaturation. It was concluded that the molecular interaction plays a decisive role for vitro and in vivo performance of oral formulations [54]. The use of polymers to inhibit crystallization in the supersaturated solutions is also one of the challenges to deliver a poorly water-soluble drug. It is important to maintain the supersaturation using a polymeric carrier which helps to inhibit nucleation and crystal growth. Ilevbare et al. investigated the impact of polymers on the nucleation behavior of the APIs celecoxib, efavirenz and ritonavir. The interplay of polymer and drug properties influences the nucleation kinetics. They revealed that the polymers having hydrophobic property similar to the hydrophobicity of the drug molecule are effective nucleation inhibitors and that the polymer structure has an effect on the nucleation kinetics. They found that cellulose derivatives with bulky side groups were more effective nucleation inhibitors compared to other synthetic polymers. This observation can be attributed to polymer-solute interactions that hinder the reorganization of a cluster of solute

molecules into an ordered crystal structure. Thus, there is increasing demand for the development of new excipients with superior crystallization inhibition properties for stabilizing supersaturated solutions [55].

The rational assessment of solubility (crystalline drug) and miscibility (amorphous drug) in the polymeric carrier is important for the development of a stable amorphous solid dispersion during storage. The method of manufacture of solid dispersions is also important as it affects the pill burden and also the shelf life of product such as Kaletra.

The selection of synthetic polymer which provide adequate stability during shelf life is challenging. The use of low peroxide containing excipients is also important as it ultimately affects the stability for APIs sensitive to peroxide residues. The increase in quantity of synthetic polymers used in combination or alone will ultimately cause side effects in the body after the administration. Therefore, it is important to consider a maximum daily dose of excipients (synthetic polymers) administered to the patients. The excipient manufacturer is less encouraged to invest in the development of novel synthetic polymers because of the long development timeline of 8 to 10 years, expensive toxicity studies and the lack of safety study guideline for novel excipients by USFDA. In the current USFDA drug approval process, novel excipients are not independently evaluated but are reviewed in context of new drug application. There is a lack of regulatory processes for approval of new excipient as a unique molecule. As per definition from USFDA and from the International council on Hormonisation (ICH) the excipient is considered as ‘novel’ if it is used for the first time in a human drug product. The USFDA maintains a database for inactive ingredient but it does not distinguish between new chemical entities and minor modifications of approved excipients, co-processed mixtures of existing excipients and approved excipients for new routes of administration. It is thus difficult for the excipient manufacturer to interpret the requirements of a new chemical entity excipient application process from regulatory agencies in relation to a new chemical entity excipient application process [56]. The excipient manufacturing companies urge pharmaceutical companies to use new excipients in their new products so that this excipient is reviewed as a part of the regulatory process by USFDA. Nevertheless, the

regulatory authorities are collaborating with the excipient manufacturers to overcome this hurdle and provide a faster approval.

Due to processing difficulties only, few polymers are suitable for HME, while also the use in spray drying processes (e.g., PVA Parteck MXP) is restricted due to its limitations on the required solubility in organic solvents. The down streaming of semisynthetic polymers into suitable dosage form is difficult (e.g., HPMC based HME extrudates are difficult for hammer mill compared to synthetic polymer co-povidone). The focus needs to be changed in a direction that will lead to the use of polymers that occur naturally which are already widely applied in food ingredients and most importantly GRAS listed which will help to overcome regulatory restrictions and encourage the excipient manufacturers along with pharmaceutical industry professionals. Natural polymers can be obtained from various sources. The first use of biomolecules as was reported in 1988 by Imai et al. The authors investigated the influence of egg albumin on several acidic drugs and reported that biomolecules can be used to improve the dissolution rate by preparing solid dispersions [57]. However, thereafter there is very scarce information and data related to the use of such biomolecules. Casein and bovine serum albumin have been reported as additional carriers for ASDs manufacturing. There is still some limitation related to the commercial launch of ASDs products that use biomolecules/natural polymers per se. Recently, Pas et. al have used gelatin type 50PS and screened twelve different poorly soluble drug substances which were prepared as ASDs using a freeze-drying technique showing a pronounced improvement in the dissolution rate of poorly soluble drugs [58].

The limitation for using natural polymers consists firstly is the solubility of the polymer in suitable organic solvents (required for spray drying and freeze drying). The natural polymers/excipients are commonly hydrophilic in nature and therefore exhibit often limited solubility in organic solvents. To overcome the limited organic solubility, they need to be mixed with co-solvents (hydro: alcoholic) making the process success more likely. Another limitation is the fact that the natural polymers/excipients are subject to batch-to-batch variations. This variability is a completely independent parameter which needs careful attention because the crop harvesting, collection, purification and final finished polymer/excipient varies from manufacturer to manufacturer and season to

season. This challenge can be solved by implementing vendor validation and performing batch to batch variation validation studies. The selection of the appropriate natural polymer/excipient is a little bit challenging as these are prone to decomposition under environmental stress conditions like heat or shear stress. Other drawbacks include the potential immiscibility with synthetic polymers or pure APIs and the lack of expertise and data for the use of various insoluble drug substances and manufacturing their respective ASDs. This knowledge gap is a big hurdle for the breakthrough of using natural polymers/excipients as ASDs matrix. On the other hand, the lower glass transition temperatures of natural polymers facilitate a wider process window for ASDs manufacturing, especially for HME.

To narrow this gap of natural polymers/excipients we have included natural polymers/excipients, that can be the potential candidates as matrix for ASDs formulation using spray drying and HME, in our study.

2 *Aim and scope of the work*

The appropriate selection of polymers as a matrix in ASDs is important as it affects the physical stability, wetting property, dissolution performance and overall bioavailability of poorly soluble drug substances. The synthetic polymers are used as carrier matrix but its total amount needs to be carefully considered due to safety limits or maximum daily intake which must not exceed the inactive ingredient limit defined by the FDA. The natural excipients/polymers are widely used as food ingredients and most importantly they are GRAS listed making them attractive to use as ASDs matrix. Although they are already widely applied in food industry, the direction must be shifted to pharma industry especially for ASDs matrix. The chemical space of available polymers needs to be extended. The pre-screening of natural polymers/excipients should preselect suitable polymer candidates which do not trigger recrystallization and phase separation of the amorphous API from the matrix. This would diminish the advantage of ASDs for improved solubility and bioavailability enhancement. The natural polymers/excipients can be used alone or in combination with synthetic/semi-synthetic polymers which will assist in tailor release profiles for the respective therapeutic indication using the industrially applicable process technique of hot- melt extrusion and spray drying. Secondly, an effective delivery to the colon is another need which can be addressed by using a natural excipient with increased site-specific delivery to the colon.

Thus, taking into account the above-mentioned challenges for the selection of the appropriate natural polymer, the following aims of thesis have been pursued:

- The natural/ synthetic polymers including one immediate release and one gastric resistant polymer are mixed for miscibility assessment. These preliminary studies will enable the selection of polymer candidates showing the desired miscibility and thermal properties. This will help to extend the set of available polymers for solid dispersions of poorly soluble APIs. Thus, overcoming solubility limited bioavailability.

- Investigations of the processability towards solid dispersions depending on the polymer and the respective excipients as prerequisite (hot melt extrusion and/or spray drying)

- understanding the interaction between the polymer and the API in order to select a suitable dispersion of polymer or mixtures thereof

- Feasibility study and evaluation of natural excipients for targeting the colonic site

- **Goal**: Decision tree for selecting the appropriate preparation method for solid dispersions (input: API, output: polymer and process) by using natural and(semi) synthetic polymers or mixtures thereof.

2.1 Experimental model

2.1.1 Selection of Model APIs

To overcome the existing gaps in use of natural polymers and improving solubility of poorly soluble drugs solid dispersions were prepared using natural and synthetic polymers as well as mixtures thereof. The following research tools, technologies, equipment and materials were selected:

The model APIs loratadine and indomethacin were selected based on their poor solubility in order to assess their dissolution enhancement and site-specific delivery. The general physicochemical properties and clinical usage of the applied APIs is summarized subsequently. The screening of polymers mixtures (natural/synthetic) is described in chapter 3. The preparation and evaluation of ASDs is described and discussed in detail in chapter 4 and 5.

2.1.1.1 Loratadine (LOR)

LOR is a second-generation anti-histaminic drug and clinically used in symptomatic treatment of allergic rhinitis, hay fever. LOR is a weak base with its low solubility and high permeability its categorized as BCS class II compound. It is having pH dependent solubility for its weakly basic API is critical, thus its solubility will vary with increase in intestinal pH (pH 1 to 8) and precipitation may occur. It is having glass transition temperature of 34 °C and melting point of 137 °C. This makes it interesting candidate for improving solubility using Spray drying and HME. The chemical structure is presented in Figure 2 and physicochemical properties are summarized in Table 3.

2.1.1.2 Indomethacin (IND)

IND is a non-steroidal anti-inflammatory drug (NSAID) with analgesic and antipyretic properties belonging to COX 2 inhibitor category. It is clinically used in treatment of acute

to severe rheumatoid arthritis and acute gouty arthritis, decrease pain and swelling by inhibiting the prostaglandin production.

It is a weak acid with its low solubility and high permeability it is categorized as BCS class II compound in which its dissolution in gastro-intestinal tract is rate limiting process to exert the therapeutic effect. It has been also reported in supportive indication of colon cancer [93]. IND shows low glass transition temperature of 45.1 °C and melting point of 160.3 °C. The crystalline indomethacin exists in polymorphic form α, γ and δ form. The γ form is the most stable form followed by α and δ form. It exists as dimer in which are associated with hydrogen bond [60], [88]. Figure 2 and Table 3 presents the chemical structure and physicochemical properties of indomethacin.

a **b**

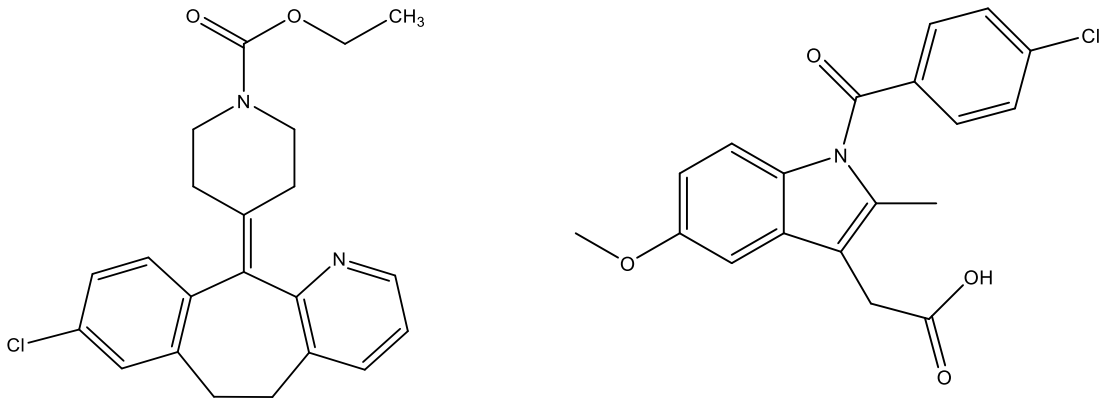

Figure 2: Chemical structure a) Loratadine and b) Indomethacin

Table 3: Physiochemical properties of Loratadine and Indomethacin

API	**Loratadine**	**Indomethacin**
IUPAC chemical name	ethyl 4-(13-chloro-4-azatricyclo pentadeca-1(11),3(8),4,6,12,14-hexaen-2-ylidene) piperidine-1-carboxylate	2-[1-(4-chlorobenzoyl)-5-methoxy-2-methylindol-3-yl] acetic acid
Formula	$C_{22}H_{23}ClN_2O_2$	$C_{19}H_{16}ClNO_4$
Molecular weight [g/mol]	382.8	357.79
Melting point [°C]	134 to 137	160.3 [γ form]
Glass transition temperature [°C]	34.3	45.1
pKa	5.26 [95]	4.5
Solubility	0.1 N HCl: 0.168 mg/ml PBS, pH 5.5: 0.016 mg/ml PBS, pH 6.8: 0.010 mg/ml	0.1 N HCl: 1.5 µg/ml [18] PBS, pH 5.5: 42.6 µg/ml [96] PBS, pH 6.8: 388.5 µg/ml[96]

2.1.2 Polymer selection

A range of natural polymers with synthetic polymers and active pharmaceutical ingredients (API) were used for the investigations. The different set of polymers assessed were inulin, shellac, α-glycosyl hesperidin and the cellulose based materials such as hydroxypropyl methyl cellulose new grade and the hydroxypropyl methyl cellulose acetate succinate. They are presented in Figure 1 explaining their physicochemical properties in respective monographs (1.5.1 – 1.5.5). The polymers suitable for spray drying and hot melt extrusion and are selected based on their broad range of their physical and chemical properties. The solid dispersions were prepared using spray drying and hot melt extrusion. To understand the characteristics and performance of manufactured solid dispersions, various techniques were used to characterize the thermal and physicochemical properties of the raw materials and prepared formulations. These techniques include differential scanning calorimetry, in standard or modulated mode (DSC or TOPEM-DSC), to characterize the thermal behavior of materials, i.e. melting temperature and/or glass transition temperature, thermogravimetric analysis to determine the degradation temperature of polymers, AT-IR to obtain information of intermolecular interaction in solid dispersion, Karl Fischer titration to investigate the water content, and X-ray powder diffraction (XRPD) for solid state characteristics. Further, to evaluate the dissolution characteristics of drug and different formulation experiments were performed using conventional USP equipment (USP apparatus I and II).

3. Selection of suitable polymers/mixtures as matrix for ASDs

3.1 Introduction

The first challenge prior to manufacturing amorphous solid dispersions, is the selection of the appropriate polymer as matrix in ASDs. The polymer and API should completely dissolve in the organic solvent without degradation at the applied process conditions. It must have a low glass transition temperature allowing for easier processability during extrusion, with the capability to reduce molecular mobility of the amorphous system to retain its advantage of improved dissolution performance, even upon storage. [25], [97]. The hygroscopicity plays a vital role for crystallization during storage and should therefore be minimized. A pre-drying step is recommended to avoid detrimental effects during storage of ASDs [98]. The amount of proton donor/acceptor groups plays an important role for intermolecular interactions between the polymer and the respective incorporated drug. These intermolecular interactions influence the drug-polymer miscibility, which will increase physical stability of the amorphous solid dispersion [58], [89].

Therefore, it is important to investigate the polymer-polymer matrix with pre-screening in terms of solubility and miscibility to provide a future direction for the selection of a suited polymer for the ASDs matrix. The use of differential scanning calorimetry helps to understand the miscibility of polymer-polymer mixtures, in which one glass transition temperature is indicative of a miscible system, while two glass transition temperatures suggests that an immiscible system is likely to be present. Those immiscible polymer-polymer mixtures should be avoided as an ASDs matrix. In case of film cast, the soluble polymer system will show a uniform film formation with a single glass transition temperature.

3.2 Evaluation of solid-state dependency from processing principles

3.2.1 Differential scanning calorimetry (DSC)

Table 4: Physical properties of natural and synthetic polymers neat and their mixtures

Name of Excipient/mixture	DSC		XRPD	Solubility in organic solvent
	Phases	Tg (°C)		
Inulin	1	123.4	Amorphous	Slightly soluble in acetone, ethanol, freely soluble in water
HPMC-AS	1	120	Amorphous	Soluble in acetone, ethanol, insoluble in water
Shellac	1	38.9	Amorphous	Soluble in ethanol, slightly soluble in acetone, insoluble in water
A15	1	98.8	Amorphous	Soluble in acetone, water, slightly soluble in water
Inulin + HPMC-AS PM (50:50)	1	123.8	Amorphous	These mixtures were dissolved in different solvents and are described in table below
Shellac + A15 PM (50:50)	1	58.2	Amorphous	
Inulin + Shellac PM (50:50)	1	112.7	Amorphous	
A15 + HPMC-AS PM (50:50)	1	122.5	Amorphous	

The glass transition temperature of the pure polymer, the mixture of natural with synthetic polymer and the mixture of natural with natural polymer were investigated to assess the miscibility using DSC. The single-phase system of all physical mixture showed one glass transition temperature (Table 4) and the biphasic system of a mixture of two natural polymers (shellac and inulin) showed two glass transition temperatures indicating their immiscibility after film casting in organic solvent (Table 5). The physical mixtures of the polymers were prepared in an equivalent ratio. DSC measurements revealed a decrease in glass transition temperature indicating that they are miscible with each other.

3.2.2 Film casting of mixtures

The polymers were dissolved in organic solvent/s (mixture). It is challenging to use a common solvent for binary mixtures in case of natural/synthetic and natural/natural polymers. The solubility is governed by hydrophilicity and hydrophobicity of the individual polymer i.e. the higher the number of hydrophilic groups, the more soluble it will be in water and vice-versa. The organic solvent needs to be carefully assessed due to their environmental issues. ICH guidelines suggest the use of such solvents and in the present study we have used class III solvents which are used widely for pharmaceutical industrial applications.

Table 5: Solubility and glass transition temperature for various film cast samples in different solvent

Name of physical mixtures	Solvent used	Solubility in Aqueous/organic solvent mixture	DSC	
			Film cast	
			Phases	Tg (°C)
Inulin + HPMC-AS	Acetone	slight undissolved particles	1	120.4
	Ethanol	slight undissolved particles	1	120.1
	Acetone/Ethanol (50:50)	slight undissolved particles	1	121
	Ethanol/Water (95:5)	slight undissolved particles	1	121.2
Shellac + A15	Acetone	Yes, dissolved completely	1	56.8
	Ethanol	Yes dissolved	1	56.2
	Acetone/Ethanol (50:50)	Yes dissolved	1	56.3
	Ethanol/Water (95:5)	Yes dissolved	1	59.3
Inulin + Shellac	Acetone	No	2	36.4 97.5
	Ethanol	Film cast was not possible	NA	NA
	Acetone/Ethanol (50:50)	Film cast was not possible	NA	NA
	Ethanol/Water (95:5)	No	2	39.6 98.3
A15 + HPMC-AS	Acetone	Yes, dissolved completely clear solution	1	113.2
	Ethanol	Yes, dissolved clear solution	1	111.5
	Acetone/Ethanol (50:50)	Yes, dissolved completely clear solution	1	110.1
	Ethanol/Water (95:5)	Yes, dissolved clear solution	1	106.2

All mixtures of inulin and HPMC-AS that were film casted showed slight undissolved particles of inulin due to its low solubility in organic solvents, but the film cast showed one Tg indicating that they are miscible with each other. In case of the mixture of shellac with A15 the film cast was clear in appearance with a single Tg clearly showing that these mixtures are miscible with each other. The mixtures of inulin with shellac were insoluble in all organic solvent mixtures and the film cast for acetone/ethanol and ethanol was uneven and difficult to collect from Teflon petri-plate. In the film cast, two phases and two Tgs (36.6 °C of shellac and 97.5 °C for inulin) were observed indicating immiscibility of this mixture of two natural excipients. For the mixture of A15 with HPMC-AS, the film cast was clear in different organic solvent mixtures with a single Tg indicating miscibility of all these mixtures. Thus, it was observed that Shellac with A15 and A15 with HPMC-AS showed better solubility and miscibility in organic solvent**.**

3.3 Decision tree for selecting suitable polymers or mixtures thereof for ASDs matrix processing

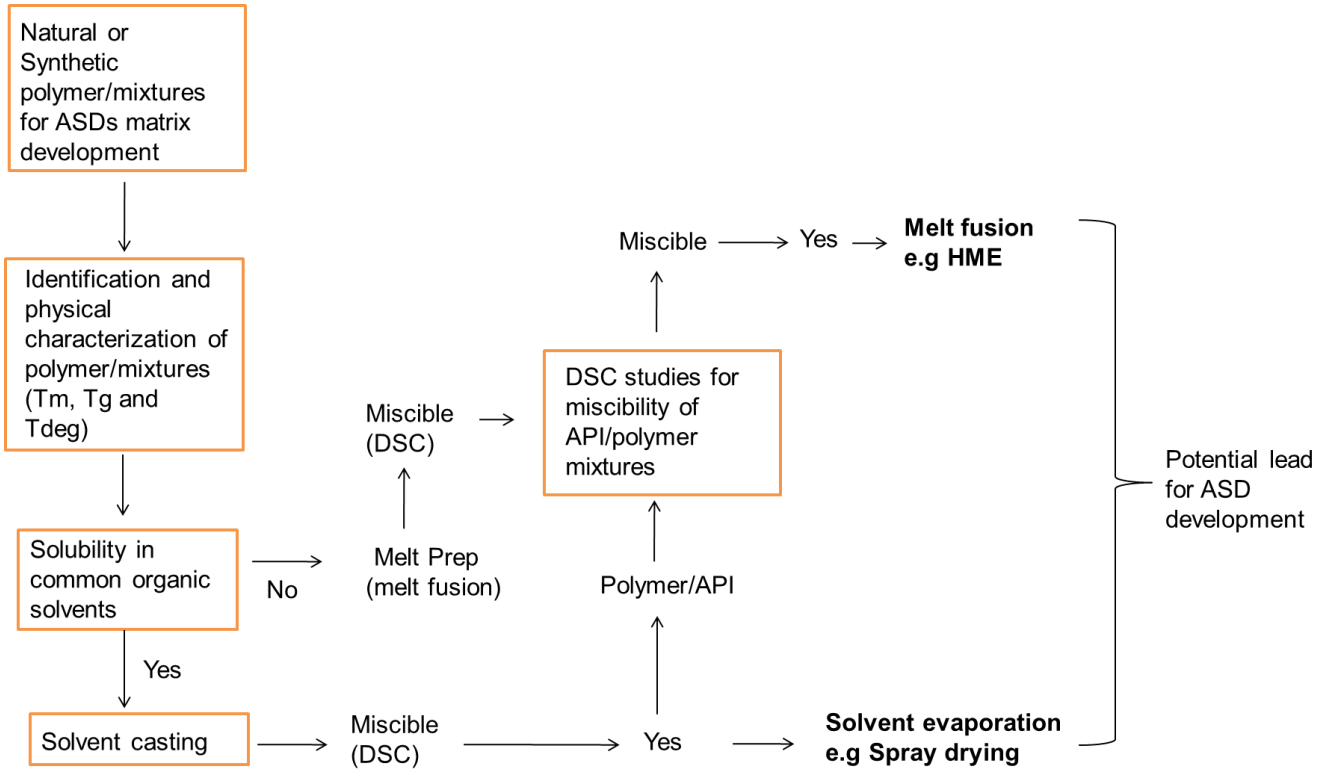

Figure 3: Decision tree for excipient/polymer selection for ASDs development

3.4 Summary and conclusion of the chapter

The natural polymer inulin in combination in a binary mixture with HPMC-AS was slightly soluble in organic solvents and the film cast showed a single glass transition temperature indicating that these two polymers are miscible with each other which might be suitable for spray drying. Other mixtures of shellac with A15 showed a better solubility in organic solvent mixtures and the film cast showed a single Tg, in this case, a solvent mixture of acetone/ethanol (50/50) showed the best results in terms of clearity of casted film. The mixture containing inulin with shellac was insoluble in different organic solvents and immiscible showing two Tgs in DSC measurements, thereby clearly indicating that this combination is not a suitable matrix for manufacturing of ASDs. Lastly, A15 with HPMC-AS was soluble in all tested organic solvents (acetone, ethanol) and mixtures acetone/ethanol (50/50) and ethanol/water (95/5) showing a single Tg in DSC measurements making this combination one of potential lead candidates for the manufacturing of ASDs. Thus, using the pre-screening enabled the selection of natural excipients alone or in combination as matrix in ASDs development. This strategy is summarized in Figure 3 as decision tree for the selection of a suitable polymer (combination) for ASD development.

4 Influence of shellac to improve solubility and supersaturation of loratadine amorphous solid dispersion using new grade of HPMC

4.1 Introduction

The recent years have witnessed an exponential increase in the number of new low water-soluble compounds in the drug discovery pipeline. [100]. Most of these belong to class II of the biopharmaceutical classification system (BCS), which suffer from a low water solubility-related limited bioavailability [101]. Various strategies have been developed to overcome low water solubility challenges. These include the development of water-soluble pro-drugs [102], salt forms [103], co-crystals [104] and amorphous solid dispersion (ASDs) [75].

There has been an increase in the number of studies dedicated to improve the solubility and delay the crystallization of poorly soluble drugs using different polymers through the formulation of binary ASDs. Within this context, the selection of appropriate polymers in proper quantity is highly essential, as it is decisive in the success of such binary systems. Also, the physical stability of the ASD formulation with respect to the generation and maintenance of drug supersaturation during dissolution is equally important. Within this context, combination of polymers with surfactants was employed to improve the delivery of poorly water-soluble drugs [95]. Examples include the preparation of ternary spray-dried dispersion of dipyridamole and cinnarizine with surfactant sodium dodecyl sulfate, poloxamer 188 and polymers polyvinylpyrrolidone K30 and hydroxypropyl methylcellulose K100. It has been observed that the maximum supersaturation level can be achieved using drug-polymer-polymer ternary dispersions, but that the incorporation of surfactant into binary (drug-polymer) and ternary (drug-polymer-polymer) systems has an adverse effect on the physical stability and dissolution of the system, promoting crystallization. Thus, it is necessary to study the effect of adding a ternary polymer or additive on the dissolution and supersaturation performance of ASDs. [106] studied ternary systems for the weakly basic drug dipyridamole using HPMCAS in combination with hydroxypropyl cellulose (HPC-SSL), which showed improved performance in terms of solubility and supersaturation. They observed that for weak bases readily soluble at low pH, ternary mixtures of HPMC-AS and HPC-SSL combined the advantage of fast dissolution at low pH (HPC-SSL controlled)

with superior supersaturation at pH 5.5 and 6.8 (HPMC-AS controlled). This study investigated whether a similar effect occurs with the natural excipient shellac in combination with Affinisol® HPMC HME 15 LV (A15) having low Tg with flipped proportion.

Shellac is a natural resinous complex mixture of different acids, mainly alueritic acid, jalaric acid, shellolic acid and butolic acid [107] with a molecular weight of 1006 g/mol. It is derived from the insect strain of kerria lacca through solvent extraction [108]. Shellac is non-toxic, physiologically harmless, GRAS listed by FDA, renewable and economically available [109]. It is used for various purposes such as enteric-coating and colon targeting, as well as the development of extended-release matrices in tablets [110]. However, to the best of our knowledge, shellac has not been used as additive to optimize and maintain supersaturation with solubility improvement for the poorly soluble drugs.

The challenge in using shellac lays within in its pH-dependent dissolution, as it begins to dissolve at pH 7.0 with full dissolution at pH 7.3. This is due to the high pKa of shellac, which is between 5.8 and 7.5 [110], [111]. Shellac is amorphous, brittle in nature and soluble in ethanol. Given all such properties and having a low glass transition temperature, it can serve as an interesting polymer for the preparation of ASDs, both through spray drying (SD) and hot melt extrusion (HME). There, however, might be a risk for pronounced recrystallization of the molecularly dispersed drug. Hence, shellac should be used in combination with hydrophilic polymers to achieve pH-independent solubility. The new grade of HPMC with a molecular weight of 84,400 g/mol is an interesting candidate for this purpose, as it possesses a low glass transition temperature, low melt viscosity and low hygroscopicity compared to traditionally available grades of HPMC, which often require plasticizers for processing through HME [5], [102]. We hypothesized that the lower molecular weight of shellac might enable a high mobility of shellac acids into HPMC, leading to increased potentials of interaction.

Loratadine (LOR) is a weakly basic compound having a solubility of 0.168 mg/ml at pH 1.1 that drops to 0.010 mg/ml at pH 6.8. As it belongs to the BCS class II category, it is used as a model drug for ASD preparation. It has a melting point of 137 °C and a glass transition temperature of 34 °C. The goal of the present study was first to

investigate the effect of various ratios of shellac as an additive in ASDs prepared using SD and HME on forming single phased glassy solutions. Secondly, we sought to investigate the impact of shellac on the dissolution profile, i.e., solubility improvement, and supersaturation maintenance. To achieve the set goal, ASDs were characterized for their solid-state and stability upon storage at accelerated conditions, correlating the amount of dissolved drug with remaining crystallinity, dependent of the crystals origin; a) undissolved crystals during processing of the ASDs or b) recrystallization upon storage. These studies will add to the understanding of the use of shellac as additive for tweaking supersaturation occurrence and maintenance for solubility enhancement, which will be advantages for future ternary ASD development for solubility enhancement purposes.

4.2 Results and Discussion

4.2.1 Physicochemical properties of the neat excipient/polymer

The shellac glass transition temperature was recorded to be 36.9 °C. Shellac was shown to be freely soluble in ethanol (96 % v/v), and to have a water content of 1.91% post drying (24 h, 40 °C, vacuum). A15 showed a glass transition temperature of 96.8 °C with a water content of 0.55 % post drying (24 h, 40 °C, vacuum). A15 was found to be soluble in ethanol and acetone mixtures.

4.2.2 Characterization of ASDs

4.2.2.1 Solid-state

a) DSC studies of LOR ASDs formulations

The DSC thermal analysis showed a melting endotherm of LOR at 137 °C confirming the identity and purity of the compound based on the reported values [113].

In all mixtures, a single glass transition temperature appeared indicating a homogenous mixture of the drug into all respective binary and ternary systems, which served as evidence of molecular interaction i.e., single phased ASDs shown in Figure 4A and Figure 4B. The glass transition temperature of the SD ASDs was used as a basis for preparing ASDs using HME, in which the mixtures were melt extruded at 40 to 50 °C above their glass transition temperature to obtain an ASD. The glass transition temperatures of SD ASDs were about 2 °C higher than that of the HME ASDs for binary mixtures and ternary mixtures up to a shellac content of 5 %. As shellac concentration further increased to 10 and 20 %, the difference in Tg became smaller down to 1 °C (Table 6), as shellac acted as a solid-state plasticizer [104]. The lower Tg for the HME products was probably related to the shear degradation of the polymer, which is reported to be responsible for shortening of the chain lengths of polymers and subsequent decrease in Tg [115], [116].

Table 6: Glass transition temperatures of LOR, A15 and SSB 55 physical mixtures, spray dried and hot-melt extruded ASDs in various ratios

Name of sample mixture	Glass transition temperature [°C]	
	SD	HME
LOR – A15 20/80	59.9 ± 0.7	57.5 ± 0.06
LOR – SSB 55 20/80	49.3 ± 0.9	47.5 ± 0.09
LOR – A15 – SSB 55 20/75/5	55.6 ± 0.7	53.8 ± 0.8
LOR – A15 – SSB 55 20/70/10	54.5 ± 0.3	53.3 ± 0.6
LOR – A15 – SSB 55 20/60/20	50.6 ± 0.3	49.3 ± 0.5
LOR – A15 – SSB 55 20/50/30	51.5 ± 0.4	50.3 ± 0.3
LOR – A15 – SSB 55 20/40/40	49.7 ± 0.2	48.7 ± 0.9

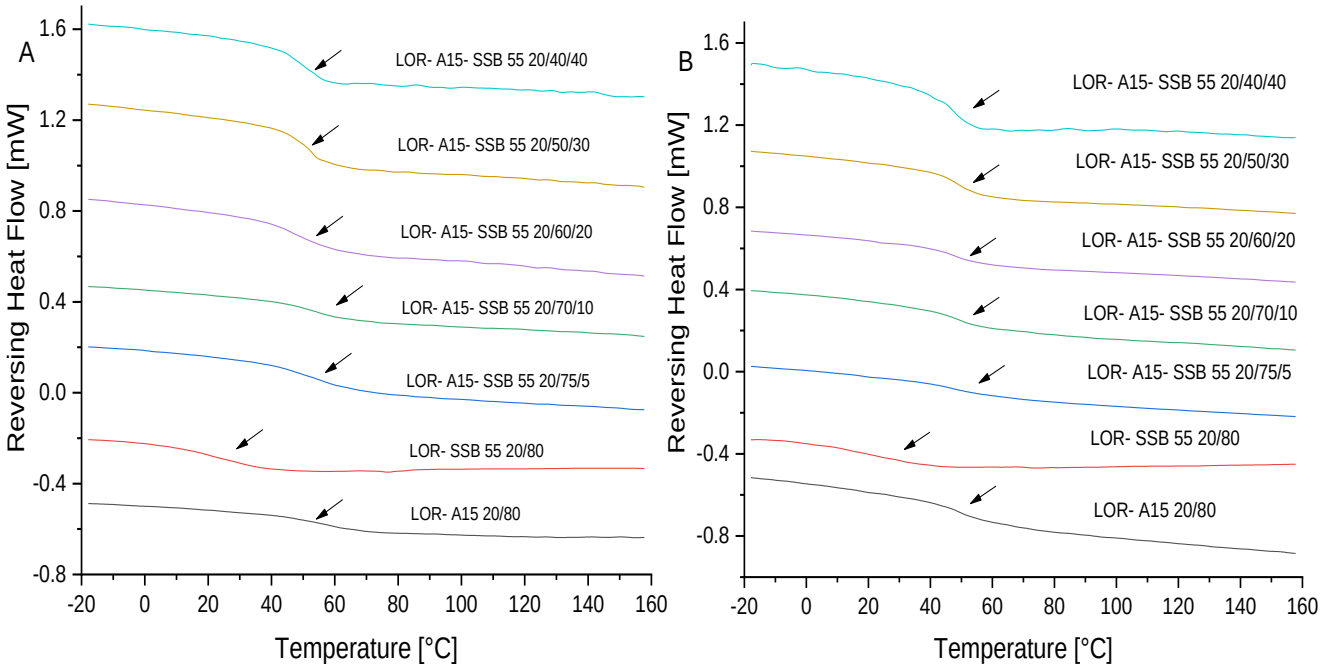

Figure 4: (A) DSC plot of spray dried binary and ternary mixtures (bottom to top): LOR-A15 SD 20/80, LOR-SSB 55 SD 20/80, LOR-A15-SSB 55 SD in ratios 20/75/5, 20/70/10, 20/60/20, 20/50/30 and 20/40/40; (B) hot melt extruded binary and ternary mixtures (bottom to top): LOR-A15 HME 20/80, LOR-SSB 55 HME 20/80, LOR-A15-SSB 55 HME in ratios 20/75/5, 20/70/10, 20/60/20,20/50/30 and 20/40/40 [Arrows indicate → Glass transition temperature]

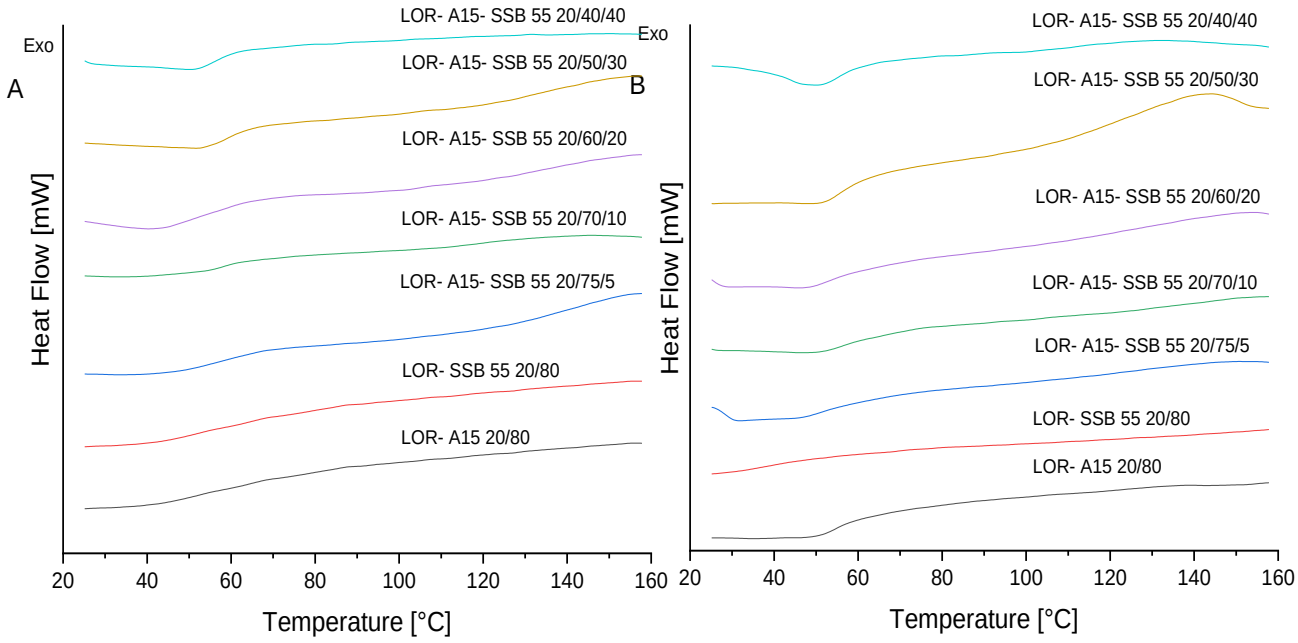

Figure 5: (A) DSC plot showing absence of melting endotherm for spray dried binary and ternary mixtures (bottom to top): LOR-A15 SD 20/80, LOR-SSB 55 SD 20/80, LOR-A15-SSB 55 SD in ratios 20/75/5, 20/70/10, 20/60/20, 20/50/30 and 20/40/40; (B) hot melt extruded binary and ternary mixtures (bottom to top): LOR-A15 HME 20/80, LOR-SSB 55 HME 20/80, LOR-A15-SSB 55 HME in ratios 20/75/5, 20/70/10, 20/60/20,20/50/30 and 20/40/40

b) XRPD studies

i) Initial samples

The diffractograms presented in Figure 6 (A) showed that neat LOR was of crystalline nature with several well-defined intense 2-theta peaks. The neat materials of A15 and SB 55 showed no intense peaks indicating their amorphous nature. The peak at 31.6 ° for A15 indicated the presence of residual sodium chloride as a by-product of its synthesis [112], [117]. The binary PMs of LOR - A15 and LOR- SB 55 were crystalline, resembling peaks of the neat LOR (Figure 6 (A)), while the ASDs prepared by SD and HME were amorphous. Figure 6(B) represents the ternary PMs showing the characteristic peak pattern of neat LOR. The ASDs of ternary mixtures obtained from SD (Figure 7 (A)) and (HME Figure 7 (B)) depict that all formulations have been converted into a completely amorphous state. These results were in accordance

with DSC, where no melting endotherm of remaining crystalline LOR could be observed (Figure 5A and Figure 5B).

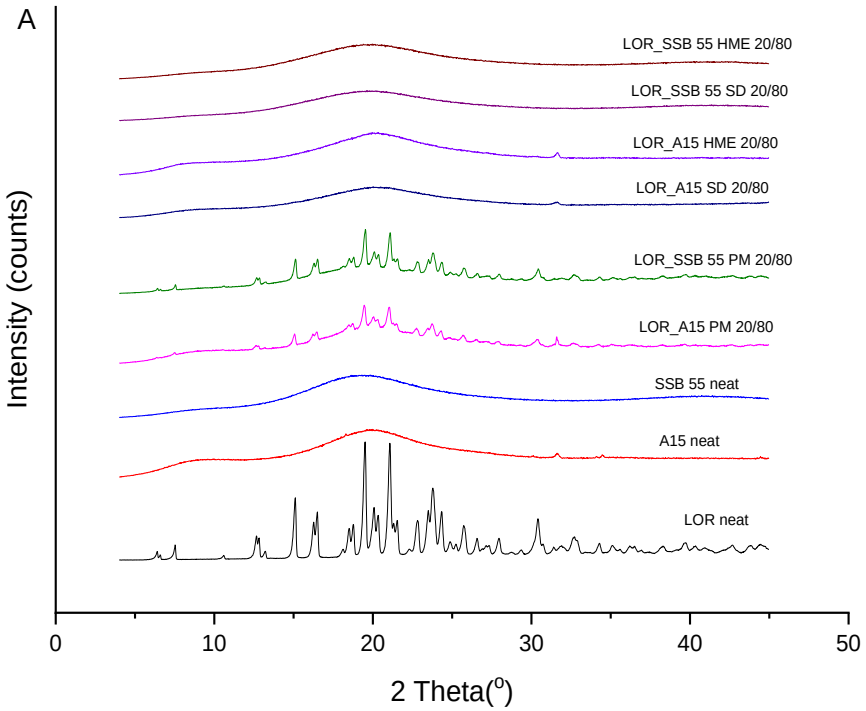

Figure 6: (A) XRD patterns for single components and binary mixtures (bottom to top): LOR neat, SSB 55 neat, A15 neat, LOR-A15 PM 20/80, LOR-SSB 55 PM, LOR-A15 SD 20/80, LOR-A15 HME 20/80, LOR-SSB 55 SD 20/80 and LOR-SSB 55 HME

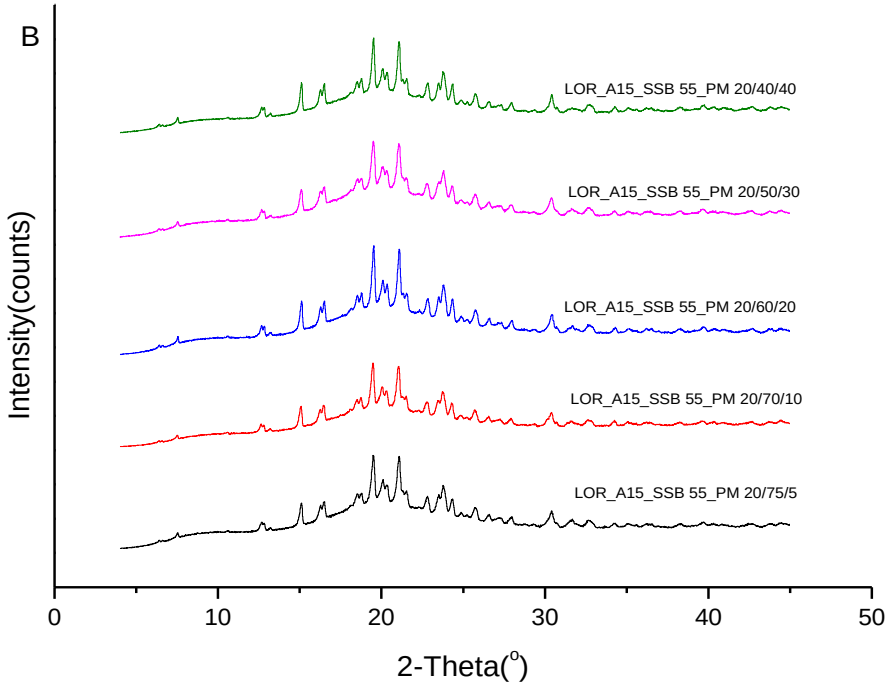

Figure 6:(B) XRD patterns for ternary physical mixtures (bottom to top): LOR-A15-SSB 55 PM in ratios 20/75/5, 20/70/10,20/60/20, 20/50/30 and 20/40/40

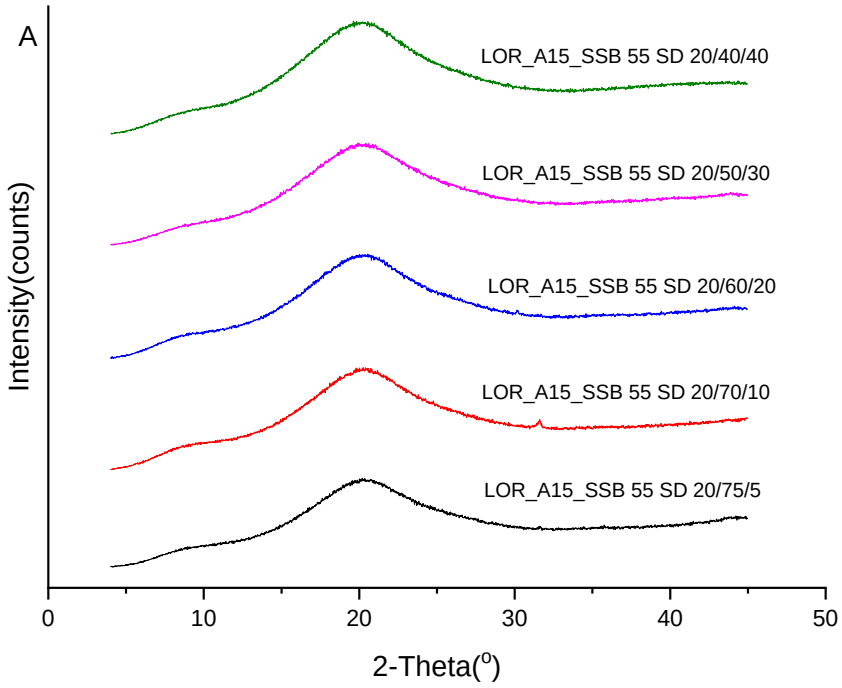

Figure 7: (A) XRD diffractograms of spray dried ternary mixtures (bottom to top): LOR-A15-SSB 55 SD in ratios 20/75/5, 20/70/10, 20/60/20, 20/50/30 and 20/40/40

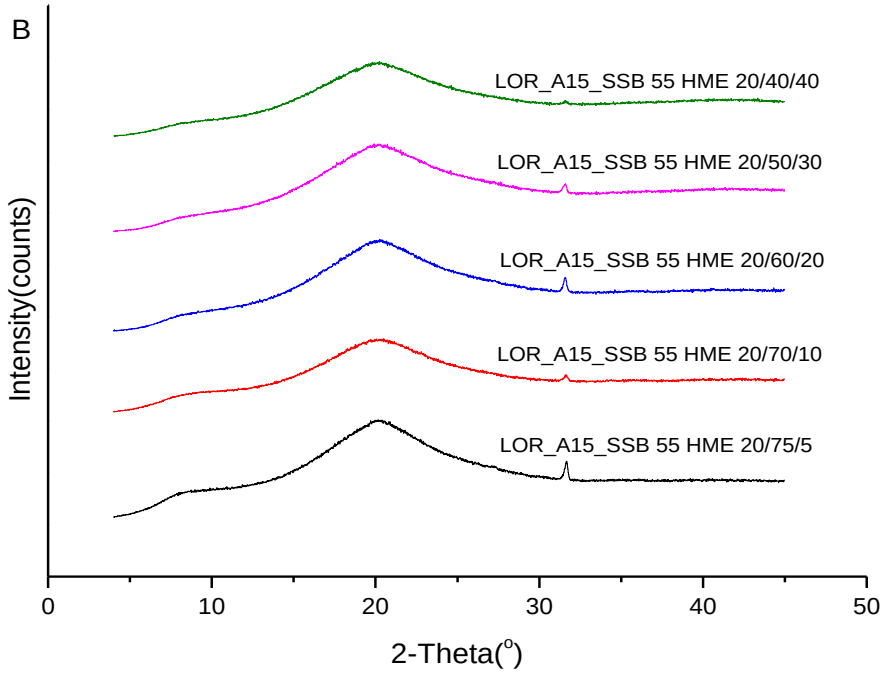

Figure 7: (B) XRD diffractograms of hot melt extruded ternary mixtures (bottom to top): LOR-A15-SSB 55 HME in ratios 20/75/5, 20/70/10, 20/60/20,20/50/30 and 20/40/40

ii) Induced crystallinity studies

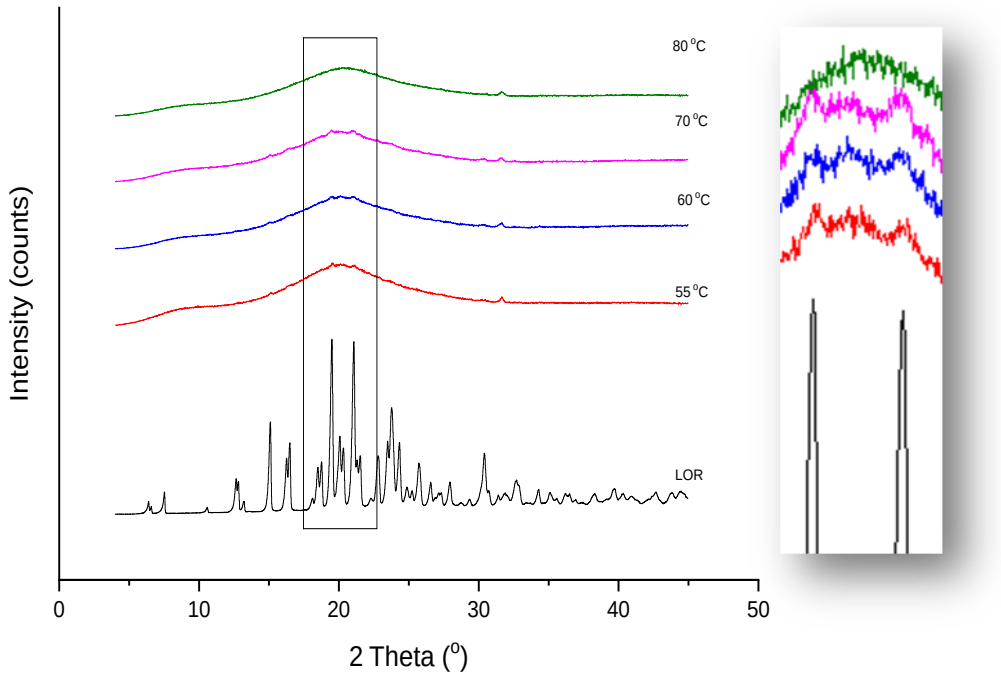

Figure 8: XRD diffractograms for LOR neat and LOR-A15-SSB 55 HME in ratio 20/70/10 hot-melt extruded at 55 °C, 60 °C, 70 °C and 80 °C (bottom to top).

The diffractograms of cryo-milled extrudates showed slight crystallinity (Figure 8). The crystallinity was dependent on the extrusion temperature, where it decreased with an increase in the HME temperature. The amount of calculated crystallinity is represented below in Table 7.

Table 7: Calculated amount of crystallinity present within the extruded samples at different temperatures

Name of sample	Crystallinity [%]
LOR- A15- SSB 55 HME 55 °C	6.2
LOR- A15- SSB 55 HME 60 °C	5.6
LOR- A15- SSB 55 HME 70 °C	4.1
LOR- A15- SSB 55 HME 80 °C	3.2
LOR- A15- SSB 55 HME 105 °C	0.0

Only at an extrusion temperature of 105 °C did LOR completely dissolve into the polymeric matrix, and hence, no remaining crystallinity was detected. At lower processing temperatures during HME, remaining crystallinity in the final ASD products was observed,

which was due to incomplete dissolution of LOR into the ASD matrix during the HME process.

iii) Stability samples

The ASDs samples were subjected to stability studies, the results of which are represented in Table 8

Table 8: The amount of crystallinity calculated for stored ASDs sample ASDs using SD and HME

Name of sample	Storage vials	Stability condition	% Crystallinity
LOR- A15- SSB 55 SD	Closed	25 °C/60% RH/ 1 week	2.1 %
		25 °C/60% RH/ 2 weeks	2.5 %
		25 °C/60% RH/ 4 weeks	3.3 %
		40 °C/75 % RH/1 week	2.3 %
		40 °C/75 % RH/2 weeks	2.7 %
		40 °C/75 % RH/4 weeks	3.5 %
	Activ® vials (closed with desiccant)	40 °C/75 % RH/4 weeks	2.5 %
LOR- A15- SSB 55 HME	Closed	25 °C/60% RH/ 1 week	2.1 %
		25 °C/60% RH/ 2 weeks	2.3 %
		25 °C/60% RH/ 4 weeks	3.1 %
		40 °C/75 % RH/1 week	2.2 %
		40 °C/75 % RH/2 weeks	2.6 %
		40 °C/75 % RH/4 weeks	3.4 %
	Activ® vials (closed with desiccant)	40 °C/75 % RH/4 weeks	2.1 %

The ASDs prepared through both SD and HME (@ 105 °C) techniques initially comprised amorphous LOR, i.e., possessed no remaining crystallinity. The samples subjected to

accelerated conditions absorbed moisture due to exposure to humidity, while the temperature led to faster aging process changing in its physical properties. Thus, the LOR, which was initially dispersed on a molecular level, exhibited slight crystal seed formation. These were smaller during initial phase (here 1 week), but seed agglomeration occurred in later stages (here 4 weeks) [118].

c) Changes upon storage

i) Water content, glass transition and crystallinity

Figure 9(A) shows the change in glass transition temperature and water content of all formulations. Under accelerated conditions (40 °C, 75 % RH, full symbols Fig. 9), the initial water content of the sample (closed without desiccant) increased from 1.1 % to 1.9 % for SD and 2.0 % for HME after 4-week storage. The glass transition temperature, on the other hand, dropped from 54.5 °C (SD) or 53.5 °C (HME) to 46.1 °C (SD) or 45.9 % (HME), respectively. During the 4 weeks of storage at 40 °C / 75 % RH, the Tg of samples from SD and HME at respective time points were similar. However, the water content of the HME samples were always 0.1 % higher compared to the SD samples. In contrast, at 25 °C / 60 % RH, the water content after 2 and 4 weeks was identical, whereas the Tg of HME samples were always lower. Based on the samples of similar water content (Fig. 9A) at 1.5 and 1.7 %, it can be concluded that Tg is not strictly dependent on water content, but also on the manufacturing process and the storage temperature. Tg SD (25 °C) >Tg HME (25 °C) >Tg HME (40 °C) storage in closed containers including desiccant, however, reduced the starting water content from 1.1. % (SD and HME) to 0.6 (SD) and 0.7 % (HME). Accordingly, the glass transition temperature increased to 55.5 °C (SD) and 55.0 °C (HME). Nevertheless, exposure to a high temperature of 40^{o}C might have facilitated the aging process accounting for an increase in the glass transition temperature and consequently slight small microcrystal formation [119].

In general, remaining crystallinity upon storage was inversely affected by water content compared to Tg (Fig. 9B). Surprisingly, despite exhibiting higher water content and lower Tg, the HME samples at both storage conditions always showed lower crystallinity compared to the SD samples. Looking at samples of identical water content at 1.5 and 1.7

% crystallinity, the crystallinity seemed to be impacted more by storage time rather than temperature. At 40 °C/75 % RH under closed conditions with desiccant, the crystallinity did not remain at 0 % (starting value), but increased to 2.1 % for the HME samples after four weeks and 2.5 % for SD samples. This again demonstrated the dominant impact of storage time and temperature upon water content. Thus, storage in moisture-protective containers alone does not ensure a complete retention of the amorphicity, and slight recrystallization occurs over the course of storage. This is in accordance with previous reports [111] and in complete agreement with our results of Karl Fischer, DSC and XRPD.

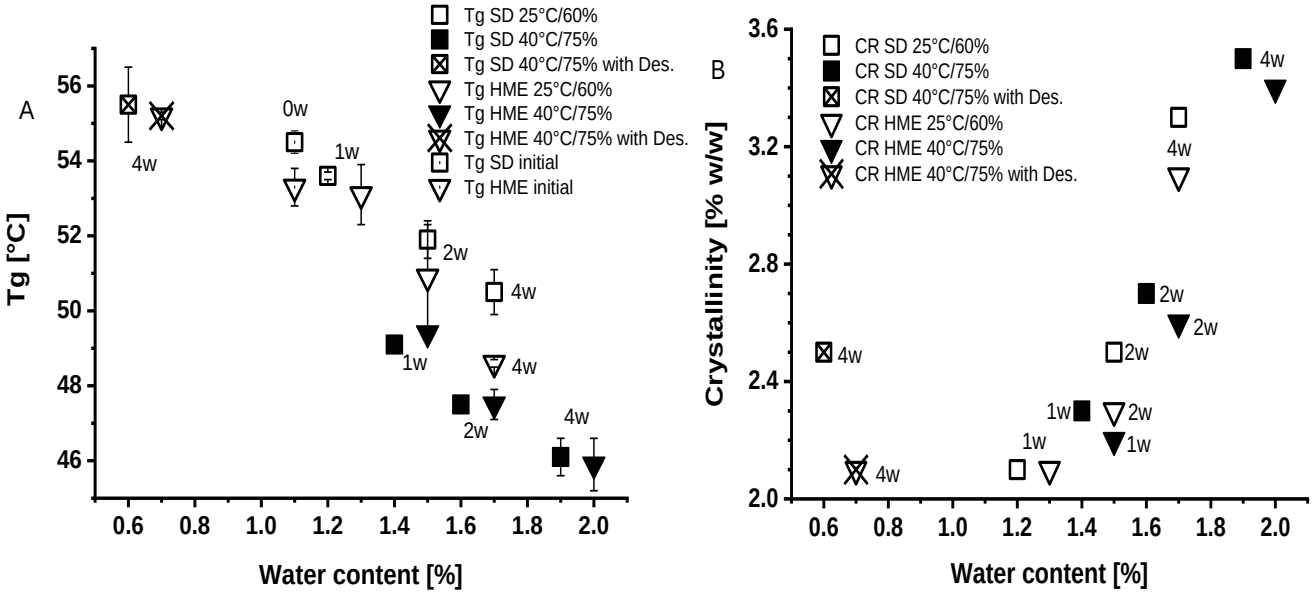

Figure 9: Correlation between the water content of LOR-A15-SSB 55 (20/70/10) ASDs form HME and SD and
(A) glass transition temperature at various storage conditions,
(B) remaining LOR crystallinity at various storage conditions

d) Drug-polymer interaction

Attenuated total reflectance infrared spectroscopy was carried out to find out the potential interactions among LOR, A15, SSB 55 in binary or ternary mixtures processed by SD and HME. The non-covalent interactions, such as hydrogen bonding, resulted in characteristic peak broadening of functional groups of the polymer and drug in infrared experiments [122]. The spectra of LOR with A15 binary mixture are presented in Figure

10, where LOR showed various characteristic bands at 2997.4 cm $^{-1}$ (=C-H stretch), 1706.5cm^{-1} (C=O group of carbonyls where intermolecular interaction might take place), 1218.8 cm^{-1} (C-O stretch), and 1559.5 cm^{-1} as well as 1472.4 cm^{-1} stretch vibration of benzene [123], [124]. The infrared spectrum of A15 exhibited a strong characteristic vibration band at 1045.5 cm^{-1} due to an alkyl substituted cyclic ring containing ether linkages and a peak at 3461.1 cm^{-1} due to the presence of a hydroxyl group (-OH stretching) [125]. LOR/A15 ASDs showed a slight decrease in the peak intensity to 1699.7 cm^{-1} with increase in O-H stretch frequency to 3463.6 cm^{-1} indicating a slight interaction in binary mixtures as shown in Figure 10.

The interaction between LOR-SSB 55 ASDs are shown in Figure 10. SSB 55 showed a single peak at 1706.1 cm^{-1} corresponding to a C=O stretching of the ester group, while the -OH stretch of the hydroxyl group was observed at 3397.2cm^{-1}. The -OH stretch of SSB 55 was not affected within the ASDs, implying no intermolecular interaction at this site.

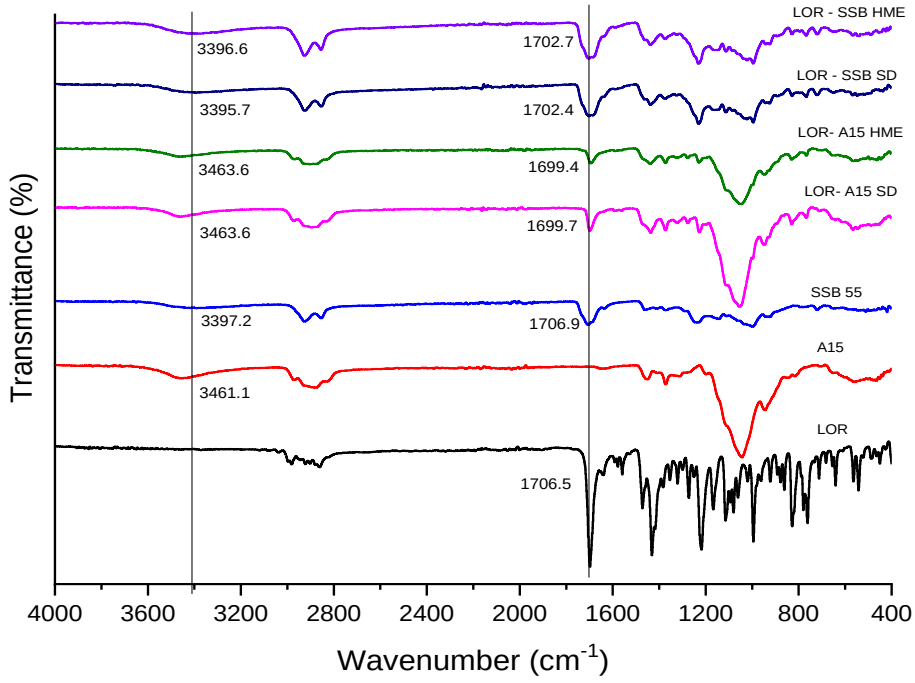

Figure 10: ATR-IR spectra of single components and binary mixtures (bottom to top): LOR, A15, SSB 55 neat, LOR-A15 SD and HME (20/80), LOR-SSB 55 SD and HME (20/80). Vertical lines indicating the A15 related OH-stretch at 3461.1 cm^{-1} and the LOR related C=O-stretch at 1706.5 cm^{-1}.

The ternary ASDs for SD formulations showed a slight change in the carbonyl region (C=O) and the –OH region (Figure 11). The ATR-IR peak for the ternary system occurred at 3461.1 cm^{-1}, and was similar in case of LOR-A15-SSB 55 20/40/40 ratios indicating only slight interaction.

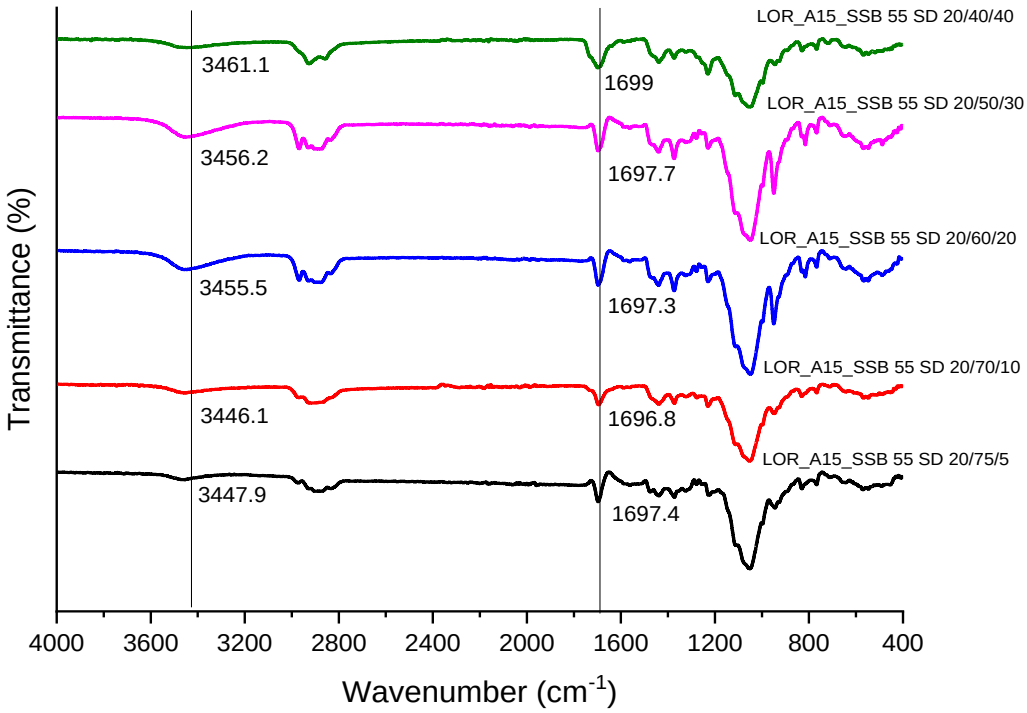

Figure 11: ATR-IR spectra of spray dried ternary mixtures (bottom to top): LOR, A15, SSB 55 in ratios of 20/75/5, 20/70/10, 20/60/20, 20/50/30 and 20/40/40. Vertical lines indicating the A15 related OH-stretch at 3461.1 cm^{-1} and the LOR related C=O-stretch at 1706.5 cm^{-1}.

The HME ASD formulations (Figure 12) showed comparable results to the SD formulations, in which the LOR-A15-SSB 55 (20/70/10) showed the marked decrease for the –OH stretch to 3446.2 cm^{-1} and decrease in (C=O) stretch to 1696.5 cm^{-1} indicating the intermolecular interaction. The formulations containing various ratios of LOR-A15-SSB 55 (20/75/5, 20/60/20 and 20/50/30) prepared through HME showed similar results to those produced by SD. In all, the results were suggestive of strong intermolecular interactions in LOR-A15-SSB 55 (20/70/10) compared to the formulations prepared with other ratios. Hence, this formulation was selected for further investigations.

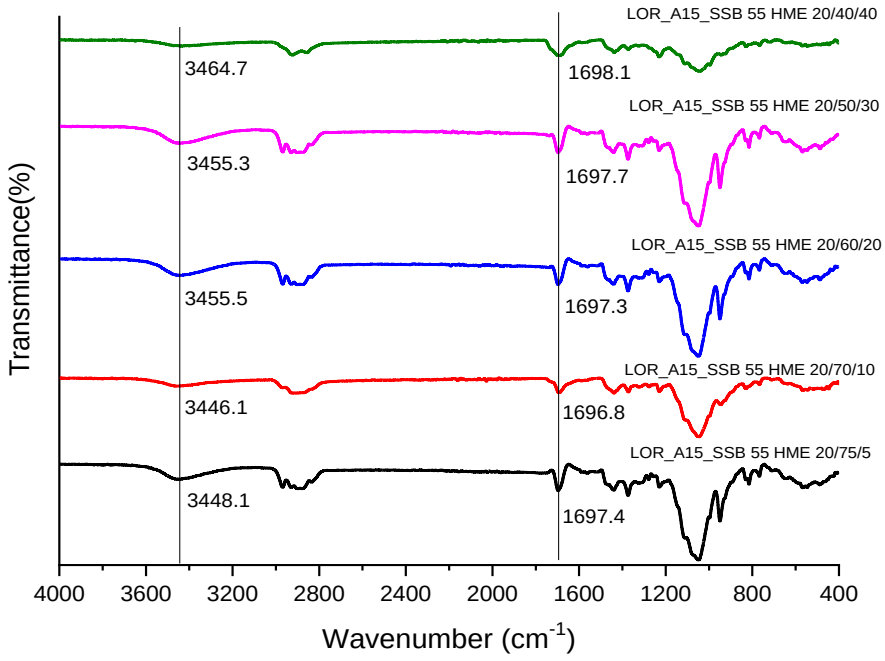

Figure 12: ATR-IR spectra of melt extruded ternary mixtures (bottom to top): LOR, A15, SSB 55 in ratios of 20/75/5, 20/70/10, 20/60/20, 20/50/30 and 20/40/40. Vertical lines indicating the A15 related OH-stretch at 3461.1 cm^{-1} and the LOR related C=O-stretch at 1706.5 cm^{-1}.

4.2.2.2 Non-sink dissolution studies of LOR ASDs formulation

a) Initial samples

i) pH 6.8

The dissolution studies performed for pure LOR (Figure 13) revealed that due to the basic character of LOR, only 2.6 % of the drug was dissolved after 180 min. The ASDs of binary mixtures of LOR-A15 had improved performance, with the SD formulation leading to 19.4 %, and the HME ASD accounting for 18.4 % LOR dissolution after 3 hours. The LOR/SSB 55 (20/80) ASDs showed drug release of 6.3 % and 5.7 % in case of SD and HME formulations, respectively. Ternary mixtures containing various amounts of LOR, A15 and SSB 55 ratios showed improved dissolution presented in Figure 13 A and B. LOR-A15-SSB 55 20/75/5 showed a slightly improved dissolution profile of 50.0 % in SD and 51.9 % in HME, respectively, in comparison to LOR. ASDs with LOR-A15-SSB 55 (20/70/10) showed higher supersaturation levels in relation to binary mixtures with a

higher dissolution profile in this ratio, where 76.7% of drug was dissolved. Concurringly, a peak shift in ATR-IR studies was observed. In contrast, the ratio of 20/40/40 only resulted in 12.5 % and 11.7 % of LOR dissolution for SD and HME formulations, respectively.

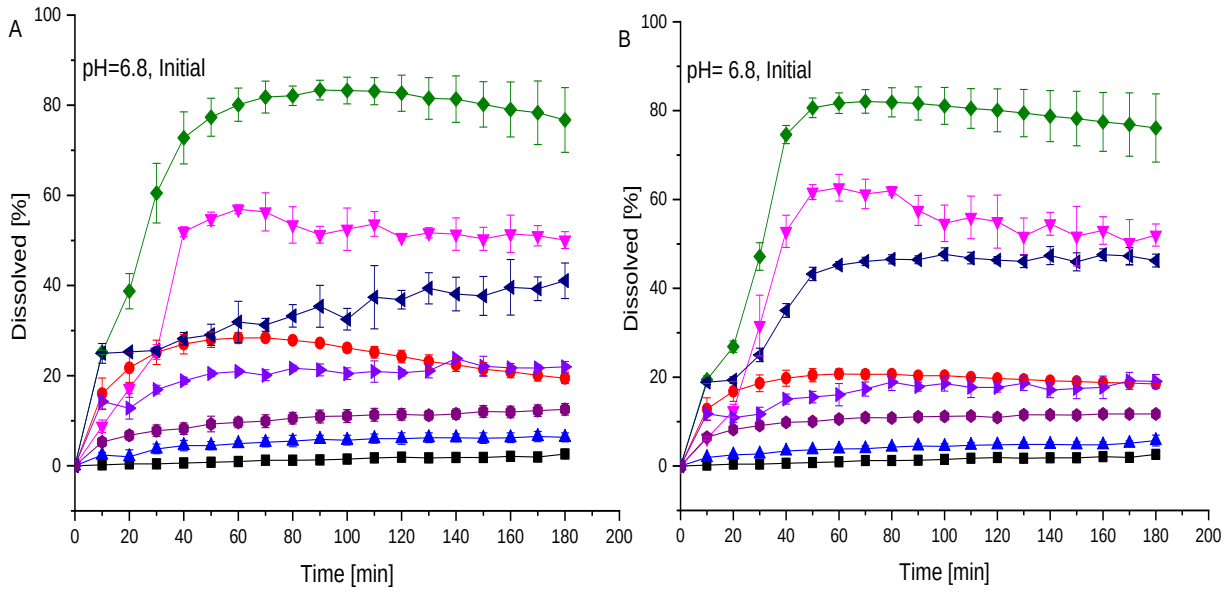

Figure 13: Non-sink dissolution (pH 6.8; 100 % = 40 µg/ml) of ■ pure LOR, binary ASDs: ● LOR- A15 20/80,▲ LOR- SSB 55 20/80, ternary ASDs: ▼LOR-A15-SSB 55 20/75/5, ◆20/70/10, ◀20/60/20, ▶20/50/30 and ⬢20/40/40 prepared through (A) SD and (B) HME

The other ratios with 20/60/20 resulted in a dissolved amount of LOR to 41 % for SD and 46.2 % in HME. The ASDs with the 20/50/30 ratio led to a LOR release of 21.9 % in SD and 19 % in HME. The order of dissolution rate enhancement was LOR-A15-SSB 55 20/70/10 > 20/75/5 > 20/60/20 > 20/50/30 > LOR - A15 20/80 > LOR-A15-SSB 55 20/40/40 > LOR-SSB 55 20/80. For easier dissolution performance comparison of the various ASDs, a solubility factor was calculated based on the LOR concentration at 180 min in relation to the crystalline neat LOR (Fig. 14). The solubility factor (SF) for the neat LOR was by definition 1.0 at pH 6.8. The A15 based binary ASD exhibited a SF of 7.0, whereas the one with SSB 55 had an SF of 2.0. In case of ternary mixtures, ASDs resulted in higher levels of solubility improvement. The ASDs with LOR/A15/SB 55 (20/70/10) resulted in the

overall highest SF of 30, implying 30-fold improvement in solubility compared to crystalline LOR. On the other hand, the other ratios of LOR/A15/SSB 55 (20/75/5) led to a SF of 17– 20. In case of LOR/A15/SSB 55 (20/50/30), however, the dissolved concentration at the final timepoint with SF 0.7 to 0.8 was comparable to a binary mixture of A15 ASDs. The ASDs comprising LOR/A15/SSB 55 (20/40/40) only provided an SF of 5.0 at pH 6.8.

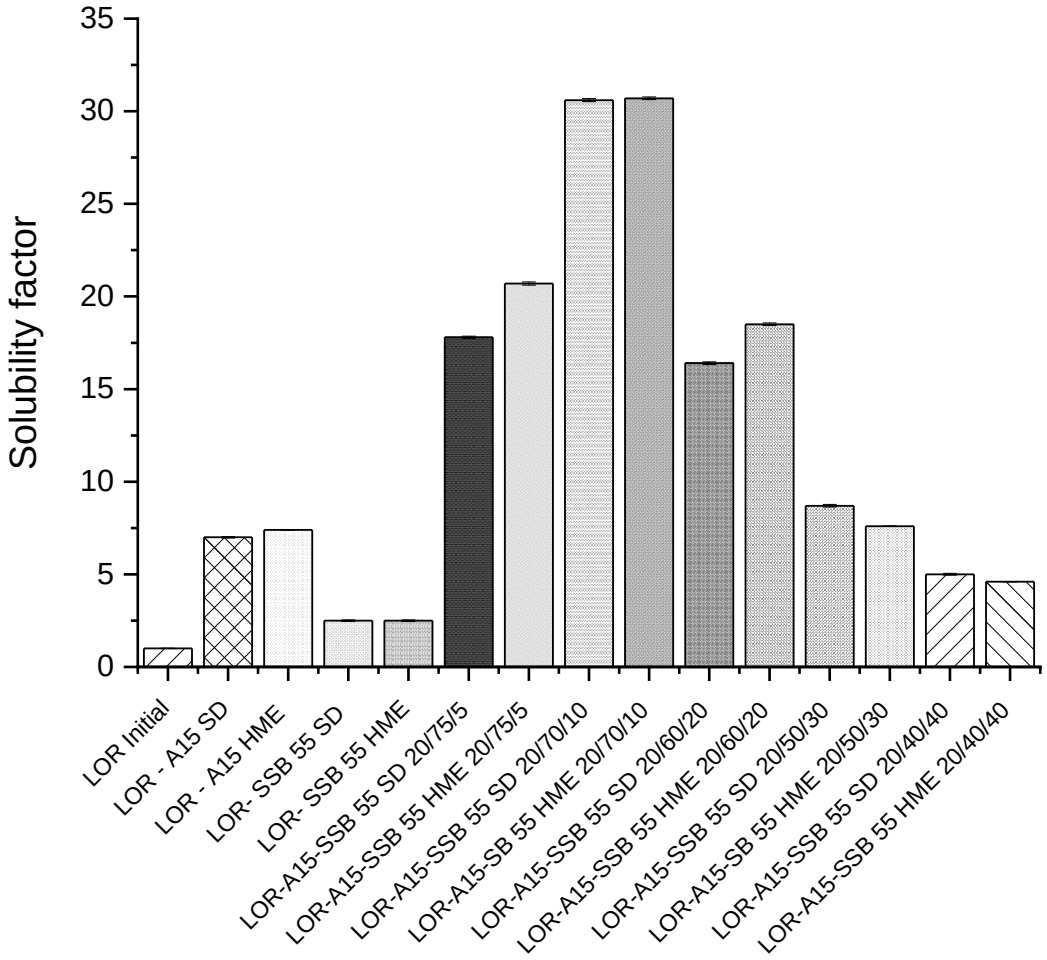

Figure 14: Solubility factors of pure LOR, LOR-A15 (20/80), LOR-SSB 55(20/80), LOR-A15-SSB 55 (20/75/5, 20/70/10, 20/60/20, 20/50/30, 20/40/40) prepared through SD and HME at pH 6.8

The presented results for the LOR ternary ASDs in (20/70/10) reveal the highest amount of LOR dissolution in case of this formulation when compared with all other ternary and binary ASDs. 10 % weight fraction of SSB 55 was hence the optimum ratio to enhance the solubility and supersaturation of LOR. It seems that A15 and SSB 55 act synergistically, the former being a hydrophilic polymer and the latter a more hydrophobic excipient

leading to increased shellac acids mobility within the A15 polymer. The observed synergistic effect in combination of an optimum at 10 % SSB 55 could arise from different phenomena i) improved miscibility of the ternary system with melting point depression of LOR [116] ii) the molecular level mixing of the ternary system during the manufacturing of SD and HME [105], [127]iii) intense peak broadening with shift to lower wavenumber indicating strong intermolecular interaction in this specific ratio confirmed by ATR-IR [52] iv) improved wetting properties of amorphous LOR dispersion that can be observed from the dissolution results[124] and v) maintenance of supersaturation and hindrance of LOR precipitation [18], [128].

Based on the dissolution studies and ATR-IR, it can be concluded that LOR/A15/SSB 55 (20/70/10) showed optimal dissolution performance in pH 6.8, and hence, the dissolution studies for stability tests were performed at this pH.

ii) pH 5.5

The neat LOR dissolution behavior was also examined at pH 5.5 and the results are depicted in Figure 15. As observed, about 5.21 % of the drug was dissolved after 180 min, which was slightly higher than in pH 6.8, due to pH-dependent solubility of the drug. The equilibrium solubility in this case was about 0.016 mg/ml. The binary ASDs containing LOR/A15 (20/80) prepared through SD dissolved 15 % of the incorporated LOR, while the HME counterparts led to 16 % LOR dissolution. On the contrary, the LOR/SSB 55 (20/80) only led to 5.8 % of drug dissolution, which might be due to lower solubility of SSB 55, making the drug release matrix dependent.

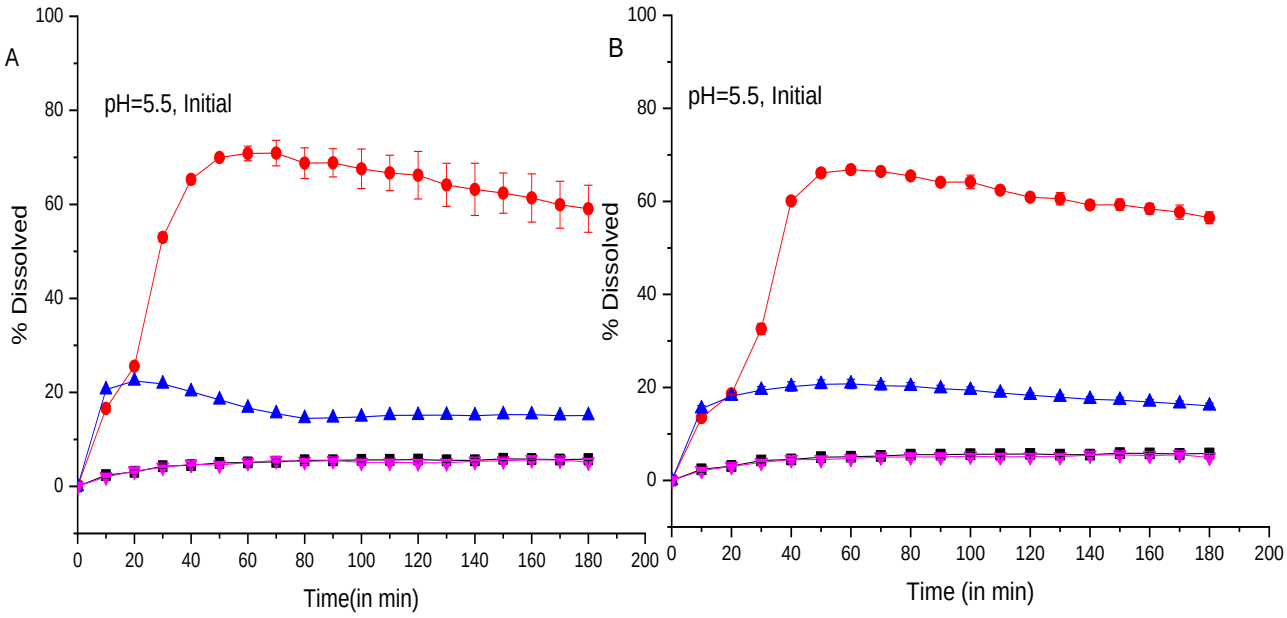

Figure 15: Non-sink dissolution (pH 5.5; 100 % = 40 µg/ml) of ■ pure LOR, binary ASDs: ▲ LOR- A15 20/80, ▼ LOR- SSB 55 20/80, ternary ASDs: ● LOR-A15-SSB 55 20/70/10 prepared through (A) SD and (B) HME

The ASDs from ternary mixtures with LOR/A15/SSB 55 (20/70/10) showed better drug dissolution profiles of 59.3 % (SD) and 56.5 % (HME). Nevertheless, LOR dissolution in these cases was less than at pH 6.8, which may be explained by the lower solubility of SSB 55 at pH 5.5, limiting the dissolution of the drug from ASD matrix (Figure 15 A and B).

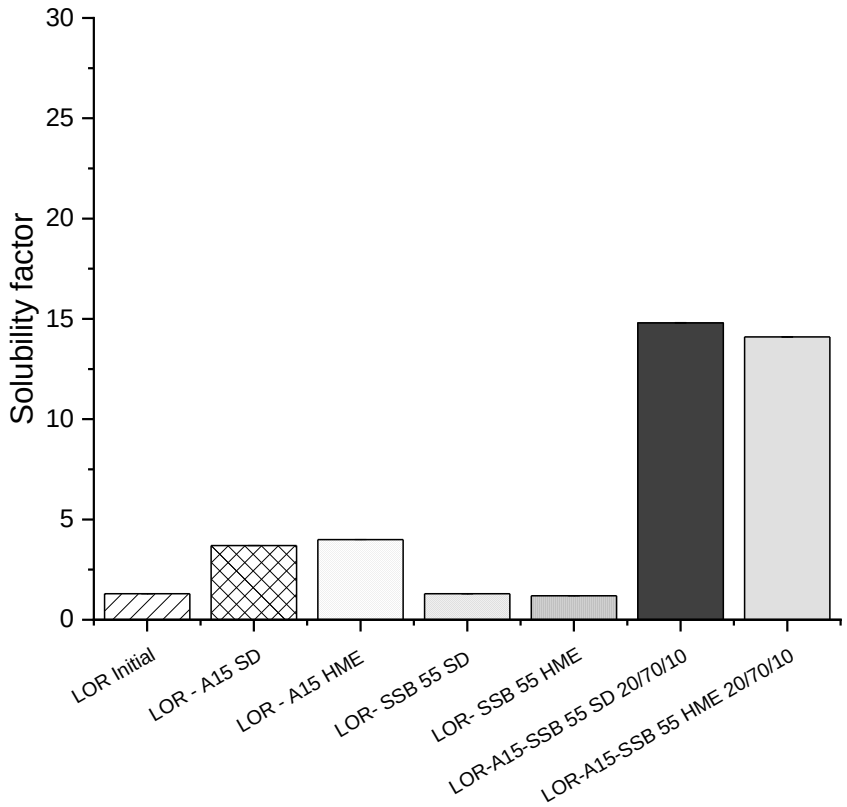

Figure 16: Solubility factor of pure LOR, LOR-A15 (20/80), LOR –SSB 55 (20/80) and LOR-A15-SSB 55 (20/70/10) prepared through SD and HME at pH 5.5

The solubility performance for ASDs in pH 5.5 was assessed as in terms of SF (Figure 16), assigning the pure LOR an SF of 1.3. The ASDs prepared with binary mixtures of LOR and A15 yielded an SF of 3.0 – 4.0, whereas those prepared with SSB 55 led to an SF of 1.0 similar to the pure drug. Once again, this could be associated with the slight solubility of SSB 55 at pH 5.5. However, in case the ASDs with LOR/A15/SB 55 (20/70/10) the observed SF of 14 implied 14 folds improvement in solubility compared to crystalline LOR. Thus, based on dissolution studies and ATR-IR, it was concluded that LOR/A15/SSB 55 (20/70/10) showed optimal dissolution performance in pH 6.8, and hence, the dissolution studies for stability tests were performed at this pH.

b) Stability samples

Storage: closed without desiccant

The HME and SD ASDs samples exposed to two storage conditions were evaluated for their individual stability and dissolution performance. Compared to the freshly prepared ASDs, the dissolution rate of LOR from the SD ASDs stored for 1 and 2 weeks at ambient conditions (25 °C /60 % RH, Figure 17A) dropped by 2 to 3 %. In case of 4-week storage, the rate of dissolution decreased to 68.2 % (drop of 8 %), highlighting the generation of microcrystals, as the dissolution profile does not drop to the level of pure LOR and the formulation still maintains supersaturation. Under accelerated conditions of 40 °C /75 % RH (Figure 17B) in snap cap vials, however, the dissolution was reduced by 2 and 6 % after 1- and 2-weeks storage, respectively. Following 4 weeks of storage, the LOR dissolution from the SD formulation decreased further to 66.9 % (drop of 10 %).

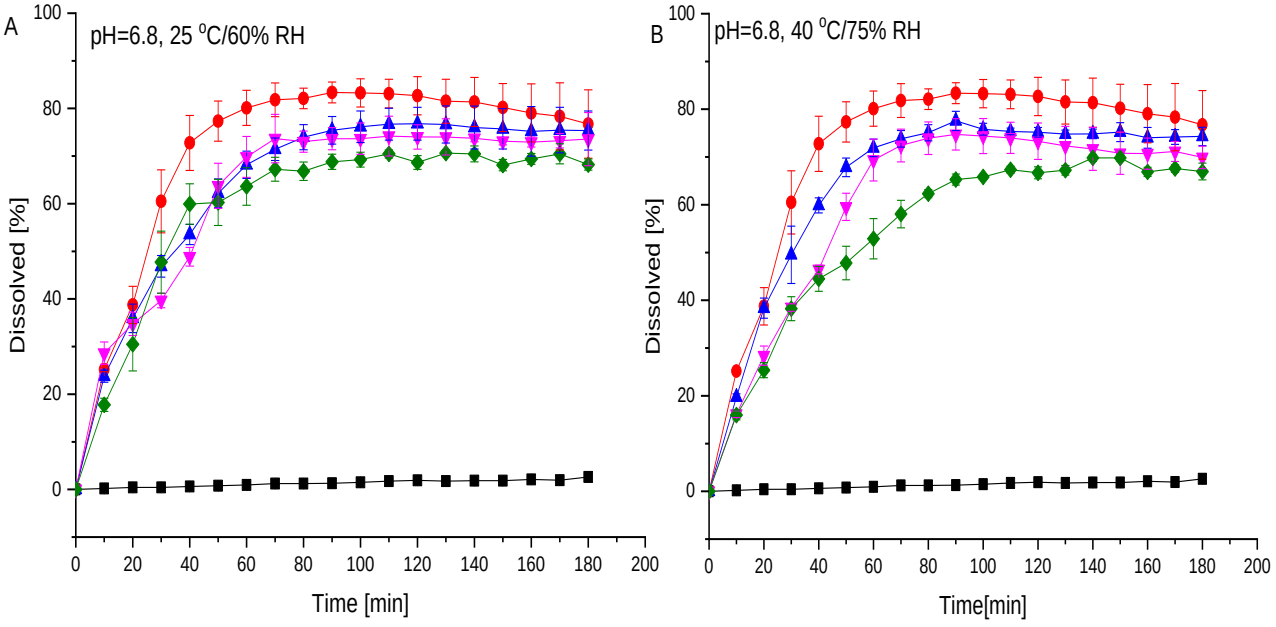

Figure 17: Non-sink dissolution (pH 6.8; 100 % = 40 µg/ml) of ■ pure LOR and ternary ASD

Initial: ● LOR- A15-SSB 55 20/70/10, 1 week: ▲ LOR- A15-SSB 55 20/70/10, 2 weeks:▼ LOR-A15-SSB 55 20/70/10, 4 weeks: ◆ LOR- A15-SSB 55 20/70/10 prepared through SD and stored in closed without desiccant at (A) 25 °C/60 % RH and (B) 40 °C/75 % RH

The dissolution behavior of HME-based formulations stored at 25 °C /60 % RH (Figure 18A) depicts a decrease in dissolution by 1 to 2 % compared with the initial formulation. Following 4 weeks of storage, the dissolution rate was reduced by 5 % indicating the formulation's ability to maintain supersaturation over this period of storage time. The ASDs stored at 40 °C /75 % (Figure 18B) for 1 and 2 weeks showed a slight decrease in dissolution rate by 3 to 4 %. Upon storage for 4 weeks, however, the rate and extent of dissolution dropped to 68.9 %.

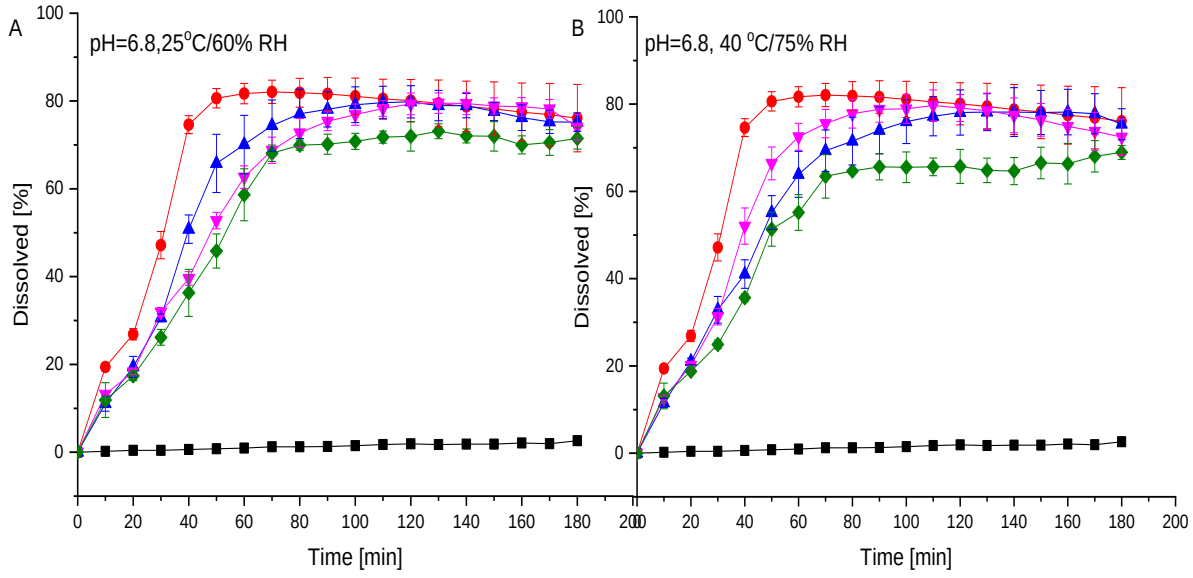

Figure 18: Non-sink dissolution (pH 6.8; 100 % = 40 µg/ml) of ■ pure LOR and ternary ASD

Initial: ● LOR- A15-SSB 55 20/70/10, 1 week: ▲ LOR- A15-SSB 55 20/70/10, 2 weeks:▼ LOR-A15-SSB 55 20/70/10, 4 weeks: ◆ LOR- A15-SSB 55 20/70/10 prepared through HME and stored in closed without desiccant at (A) 25 °C/60 % RH and (B) 40 °C/75 % RH

Storage: closed with desiccant

The ternary ASDs (LOR- A15-SSB 55 20/70/10) of optimum dissolution performance were stored under closed conditions with desiccant (Activ® vials) at accelerated conditions (40 °C /75 %) for 4 weeks in order to eliminate exposure to moisture and remove the remaining moisture available in the gas phase. The SD samples stored in this way (Figure

19A) showed decreased dissolution of 5 % compared to the initial sample, while the amount dissolved after 180 min decreased only by 2 % for the HME samples (Figure 19B). Despite of the dissolution end point after 180 min, the storage related ageing at 40 °C led to a decrease in dissolution rate and C_{max} values.

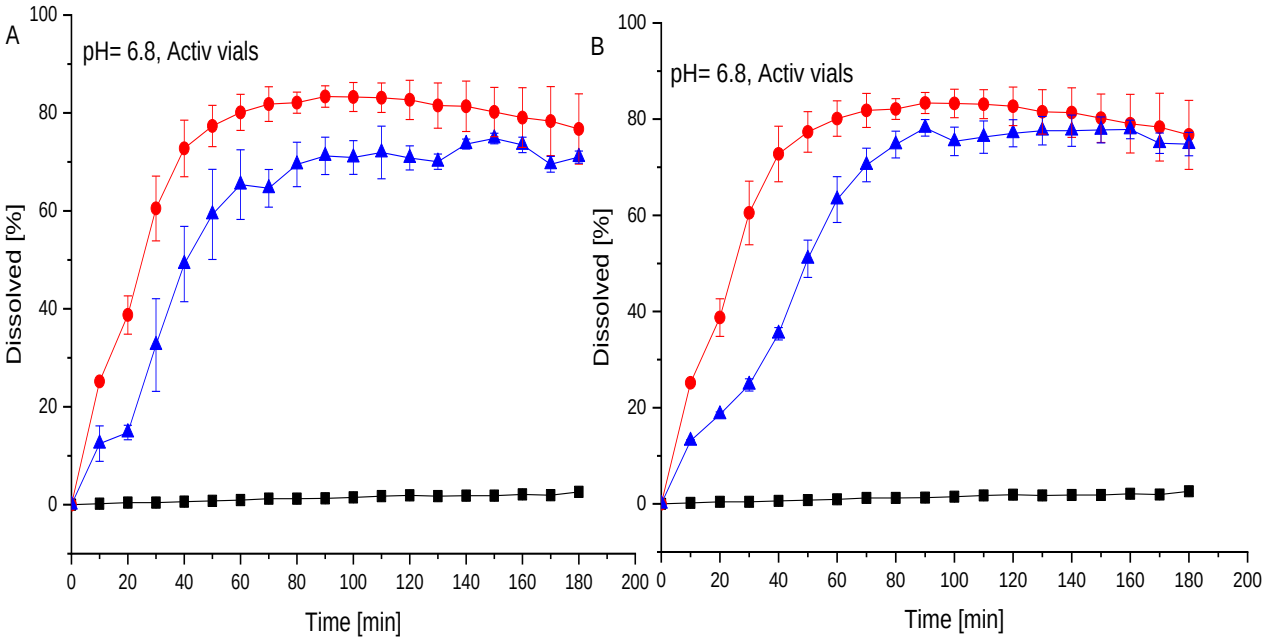

Figure 19: Non-sink dissolution (pH 6.8; 100 % = 40 µg/ml) of ■ pure LOR and ternary ASD

Initial:● LOR- A15-SSB 55 20/70/10, 4 weeks: ▲ LOR- A15-SSB 55 20/70/10 prepared through (A) SD and (B) HME stored closed with desiccant (Activ® vials) at 40 °C/75 % RH

Notwithstanding the differences between SD and HME, similar chemical interactions occur in both techniques, which leads to an improved dissolution profile. The higher intermolecular interaction among the components when used in such proportion was potentially responsible for the improved dissolution of these formulations compared to other ternary and binary ASDs. The SSB 55 contains a carboxylic acid group with high pKa, which is responsible for its complete dissolution at pH 7.4. To achieve the desired dissolution at pH 6.8, mixing SSB 55 with at least one hydrophilic excipient was necessary. However, the low fraction of SSB 55 (10 % w/w) within these formulations allowed for its

maximum interaction with A15 and LOR, enabling the amorphous matrix to dissolve completely compared with other ternary ratios and was confirmed with AT-IR results. Thus, in ternary systems prepared with proportion of the components (20/70/10), both A15 and SSB 55 acted synergistically to achieve a higher amount of dissolved drug through the maintenance of supersaturation until the endpoint.

c) Crystallinity dependent drug release

The origin of crystallinity was either the recrystallization during storage or the remaining LOR crystals from temperature dependent incomplete dissolution of drug in the polymeric matrix during ASD processing in HME at temperatures below 105 °C (Tab. 7). The extruded samples were tested on remaining crystallinity (undissolved API in the matrix) immediately after extrusion through XRPD analysis and subsequently tested for dissolution at pH 6.8 shown in Figure 20. As suspected, the dissolution performance was dependent on crystallinity. Regardless of origin of the crystals, higher crystallinity in the formulation accounted for the lower amount of LOR dissolved at 180 min (Fig. 20A). Upon storage, ASDs prepared by SD and HME showed decrease drug release with increasing crystallinity. The crystallinity of 3.1 to 3.5 % led to dissolved amounts of 66 to 68 % irrespective on the ASD's manufacturing process and were comparable to samples processed via HME at 80 °C, in which drug release was 66.9 %. The overall dependence of dissolved LOR after 180 min upon crystallinity showed a sigmoidal curve. Remarkably, the dependence of released LOR at end of the dissolution test in the range of 2.1 and 3.5 % was quite linear (R^2 = 0,861) as shown in (Fig. 20B)

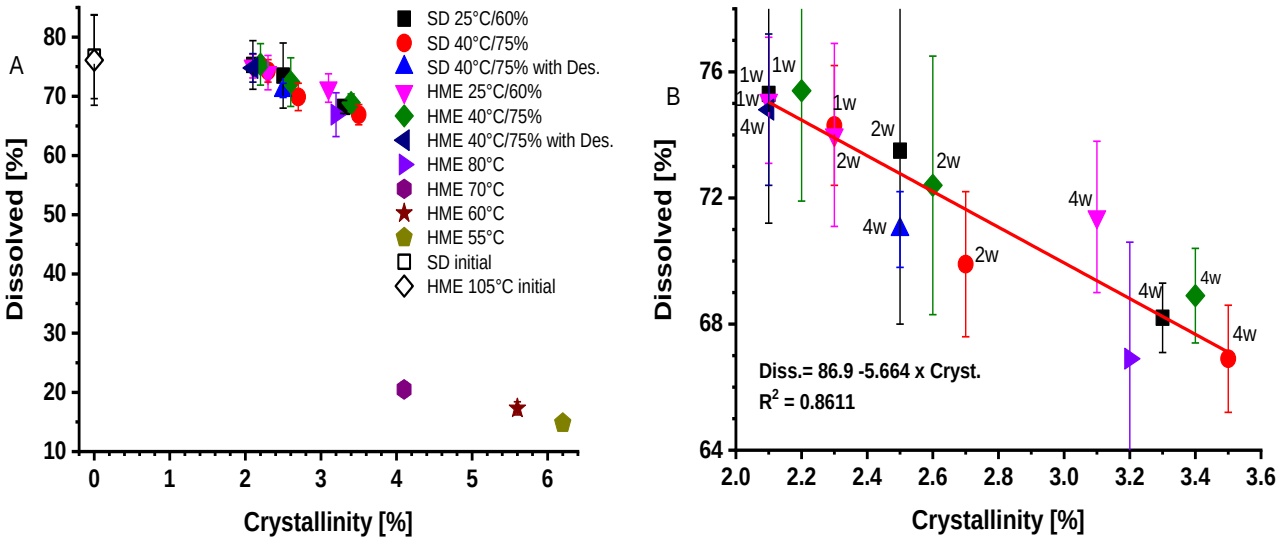

Figure 20: Non-sink dissolution (pH 6.8; 100 % = 40 µg/ml) after 180 min dependent on the remaining crystallinity. Crystallinity was induced via storage of SD and HME ASDs via closed storage at 25 °C/60 % RH and 40 °C/75 % RH (with and without desiccant) or via HME at lower processing temperatures (Tab.14).
A: all data points
B: zoom 2.1 – 3.5 % crystallinity

Below 2.1 %, no crystallinity could be detected [129], [130] and the drug release after 180 min was 76.7 and 76. 1 % for SD and HME ASDs, respectively. Above crystallinity values of 3.5 %, the dissolution dropped severely to 20.5 % at 4.1 % crystallinity and further down to 14.8 % release at 6.2 % crystallinity.

4.3 Conclusion

The findings of the current work demonstrated that preparation of LOR ASDs with shellac (SSB 55) and HPMC (A15) in an optimal ratio (LOR-A15-SSB 55 20/70/10) could result in a good control of the supersaturation, and improved dissolution behavior. This synergistic effect occurred as a result of intense intermolecular interactions as qualitatively confirmed by ATR-IR and further supported by DSC and dissolution studies as well as the findings of Baghel et al. [105]. When stored under closed conditions with desiccant (Activ® vials), HME ASDs showed better stability compared to those prepared through SD. This might be due to the less absorption of moisture compared to SD, and the lower amount of solvent involved in HME. Investigation of the samples following storage under various conditions revealed a decrease in the dissolution rate and the overall drug release caused by the generation of small microcrystals of precipitated drug in the ASDs. This recrystallization process, as confirmed by the DSC and Karl Fischer analyses, was mainly influenced by storage temperature and to lower degree by the samples' water content. Unfortunately, the ternary mixtures of LOR/A15/SSB55 were not completely stable independent from the manufacturing process, and recrystallization of amorphous LOR occurred even at 25 °C under closed conditions. The ASDs crystallinity governed the drug release and degree of supersaturation. Up to a crystallinity of 3.5 %, the amount released at the end of the dissolution test decreased linearly. Exceeding the 3.5 % crystallinity value, the drug release decreased severely and a sigmoidal correlation between the drug release and crystallinity could be observed. However, with the successful implementation of shellac within ternary ASDs for the improvement of the solubility of LOR, it will be interesting to see whether such a synergistic effect can be obtained for combinations of Shellac with other drugs and polymeric matrices resulting in stable ASDs.

4.4 Summary of the chapter

The use of shellac for preparing binary and ternary ASDs of shellac, alone or in combination with HPMC, with the model API loratadine (LOR) via spray drying and hot melt extrusion helped to achieve solubility improvement and supersaturation maintenance. It was observed that among various shellac fractions within the ternary ASDs, the 10 % weight fraction was found to increase the solubility 30 folds and maintain the supersaturation for 3 h compared to other binary and ternary formulations. This superiority was due to specific and stronger API matrix interactions detected via ATR-IR, which was further studied in terms of stability. It was found that there exists a correlation between the amount of the dissolved API and the API crystallinity, which dictates the level of supersaturation. While the crystallinity is set by the LOR concentration at the end of the test, the dissolution rate depended on the origin of the crystals. Thus, the use of shellac will add to the understanding of ternary mixture development with application of solubility improvement and supersaturation maintenance.

5. *Shellac- a natural carrier for colon targeting of indomethacin using Hot melt extrusion*

5.1 Introduction

Colon cancer is the third most common type of malignant neoplasm worldwide, the fourth-largest cause of death related to cancer, and the main cause of gastrointestinal cancer[131]. These necessities focus on investing in drug discovery and the development of new anticancer substances. Despite the pharmaceutical industry is in search of new chemical entities that can be potential new anticancer drugs[132], another approach is the repositioning of the existing approved non-anticancer drug for their anticancer activity. Repositioning is becoming popular as it involves less investment compared to a new drug discovery cycle. The main challenge is the frequent lack of suitable physicochemical properties of the drugs, which is the limiting step in new anticancer drug development [133]. One of these candidates is indomethacin. Indomethacin is indicated for the treatment of moderate to severe rheumatoid arthritis and acute gouty arthritis; it has been approved by the United States Food and Drug Administration (FDA) in 1965 and is a non-selective COX 2 inhibitor. Zhang and Wang reported that indomethacin significantly decreased viability of cultured HCT116 cells and that the active pharmaceutical ingredient (API) is also able to retard human colorectal HCT116 cell tumor growth via inhibiting tumor angiogenesis, which might be through reduction of VEGF expression [128]. Indomethacin has been also reported as anti-tumor agent for the treatment of later stages of colorectal carcinogenesis in humans. In a randomized, placebo-controlled trial of indomethacin (50 mg twice daily) or prednisolone (10 mg twice daily) in patients with disseminated solid malignancy (CRC 22% cases, liver/pancreatic cancer 33% cases), indomethacin prolonged mean survival from 250 ± 28 days to 510 ± 28 days ($p < 0:05$) compared with placebo [87], [129]. However, the main hurdle for effective drug delivery to targeted the colon is to protect the drug from dissolving at lower pH < 6.8. This problem needs to be addressed using a strategy that will improve delivery to achieve a maximized therapeutic effect. There are different strategies to target the colonic site i.e. prodrugs [102], pH-sensitive polymers for the coating of drug-loaded pellets[136], compression coating using guar gums[137], electrospun nanofibers [138] as well as, Hot melt extrusion[139]. Hot-melt extrusion

(HME) has attracted a lot of attention in the past few years due to the increasing number of pharmaceutical product approvals from the FDA [134]. HME enables the formation of solid dispersions (SDD). Especially, a single phasic amorphous solid dispersion (ASD) as a special case of SDD was reported to be useful for pH protection, solubility improvement with the ability of supersaturation maintenance making it advantageous for targeted delivery application [77].

There are several ways to target the colon, for example, by the use of a pro-drug which will be metabolized by active compound of colonic bacteria to release the active compound. In this case the prodrug is embedded drug in a biodegradable matrix [135]. The simplest approach, however, is to use a polymer possessing pH-dependent solubility and which enables the release of the drug substance at the respective targeted site [136]. The delivery of class II drugs in the colon remains challenging due to the low colonic fluid volume and higher viscosity of luminal content leading to reduced drug absorption and mucosal absorption [137]. An interesting approach might be to prepare solubility enhanced solid dispersion using pH-dependent soluble matrix polymers via e.g., hot-melt extrusion, A potential excipient candidate facilitating pH-dependent dissolution is Shellac, which is obtained from an animal source and is a GRAS listed natural carrier [103]. It is not a polymer but a mixture of different organic acids like aleuritic acid, jalaric acid, shellolic acid, and laksholic acid [101]. It has a molecular weight of about 1006 g/mole, dissolves at pH 7.0, and is completely soluble at pH 7.4; its low glass transition temperature and low melt viscosity make Shellac an interesting additive for HME [102], [104]. Thus, to achieve improved processability during extrusion shellac needs to be mix with suitable hydrophilic polymer to tailor a desired release profile. Within this context we sought to investigate the use of a new grade of HPMC with a molecular weight of 84,400 g/mol making it one potential choice for this purpose, as it is having a low glass transition temperature, low melt viscosity and low hygroscopicity compared to other available grades of HPMC, which often require plasticizers for HME [5],[102]. Another interesting excipient candidate is the pH-dependent soluble Polymer Eudragit FS 100 (EFS). EFS is an anionic copolymer of methyl acrylate, methyl methacrylate, and methacrylic acid, which is available in solid form. It is soluble at pH 7.0 and above exhibits low glass transition temperature without the need of plasticization for HME processing [133],[135]. Apart from its enteric property,

it is applicable for solubility enhancement of poorly soluble drugs at pH > 7[144]. Thus, it is an interesting polymer candidate to prepare solid dispersions in combination with pH-dependent colon drug targeting.

Indomethacin (IND) is a weak acid belonging to BCS II with pH-dependent solubility 1.51 µg/ml at pH 1.2[136], 42.6 µg/ml at pH 5.5 and 388.5 µg/ml at pH 6.8 [96] as equilibrium solubility. It has been reported that the orally administered IND shows dose-dependent systemic and upper gastrointestinal tract side-effects [140]. Thus, there is a need to overcome this GIT side-effect using a formulation having no release in the upper GIT tract and controlled release of the formulation at the colonic site leading to an effective therapeutic concentration. A pH-dependent targeting approach would hence improve drug safety and efficacy. Asghar et. al prepared controlled release formulations of indomethacin for colon specific delivery using Eudragit L100 and S100 in matrix-based tablets using xanthan gum. They prepared the directly compressible extended-release matrix tablets and found the negligible release of IND in acidic media pH 1.1 for 2 hours; with pH shift to 7.4, the extended release of indomethacin started for a period of 14 to 16 hours controlled by erosion [139]. The objective of the present study was firstly to assess the feasibility of shellac as a matrix polymer in SDD preparation and to, test subsequently its gastric protective effect against pH shift during dissolution alone, and in combination with a pH-independent soluble HPMC polymer grade of low molecular weight for the generation of a delayed-release formulation. Furthermore, the impact of the crystallinity of the SDD on the dissolution kinetics was assessed. As a comparison to the pH-dependent soluble excipient Shellac, Eudragit FS as a pH-dependent soluble polymethacrylate has been chosen. SDD of IND were prepared using HME, characterized for their solid-state properties and stability upon storage. The present study will add to the understanding and application of shellac for colon targeting via HME. Thus, it will help to extend the existing set of synthetic polymers for SDD manufacturing using HME and colon targeting for various drugs.

5.2 Results and discussion

5.2.1 DSC (Glass transition temperature)

The neat IND showed a melting endotherm at 160.3 °C indicating the identity and purity of the compound with the reported values in the literature [145] with an observed glass transition temperature (Tg) of 45.1 °C. Table 9 presents the glass transition temperatures of the pure substances, binary and ternary mixtures. The binary mixtures and ternary mixtures of SDDwere showing single glass transition temperatures indicating a homogenous amorphous dispersion of IND into the polymer matrix with confirmation of molecular interaction due to monophasic ASDs formation. The Tg of binary SDD on storage at 40 °C (closed with desiccant) increased from 2 to 6 °C upon 4 weeks storage, while for ternary ASDs the Tg increased from 3 to 5 °C. This higher Tg was likely due to slight microcrystal formation at the elevated temperature leading to the aging of SDD as there was no additional melting endotherm detected.

Table 9: Glass transition temperatures of neat IND, polymers, and SDD prepared by HME

Composition of the mixture	Glass transition temperature [°C]			
		40 °C /75 % RH		
	Initial	1 week	2 weeks	4 weeks
IND	45.1 ± 0.2	--	--	--
SSB 55	36.9 ± 0.2	--	--	--
EFS	50.8 ± 0.3	--	--	--
A15	96.8 ± 0.04	--	--	--
IND – SSB 55 HME (20/80)	38.3 ± 1.3	41.4 ± 0.06	42.7 ± 1.1	45.3 ± 0.2
IND – EFS HME (20/80)	36.9 ± 1.2	42.5 ± 1.1	42.1 ± 0.04	43.1 ± 0.3
IND – A15 HME (20/80)	53.3 ± 1.2	57.0 ± 1.1	58.8 ± 0.9	59.9 ± 0.5
IND – SSB 55 – A15 (20/70/10)	43.0 ± 0.1	46.8 ± 0.4	48.1 ± 0.7	48.2 ± 0.1

5.2.2 Powder *X-ray* diffraction

a) Initial

The XRPD results are presented in Figure 21 (A) shows that IND neat is having a crystalline nature with distinct peaks at various 2θ angle. The neat A15, SSB 55, and EFS were showing a broad halo pattern indicating that they are amorphous. The physical mixture of IND-SSB 55, IND-EFS, IND-A15, and IND-SSB 55-A15 showed peaks related to the crystalline neat IND at reduced intensity. In contrast to the DSC measurements, XRPD showed some crystalline structures of about 3.0 % for the binary SDD of IND-SSB 55 prepared by HME shown in Figure 21 (B). All other SDD IND-EFS, IND-A15, and IND-SSB 55-A15 exhibited halo patterns with humps indicating complete conversion of crystalline IND into the amorphous form. Thus, these results confirm that the SDD exist in amorphous nature except for IND-SSB 55 occurring in partially crystalline form. This finding was in partial contradiction to the results obtained by DSC, where higher Tg upon storage has been found, however, no melting endotherm of crystalline IND. This was likely due to the redissolution of the proposed microcrystals during the Tg-assay at the slow heat rate of 2 K/min.

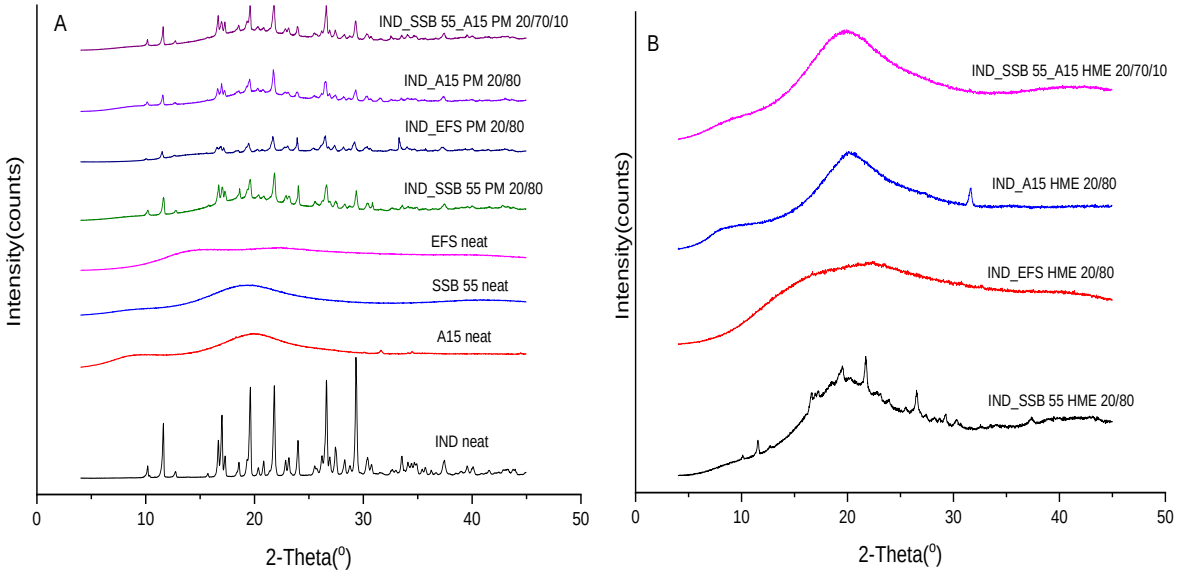

Figure 21: (A) XRD patterns for single components, binary and ternary mixtures (bottom to top): IND neat, A15 neat, SSB 55 neat, EFS 100 neat, IND-SSB 55 PM 20/80, IND- EFS PM 20/80, IND- A15 PM 20/80, IND- SSB 55-A15 PM 20/70/10. (B) Hot melt extrudates (bottom to top): IND- SSB 55 HME 20/80, IND-EFS HME 20/80, IND-A15 HME 20/80 and IND-SSB 55-A15 HME 20/70/10.

b) Stability

The XRPD data presented in Figure 22 depict the HME sample stored at accelerated condition of 40 °C/ 75 % RH for 1, 2, and 4 weeks under closed conditions with desiccant. IND-SSB 55 HME showed an increase in crystallinity from 4.9 % (one week) to 5.7 % (four weeks) when stored at accelerated conditions Figure 22(A). For IND-EFS samples the onset of occurrence of crystallinity is delayed compared to IND-SSB 55. The samples showed a halo pattern until week one but, after two and four weeks of exposure to the elevated temperature, the crystallinity increased to 2.5 % after 2 weeks and remained at this level up to week four. A15 HME samples Figure 22(B) showed no diffraction peaks for the entire storage period of four weeks. Lastly, in the case of IND-SSB 55-A15 slight amounts of crystallinity 2.2 % (one week) were detected which increased gradually to 3.1 % (four weeks) indicating a slight crystallization tendency compared to the initial 0 % crystallinity of the ASD.

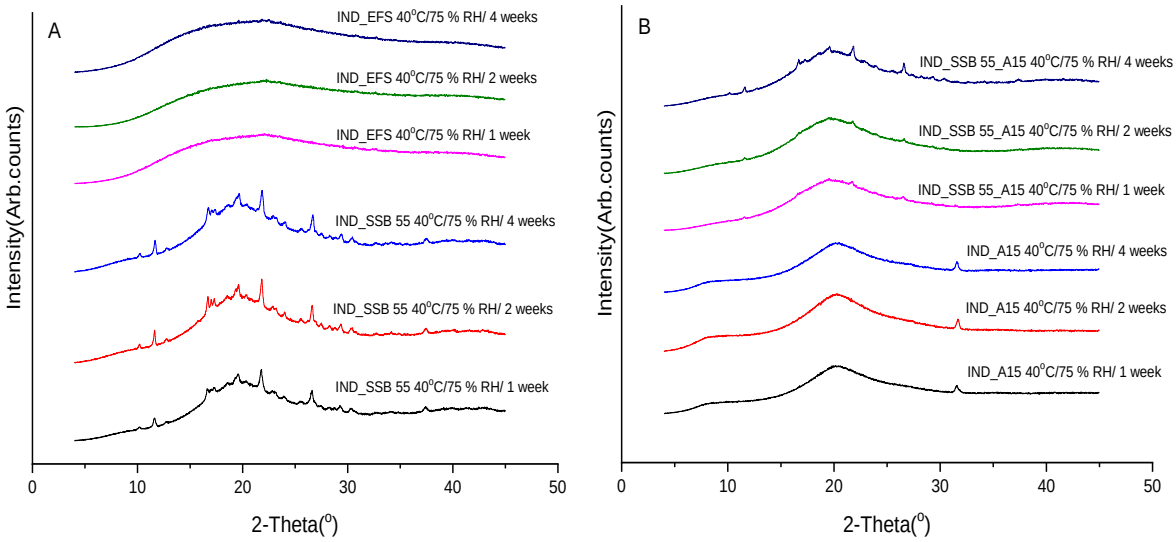

Figure 22: (A) XRPD pattern of IND-SSB 55 HME (20/80) and IND-EFS (20/80) (bottom to top): stored at 40 °C/75 % RH for 1 week, 2 weeks, and 4 weeks using Activ® vials (closed with desiccant).

(B) IND-A15 HME 20/80 and IND-SSB 55-A15 HME 20/70/10 (bottom to top): stored at 40 °C/75 % RH for 1 week, 2 weeks, and 4 weeks.

5.2.3 ATR-IR

Figure 23 represents the overlay of ATR spectra of neat samples of polymers and IND. IND exhibits two different C=O groups due to carboxylic acid and the benzoyl functional groups showing two carbonyl stretches. IND neat showed vibration of two C=O groups in which benzoyl group vibration was observed at 1690.2 cm^{-1} while the other observed band was at 1712.4 cm^{-1}. This band was attributed to the asymmetric stretch of the carboxylic acid C=O bond, which is characteristic for the cyclic dimer of the γ-form (1712.2 cm^{-1}) [60], [88]. The infrared spectrum of A15 exhibited a strong characteristic vibration band at 1045.5 cm^{-1} due to an alkyl substituted cyclic ring containing ether linkages. A peak at 3461.1 cm^{-1} is due to the presence of a hydroxyl group (-OH stretching). SSB 55 showed a prominent peak at 1706.1 cm^{-1} corresponding to C=O stretching of an ester group, while the -OH stretch of the hydroxyl group was observed at 3397.2 cm^{-1}. EFS showed a sharp peak at 1725.4 cm^{-1} which is attributed to the C=O group that has been esterified during synthesis.

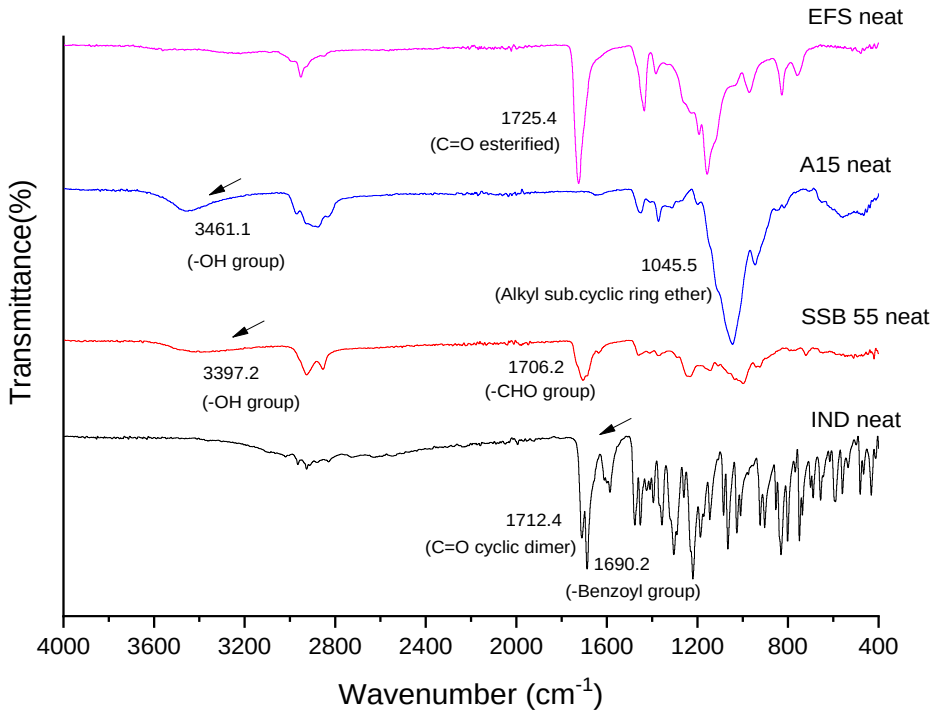

Figure 23: AT-IR spectra of single components (bottom to top): IND, SSB 55, A15, and EFS neat samples. Arrows indicate the A15 related OH-stretch at 3461.1 cm^{-1}, SSB 55 related OH-stretch at 3397.2 cm^{-1}, and the IND related C=O-stretch at 1712.4 cm^{-1}.

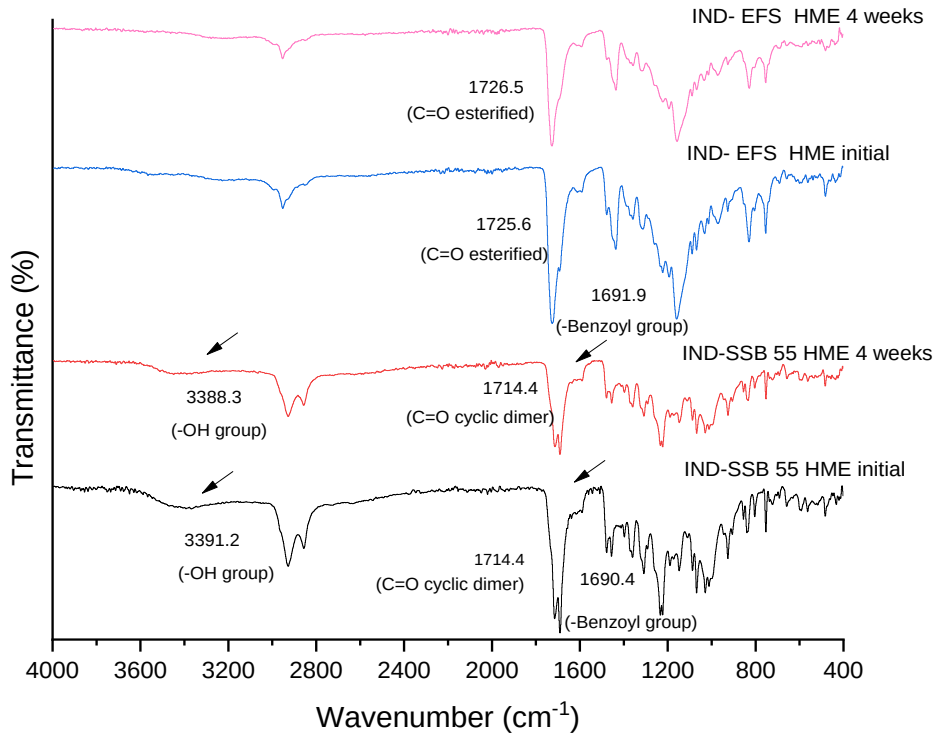

Figure 24: ATR-IR spectra of hot melt extrudates binary ASDs (bottom to top): IND-SSB 55 HME 20/80 initial, stored at 40 °C/75 % RH for 4 weeks and IND-EFS HME 20/80 initial, stored at 40 °C/75 % RH for 4 weeks. Arrow indicate the SSB 55 related OH-stretch at 3397.2 cm^{-1} and the IND related C=O-stretch at 1712.4 cm^{-1}.

Figure 24 indicates that the -OH stretch of SSB 55 was not effected within the ASDs, implying no intermolecular interaction at this site. The SDs stored at the accelerated condition of 40 °C/75 % RH for 4 weeks show that the -OH stretch of IND-SSB 55 was not affected irrespective of the storage condition for 4 weeks. IND-EFS HME showed the absence of the cyclic dimer group in comparison to IND neat and was not affected even after the storage period of 4 weeks.

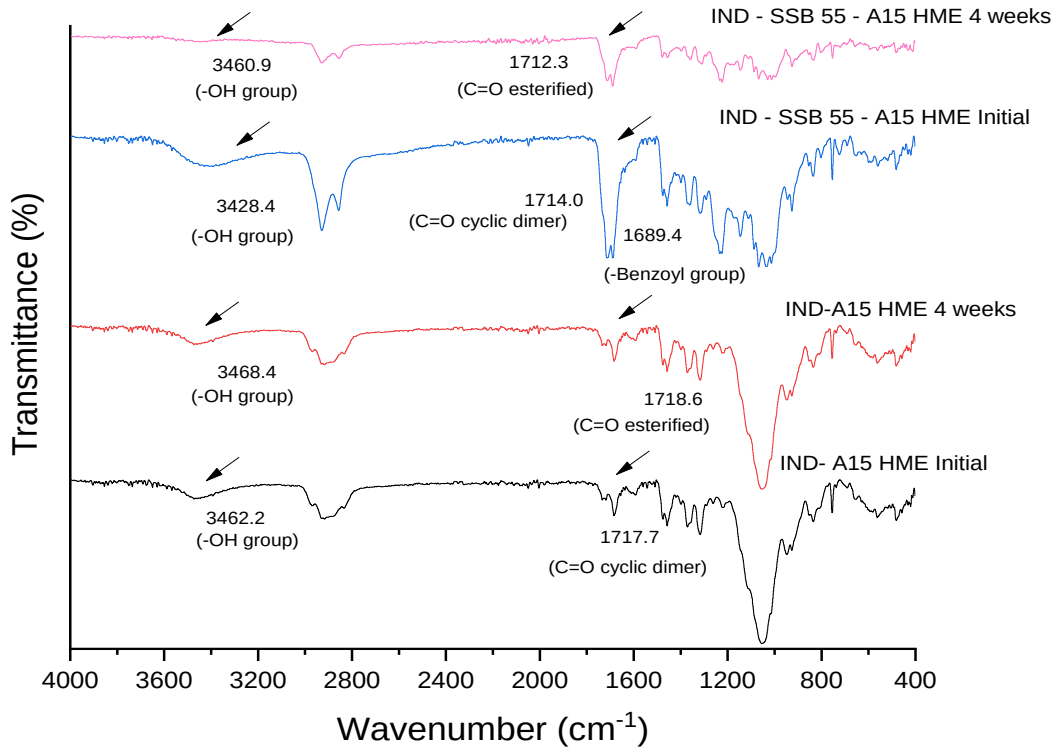

Figure 25: ATR-IR spectra of hot melt extrudates of binary and ternary ASDs (bottom to top): IND-A15 HME 20/80 and IND-SSB 55-A15 HME 20/70/10 initial and stored at 40 °C/75% RH for 4 weeks. Arrows indicates the A15 related OH-stretch at 3461.1 cm^{-1}, SSB 55 related OH-stretch at 3397.2 cm^{-1}, and the IND related C=O-stretch at 1712.4 cm^{-1}

In Figure 25, AT-IR spectra for IND- A15 HME showed the shift of the C=O group of the cyclic dimers to a higher wavenumber. Stored samples implied a slight increase in IR frequency from 3462.2 to 3468.4 cm^{-1}. While in ternary systems, IND-SSB 55-A15 HME showed a shift of the -OH group to a lower wavenumber indicating higher intermolecular interaction. But the samples of IND-SSB 55-A15 HME after 4 weeks storage had a pronounced effect of temperature and moisture leading to a significant decrease in the peak intensity as well as an increase in the IR frequency from 3428.4 to 3460.9 cm^{-1} which is indicative of weaker intermolecular hydrogen bonding interactions [44], [148] that might affect the solid-state property of the SDs.

5.3 Non-sink Dissolution studies of IND ASDs formulations

a) Initial (pH shift)

The dissolution studies performed for neat IND (Figure 26) showed that the weak acid IND which is almost insoluble at pH 1.1 (1.68 µg/ml) dissolved fast without embedding in a pH-dependent soluble matrix at pH 5.5 (38.71 µg/ml) and 6.8 (59.40 µg/ml) resulting in an almost 66.9 % drug release after 240 min already at pH 6.8 hence, most of the drug would have been released before reaching the target site. After the pH shift to 7.4 80.5 % (71.48 µg/ml) got dissolved. The SDs of the binary mixtures of IND-A15 (20/80) showed dissolution of 18 % at pH 1.1 and with a change to pH 5.5 almost 87 % were dissolved; the complete dissolution of IND (98 %) occurred already at pH 6.8, which might limit the targeting effect to the colonic site. The IND-SSB 55 (20/80) as well as IND-EFS (20/80) were able to protect IND against dissolution at pH values below 7.4 to an extent of 27.5 and 36.6 % respectively. The partially crystalline SDD out of IND-SSB 55 even showed a higher level of pH-protection compared to the fully amorphous ASD made with IND-EFS at pH 5.5. As IND crystalline solubility is not limiting at higher pH values.

For IND-SSB 55-A15 (20/70/10) SDs the amount dissolved at pH 5.5 was 20.1 % however after pH shift to 6.8 dissolution increased to 59,8 % compared to binary mixtures (30 to 38 %) The pH shift to 7.4 led to a complete dissolution of IND (99.9 %). Thus, IND-SSB 55-A15 (20/70/10) showed improved protection at pH < 6.8 compared to the binary mixtures, which was attributed to its increased wetting property and intense intermolecular interaction, which was confirmed by the AT-IR results. However, the dissolution performance was compromised by a higher release (~60 %) at pH 6.8. Nonetheless, leaving at least 40 % for dissolution directly at the target site.

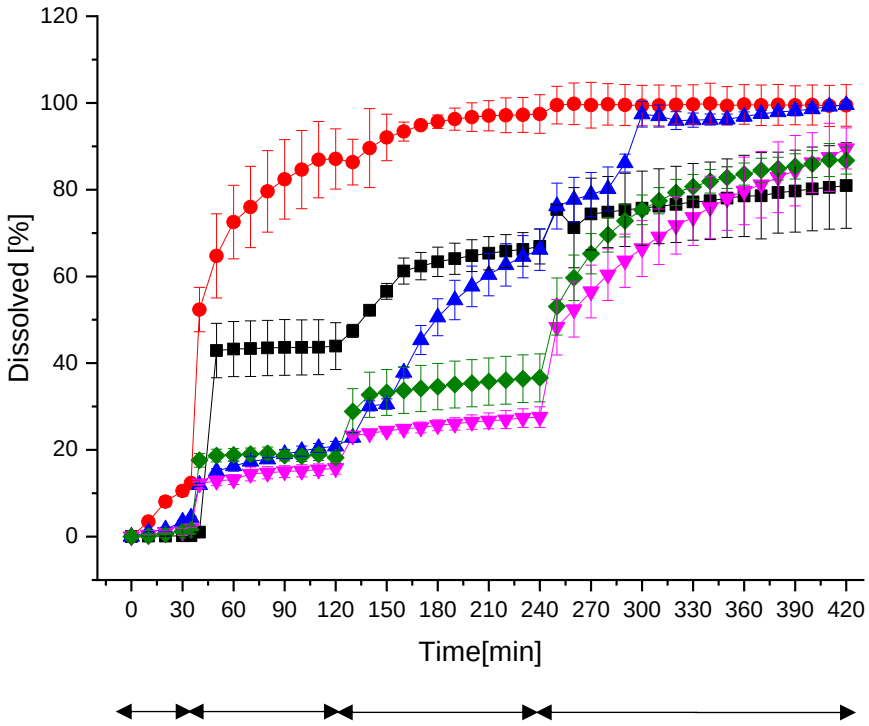

pH	**1.1**	**5.5**	**6.8**	**7.4**
Time	**30 min**	**90 min**	**120 min**	**180 min**
(Phosphate Buffer added)		38.4 ml	8 ml	2 ml
IND Solubility (µg/ml)	1.68	38.71	59.40	71.48

Figure 26: Non-sink dissolution (pH 1.1 for 30 min, pH 5.5 for 90 min, pH 6.8 for 120 min, pH 7.4 for 180 min; 100 % = 83.3 µg/ml) of ■ pure IND, binary ASDs: ● IND- A15 20/80, ▼ IND- SSB 55 20/80 and ◆ IND- EFS 20/80 ternary ASDs: ▲ IND- SSB 55- A15 20/70/10

b) Stability

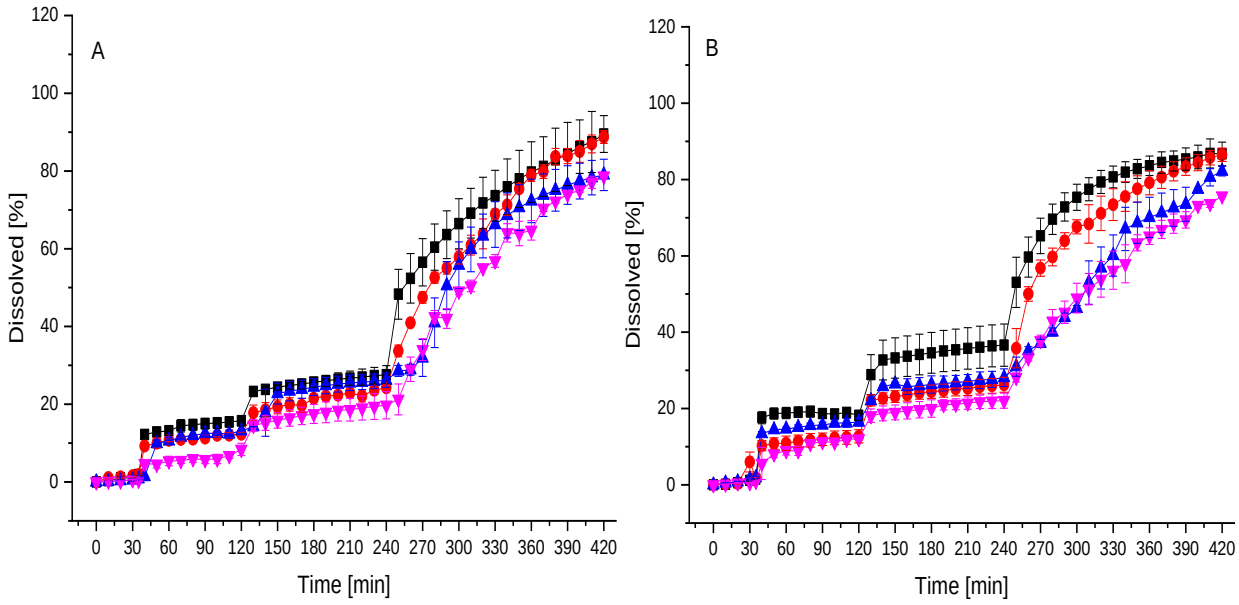

Figure 27: Non-sink dissolution (pH 1.1 for 30 min, pH 5.5 for 90 min, pH 6.8 for 120 min, pH 7.4 for 180 min; 100 % = 83.3 µg/ml) of binary ASDs stored in Activ® vials at 40 °C/75 % RH
(A) Initial: ■ IND- SSB 55 20/80, 1 week: ● IND- SSB 55 20/80,
2 weeks: ▲ IND-SSB 55 20/80, 4 weeks: ▼ IND- SSB 55 20/80
(B) Initial: ■ IND- EFS 20/80, 1 week: ● IND- EFS 20/80,
2 weeks: ▲ IND- EFS 20/80, 4 weeks: ▼ IND- EFS 20/80

The HME ASDs stored in a closed container with desiccant at accelerated condition were evaluated for dissolution performance shown in Figure 8. In comparison to freshly prepared ASDs, the dissolution decreased about 8 to 10 % for IND-SSB 55 and IND-EFS. IND-SSB 55 ASDs performance is shown in Figure 27 (A), which represents the impact of temperature and humidity on dissolution performance. The ASDs stored for 1 week showed comparable dissolution performance to the initial samples. The ASDs stored for 2 weeks and 4 weeks were effective to protect the IND release at pH < 6.8 but the rate and extent of release decreased about 10 % in pH 7.4, which might be due to the changes in solid-state i.e., aging and recrystallization (see Fig. 22A). The IND-EFS ASDs are depicted in Figure 27 (B) where 1-week ASDs samples achieved similar dissolution performance compared with the initial sample. But, over storage for 2 and 4 weeks, changes in the solid-state led to a decrease in dissolution performance of IND-EFS ASDs with dissolution values being reduced about 9 to 10 % upon storage.

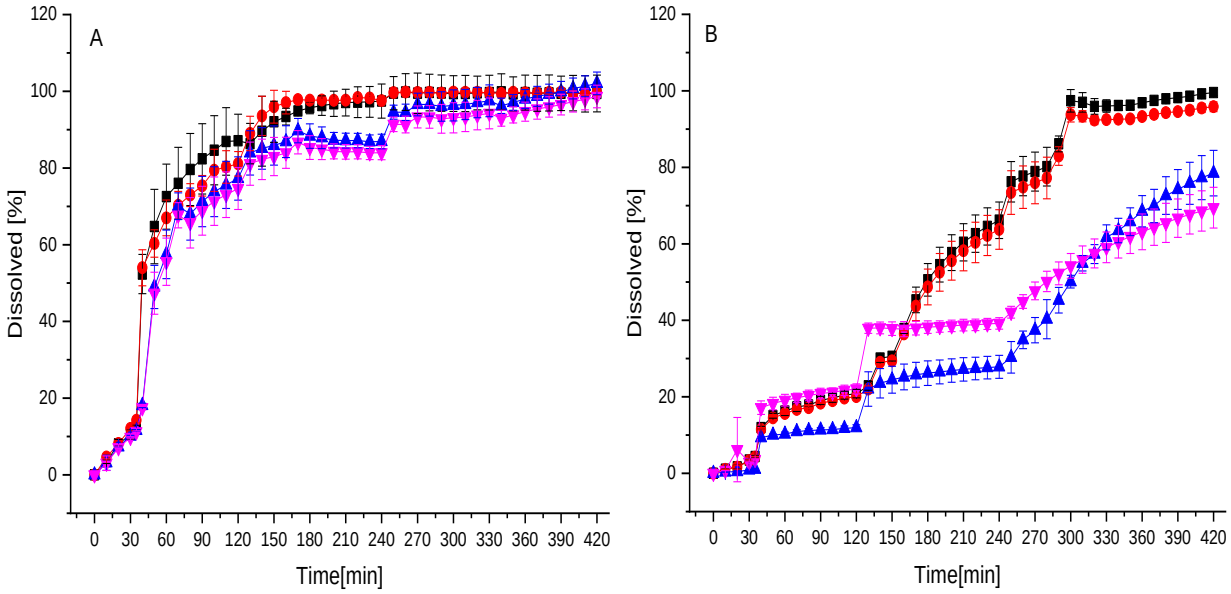

Figure 28: Non-sink dissolution (pH 1.1 for 30 min, pH 5.5 for 90 min, pH 6.8 for 120 min, pH 7.4 for 180 min; 100 % = 83.3 µg/ml) of binary and ternary ASDs stored in Activ® vials at 40 °C/75 % RH

(A) Initial: ■ IND- A15 20/80, 1 week: ● IND- A15 20/80, 2 weeks: ▲ IND- A15 20/80, 4 weeks: ▼ IND- A15 20/80

(B) Initial: ■ IND- SSB 55-A15 20/70/10, 1 week: ● IND- SSB 55-A15 20/70/10, 2 weeks: ▲ IND- SSB 55-A15 20/70/10, 4 weeks: ▼ IND- SSB 55-A15 20/70/10

Figure 28 (A) shows the IND-A15 ASDs dissolution performance for samples stored for 4 weeks, where dissolution kinetics remained similar to the initial samples. This might be attributed to A15 polymer with its higher glass transition temperature compared to other polymers showing less susceptibility to altering ASDs solid state under stress condition [36]. In contrast, IND-SSB 55-A15 showed severe changes in dissolution kinetics upon storage, especially at periods exceeding 1 week (Figure 28(B)). After 1 week the dissolution at the end of the test decreased only 4 % with identical dissolution kinetics compared to the initial samples. However, after 2 and 4 weeks, the final release rate dropped about 21 % to 28 % respectively. Interestingly, the release kinetics for samples stored for 2 and 4 weeks changed, too. At pH shifts to 5.5 and 6.8, only an initial release occurred while the dissolution rate remained almost 0 for the period of the respective pH (5.5 and 6.8). i.e., dissolution characteristics of the Shellac containing matrix were strongly

affected by time and temperature, which was attributed to aging and recrystallization tendency of ASDs upon storage and which is confirmed by XRPD results.

5.4 Comparison of crystallinity with the dissolution

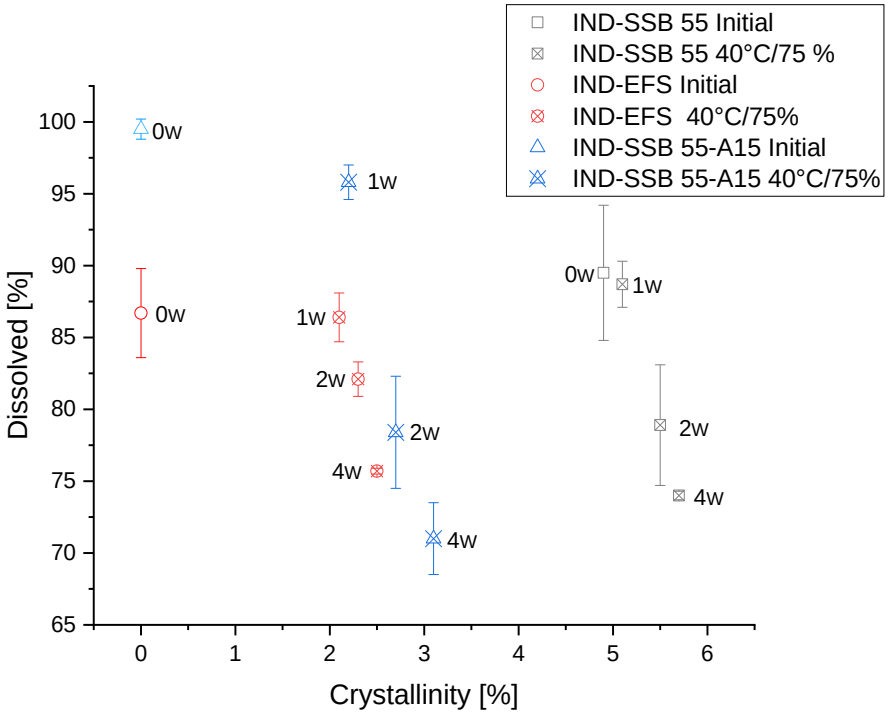

Figure 29: Non-sink dissolution (pH 7.4; 100 % = 83.3 µg/ml) after 420 min in relation to the crystallinity of binary and ternary ASDs initial values and stored at accelerated condition 40 °C/75 % RH for 1 week, 2 weeks, and 4 weeks.

It can be demonstrated that the dissolution in pH 7.4 is dependent on the changes in the crystallinity of ASDs stored at accelerated conditions shown in Figure 29. IND-SSB 55 SDs on exposure to stress condition showed decreased drug release of 16 % after 4 weeks with an increase in the amount of crystallinity from 5.1 % to 5.7 % on storage for 4 weeks. Also, the samples on storage showed increased glass transition temperature 6 °C compared to the initial value indicating occurrence of aging (exposure to higher temperature) on storage. In the case of IND-EFS, dissolution was decreased by 11 % after 4 weeks storage at increased crystallinity of > 2.5 % compared to the initial samples which were completely amorphous. The initial glass transition temperature of 36.9 °C increased to 43.1 °C after within the same 4 weeks.

This increase in glass transition temperature in DSC thermogram was likely related to the phenomenon of physical aging of SDD occurred during the 4 weeks of storage under stress conditions (40 °C/75 % RH). As proposed by Tian et al. [119] prior to recrystallization of the API, segregation of dissolved drug molecules occurred, resulting in many tiny amorphous drug clusters and eventually, an amorphous phase separation, not detectable via DSC. i.e., only the Tg of the continuous polymer phase is detected, which will increase as the concentration of dissolved drug molecules acting as solid-state plasticizer decreased upon the proposed amorphous phase separation. Even without traceable recrystallization, the aging process resulted in slower dissolution correlating with an increased Tg. While in the case of IND-A15 the dissolution rate remained similar to initial samples with no detection of crystallinity presented in Figure 28 that can be attributed to its higher glass transition temperature and viscosity showing less impact of stress storage conditions on dissolution performance. IND-SSB 55-A15 implies that due to physical changes in storage there was a decrease in dissolution rate with an increase in crystallinity > 3.1 %. There was a prominent impact of storage leading to a high increase of the glass transition temperature of 4 to 5 °C upon a 4-weeks storage. It also showed changes in -OH interactions with an increase in IR frequency and decreased peak intensity compared to the initial samples indicating the creation of weak hydrogen bond interactions confirmed by AT-IR. Thus, the use of the second polymer was ineffective to prevent the recrystallization of SDD, implying that there might be a less strong interaction between IND and polymers, resulting in a partial loss of its gastroprotective and synergistic effect leading to changed dissolution kinetics 8 upon storage for 4 weeks.

5.5 Conclusion

The findings of the present study demonstrated that the ternary mixture of IND, A15, SSB 55 prepared by HME showed improved protection at pH 5.5 with complete dissolution at pH 7.4 during pH shift compared to IND neat and other binary mixtures of IND-SSB 55, IND-EFS, and IND-A15, with the generation of delayed-release effect without the need of coating. This protective effect and delayed release properties were related to a combination of the pH-dependent soluble excipient (SSB55) and the pH-independent soluble polymer (A15) leading to improved dissolution. It was found that the ternary mixture showed improved intermolecular interaction detected via AT-IR resulting in increased hydrogen bonding. While the binary mixtures of IND-SSB 55 and IND-EFS were able to show higher protection at pH 1.1 and pH 5.5 with complete release of IND at pH 7.4 irrespective of its solid-state of IND-SSB 55 i.e., partially crystalline form. In the case of an IND-A15 mixture, complete dissolution occurred at pH 6.8 indicating its limitation to offer gastroprotective effect. When the samples were stored on stability the solid-state and dissolution kinetics changed for both binary and ternary mixtures. The ternary mixture showed recrystallization and an increase in glass transition temperature confirmed by XRPD and DSC respectively with the effect of decreased dissolution kinetics. This compromised dissolution kinetics for stored samples could be attributed to decreased intermolecular interaction confirmed by AT-IR. While, in the case of binary mixtures, the temperature led to a loss of amorphous nature of the SDD leading to physical instability of the mixtures on stress storage conditions. Thus, the increase in crystallinity led to a proportional decrease in dissolution kinetics of the stored sample. Nevertheless, with the implementation of shellac, it might be useful to achieve a gastro-protective effect with other polymers for the colonic targeting of poorly soluble drugs via HME. Thus, it will add to the existing set of synthetic polymers which might be useful for future ternary solid dispersion development.

5.5 Summary of the chapter

The use of shellac for pH-dependent soluble ternary solid dispersion of IND of improved solubility and dissolution rate at the colon without the need for a coating. The binary SDs of API (IND) with shellac (SSB 55) and Eudragit FS 100 (EFS) and ternary mixtures of IND, SSB 55 together with a new grade of HPMC (A15) were prepared using HME. To achieve gastric protection and improved dissolution performance including maintenance of supersaturation. The SDD were characterized and tested for in-vitro dissolution performance using a pH shift dissolution method from 1.1, 5.5, 6.8, and 7.4. A ternary extrudate of IND, SSB 55, and A15 showed improved protection below pH 5.5 with a complete release of 99.5 % at pH 7.4 compared to IND neat and binary extrudates from IND-A15, IND-SSB 55, and IND-EFS. It was attributed to an increased level of intermolecular interaction confirmed by AT-IR and was studied for stability. It was found that in a ternary mixture containing IND, A15 and SSB 55 an increased hydrogen bonding interaction is present, which resulted in improved dissolution performance compared to binary mixtures. Therefore, ternary SDD proved to be a promising concept for future development of colon targeting of poorly soluble drugs.

6 *Overall Summary*

The poor solubility of existing drug substances and new chemical entities is a problem in modern pharmaceutical development. There are various strategies to overcome the solubility limited bioavailability of poorly soluble drugs. One of the strategies is preparing amorphous solid dispersion using spray drying or hot-melt extrusion. Despite the efforts of several marketed formulations of ASDs, there are fewer research efforts in using natural polymers/excipients for improving solubility and supersaturation maintenance. To promote the use of natural polymers as a matrix in ASDs a comprehensive study of its application and understanding its influence on the improvement of solubility with supersaturation is essential.

To address this, we used different natural polymers in combination with synthetic polymers. Chapter 3 is dedicated to the pre-screening of the natural polymer inulin in combination in a binary mixture with HPMC-AS. The film cast in organic solvent showed a single glass transition temperature indicating that these two polymers are miscible with each other and subsequently be potentially suitable for spray drying. Other mixtures of shellac with A15 showed an improved solubility in organic solvent mixtures and the film cast showed a single Tg, in this case, a solvent mixture of acetone/ethanol (50/50) showed improved results in terms of clarity of the casted film. The mixture containing inulin with shellac was insoluble in various organic solvents (acetone, ethanol) and mixtures of acetone/ethanol (50/50) and ethanol/water (95/5). Additionally, inulin/shellac mixtures did not form a one-phasic melt or solid as was showed by two Tgs in DSC measurements, thereby clearly indicating that this combination is not a suitable matrix for manufacturing of ASDs. Lastly, A15 in combination with HPMC-AS was soluble in all tested organic solvents and mixtures thereof and showed a single Tg in DSC measurements making this combination one of the potential lead candidates for the manufacturing of ASDs. Thus, using the pre-screening enabled the selection of natural excipients alone or in combination as a matrix in ASDs development.

In continuation of the selection of two lead polymers and their miscibility in each other A15 with shellac was used for the formulation of ASDs. Chapter 4 focuses on the use of shellac for preparing binary and ternary ASDs with HPMC, using the model API loratadine

(LOR) via spray drying and hot-melt extrusion helped to achieve solubility improvement and supersaturation maintenance. We observed that among various shellac fractions within the ternary ASDs, the 10 % weight fraction optimally increased the solubility 30 folds and maintained the supersaturation for 3 h compared to other binary and ternary formulations. However, lower and higher fractions of shellac decreased the solubility again. This superiority for 10 % weight fraction was due to specific and stronger API matrix interactions detected via ATR-IR, which was further studied in terms of stability. Also, it was found that there exists a correlation between the amount of the dissolved API and the API crystallinity, which dictates the level of supersaturation. While the crystallinity is set by the LOR concentration at the end of the test, the dissolution rate (LOR in dissolution medium) depended on the origin of the crystals i.e., due to recrystallization of previously molecular dispersed LOR or undissolved LOR from HME processing. Thus, the use of shellac is proposed and it will add to the understanding of ternary mixture development with the application of solubility improvement and supersaturation maintenance.

Chapter 5 highlights the application of shellac for pH-dependent release using HME without the need for coating. The binary SDD of API (IND) with shellac (SSB 55) and IND with Eudragit FS 100 (EFS) and ternary mixtures of IND, SSB 55 together with a new grade of HPMC (A15) were prepared using HME. The SDD were characterized and tested for in-vitro dissolution performance using a pH shift dissolution method from 1.1, 5.5, 6.8, and 7.4. A ternary extrudate of IND, SSB 55, and A15 showed improved protection below pH 5.5 with a complete release of 99.5 % at pH 7.4 compared to IND neat and binary extrudates from IND-A15, IND-SSB 55, and IND-EFS. This increased level of intermolecular interaction was confirmed by AT-IR and studied for stability. It was found that in a ternary mixture containing IND, A15, and SSB 55 an increased hydrogen bonding interaction is present, which resulted in improved dissolution performance compared to binary mixtures with the maintenance of supersaturation. Therefore, ternary SDD proved to be a promising concept for the future development of colon targeting of poorly soluble drugs.

Outlook of the study

In continuation of the above work there is still some area of improvement and therefore, some future outlook is postulated:

In the chapter 3 the selection of suitable polymers/mixtures for ASDs processing was studied. However, we found out that the polymer-polymer solubility and miscibility into each other is crucial for ASD development. As some polymers or mixtures cannot be processed via spray drying due to the lack of a common solvent, others cannot be processed via HME due to high glass transition temperatures. To improve the prediction of suitable polymer-polymer miscibility on microscale further investigations are needed to optimize the processing method i.e., Melt Prep for HME and 96 well plate for polymer solubility in various organic solvent mixtures.

Additionally, we showed that the addition of ternary additive (natural excipient shellac) can be useful for the improvement of solubility and maintenance of supersaturation for ASDs. However, for further promotion of ternary polymer/excipient applications in ASDs are necessary as binary systems might not be helpful in all cases.

Furthermore, the results presented in this thesis showed the application of shellac for colon targeting using HME without the need of coating. Shellac exhibits gastric protection with delayed release property which is comparable to the synthetic polymer Eudragit FS 100 for colon targeting. Thus, its application as natural excipient in colon targeting with other APIs is promising for further studies.

The use of natural polymers as a lead polymer for ASDs is an interesting approach. It would help to expand the existing repertoire of synthetic polymers and offer alternative features. The natural polymers are the only remaining set to be explored as matrix in the solid dispersion manufacturing. The pharmaceutical companies are shifting their approach for assuring the quality in product development using QbD without sufficiently taking the patient's safety and health into account. The manufacturing of ASDs using natural polymers would help to improve the solubility and dissolution rate of poorly soluble drugs, leading to an effective therapeutic delivery. Furthermore, the amorphous solid dispersion alone or in combination with natural polymers is useful in improving the life cycle management of existing medicines. Hence, a shift of application from synthetic

polymers to natural polymers for handling poorly soluble active ingredients is needed as generalized approach for research.

7 Materials and Methods

7.1 Materials

The materials used in the experiments are listed in Table 10. Loratadine and Indomethacin were obtained from Indian suppliers (> 99 % and > 97 to 100 % respectively). Acetonitrile and methanol were of analytical HPLC grade. While all the remaining material were of pharmaceutical grade.

Table 10: Material utilization during experiments with batch number and source

Name of substance	Batch No	Company
Loratadine	LRHB5183	SRIS Pharmaceuticals. (Hyderabad, India)
Indomethacin	IND/115003	Swati Spentose Pvt. Ltd. (Mumbai, India)
Orafti GR	RRLRM4CRM4	Beneo Palatinate GmbH (Mannheim, Germany)
Alpha glycosyl hesperidin	5C06	Nagasse (Europe) GmbH (Düsseldorf, Germany)
Shellac SSB 55 Pharma FL	213680	HARKE Pharma GmbH (Mülheim an der Ruhr, Germany
Affinisol HPMC HME 15 LV	B293B20001	Dupont Nutrition and Biosciences (Bomlitz, Germany)
AQOAT-LG	4063099	SE Tylose GmbH & Co.KG (Wiesbaden, Germany)
Eudragit FS 100	-	Evonik Industries AG (Darmstadt, Germany)
Potassium dihydrogen phosphate	17G144126	VWR International bvba (Leuven, Belgium)
Sodium hydroxide pellets	H3560	Honeywell (Seelze, Germany)
Combititrant 2	HX85807902	Merck KGaA (Darmstadt, Germany)

Sodium tartarate dihydrate	FN1331364	Merck KGaA (Darmstadt, Germany)
Methanol	190312C003	Avantor Performance materials (Giwice, Poland)
Acetonitrile	19G101742	VWR International SAS (Rue Carnot, France)
Hydrochloric acid 0.1 M	182194019	VWR International SAS (Rue Carnot, France)
Tripotassium citrate monohydrate	X888.1	Carl Roth GmbH (Karlsruhe, Germany)
Tripotassium phosphate	10216213	Thermofischer(Kandel) GmbH (Kandel, Germany)
Demineralized water	-	Institute of Pharmacy (University of Bonn, Bonn, Germany)

7.2 Equipment and software

All equipment which was used to generate, analyse or characterize samples and/or data are listed in Table 11. All software programs which were used to generate and analyze data are listed in Table 12.

Table 11: Equipments utilized for experiments

Type	Name or Model	Manufacturer
Ball mill	MM400	Retsch GmbH (Haan, Germany)
Vacuum dryer	VDL-23	Binder GmbH (Tuttlingen, Germany)
-	Sirius inForm	Sirius Analytical, United Kingdom
Water content	VS 30S volumetric titrator plus stomboli KF oven changer	Mettler Toledo AG (Schwerzenbach, Switzerland)
Spray dryer	Mini spray dryer B-290	Büchi (Flawil, Switzerland)

Hot melt extruder	ThreeTec 12 mm	ThreeTec (Seon, Switzerland)
	Turbula mixer	Willy A. Bachofen AG – Maschinenfabrik, (Muttenz, Switzerland)
HPLC	Waters HPLC system 2695	Water corporation (USA)
Ultrasonicator	Sonorec digitec	Bandelin electronic (Berlin, Germany)
XRPD	X'Pert MRD Pro	PANalytical (Almelo, Netherlands)
DSC	DSC 2	Mettler Toledo (Gießen, Germany)
ATR-IR	α Alpha - T	Bruker Optik GmbH (Ettlingen, Germany)
Dissolution	AT7 smart	Sotax AG (Allschwil, Switzerland)
UV spectrometer	Agilent 8454	Agilent Technologies GmbH, Waldbronn, Germany
Hot air oven	UM 400	Memmert GmbH, Schwabach, Germany

Table 12: Software utilization for experiments

Type	**Name**	**Supplier**
Software		
XRPD data analysis	X'Pert High score plus	PANalytical (Almelo, The Netherlands)
Graphical data presentation	Origin Pro 8 software	Origin Lab Corporation (Massachusetts, USA)
AT-IR	OPUS software	Bruker Optik GmbH (Ettlingen, Germany)

7.3 Methods

7.3.1 Milling and drying of raw material

SSB 55 pharma was obtained in flakes, and was thus ball-milled using a MM400 (Retsch GmbH, Haan, Germany) at 30 Hz 2 times in each in 5 min cycles, and passed through a *355*-µm mesh sieve. The grounded SSB 55 and A15 was dried under vacuum (0.01 – 0.02 bar) using a VDL-23 (Binder GmbH, Tuttlingen, Germany) at 40^{o}C for 24 h, and stored in airtight containers until further use.

7.3.2 Solubility studies

The equilibrium solubility of LOR was investigated using the Pion inForm (Sirius Analytical, United Kingdom) using potentiometric CheqSol® method. In this method, 15-20 mg of LOR drug powder was weighed into the Pion inForm glass beaker and this was placed into the autosampler to schedule subsequent measurements. 40 mL of medium (0.15 M NaCl) was automatically added into the beaker. For the weak base (LOR), the pH was adjusted to 2.0 by means of 0.5 M HCl to allow a complete drug dissolution. The dissolution segment was 2 minutes at 300 rpm. Subsequently, the titration was performed with 0.5 NaOH until the drug first precipitated. The precipitation point was recorded UV-metrically and, depending on the behavior of the sample, the crossing point or the curve fitting method was applied. Stirring was kept constant at 300 rpm and the temperature was set to 25 °C by means of a thermometer and a Peltier device system during the entire measurement. The pH was constantly controlled by means of an inForm pH electrode and provided the *dpH*/*dt*. The evaluation of the data was performed manually by means of the inForm software (Sirius Analytical Instruments Ltd., Forest Row, UK, version 1.4.0.0). Following the refinement of the data, the equilibrium solubility, as well as the pH-dependent solubility profile were calculated.

7.3.3 Karl Fischer titration

The water content in neat A15, SSB 55 and prepared ASDs was determined using VS 30S volumetric titrator plus including Stromboli KF Oven and sample changer (Mettler Toledo AG, Schwerzenbach, Switzerland). Briefly, 20 to 25 mg of the sample was transferred to vials, which were closed with aluminum cap 19 mm (3M, USA). The sample vials were

exposed to the oven chamber and heated from 25 °C to 150 °C, the evaporated water from the sample was subjected to the titration vessel that contained methanol as a solvent and titrated with Combi titrant 2 composite under continuous stirring. All measurements were performed in triplicate. The water content was calculated using the following equation:

$$\%\, Water\ content = \frac{Wstd, theoretical}{Wstd, practical} \times Ws$$

where, $W_{std,\ theoretical}$ is the water content of standard sodium tartrate dihydrate; $W_{std,\ practical}$ is the water content of standard sodium tartrate dihydrate and W_s is the water content of the sample recorded by Karl Fischer titration.

7.3.4 Preparation of physical mixtures (PM)

For XRPD measurements, samples of LOR/A15 (20/80), LOR/SSB55 (20/80), LOR/A15/SSB 55 (20/75/5, 20/70/10, 20/60/20, 20/50/30 and 20/40/40) were prepared using a porcelain mortar. While, the IND - SSB 55 (20/80), IND - EFS (20/80), IND - A15 (20/80), and IND-SSB 55-A15 (20/70/10) were prepared using a porcelain mortar for XRPD measurements. For DSC experiments, 400 mg of the physical mixture containing API and one or both polymers in the weight fractions mentioned above was weighed separately and ball milled using a MM400 (Retsch GmbH, Haan, Germany) at 30 Hz 3 times each in 5 min cycle. After each cycle of 5 min, a break was taken to minimize thermal energy intake.

7.3.5 Manufacturing of amorphous solid dispersion

7.3.5.1 Spray drying (SD)

SD operation was carried out by using the B-290 mini spray dryer consisting of an inert loop B-295 and dehumidifier B-296 (BÜCHI, Flawil, Switzerland). The binary LOR-A15 20/80, LOR-SSB 55 20/80 and ternary mixtures of LOR-A15 -SSB 55 in 20/75/5, 20/70/10, 20/60/20, 20/50/30, and 20/40/40 ratios were dissolved separately in a mixture of acetone and ethanol in the ratio of 70:30, and subsequently spray-dried with solid

content of 6 % using the following parameters: inlet temperature was set to achieve outlet temperature of 65 °C, aspirator rate was kept at 90 %, atomization pressure 4 to 5 bar with spray rate of 4 to 5 ml/min. The respective spray-dried powder formulations were dried under a vacuum (0.01- 0.02 bar) (VDL-23, Binder GmbH, Tuttlingen, Germany) at 40 °C for 48 h to remove the residual solvent in the final product. The products were then transferred to airtight containers and stored at -20°C until further characterization.

7.3.5.2 Hot-Melt Extrusion(HME)

a) Extruder setup

The extruder barrel was composed of five individually adjustable heating zones to ensure a desirable melting and distribution of the respective mixture mentioned in table 13,14 and 15. The process temperature was set up at 65 to 80 °C and above depending on the mixture in the high shear regions of the extruder screws (zone 1: conveying; zone 2: 30°-, 60 °; zone 3: 60°- and 90°- 4-disc-kneading elements, zone 5: terminal zone consisted conveying elements presented in Figure 30.

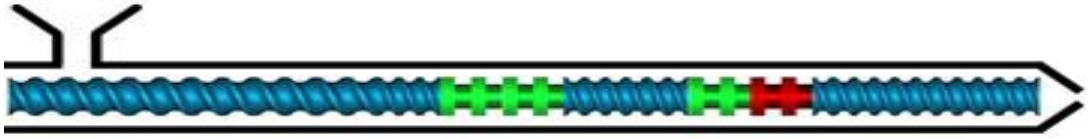

Conveying element	Kneading element at 30 °/60 °	Melt conveying	Kneading element at 60 °/90 °	Degassing and discharging

Figure 30: ThreeTec extruder set up and screw configuration

b) HME for mixtures:

HME for mixtures was performed using a 12 mm twin-screw extruder (Three Tec, Seon, Switzerland) equipped with a 2 mm die. 50 g of the powder mixtures of binary and ternary samples mentioned in 7.3.4 was mixed in a TurbulaMixer (Willy A. Bachofen AG – Maschinenfabrik, Muttenz, Switzerland) for 10 min at 22 rpm. The respective blends were transferred into the volumetric dosing feeder, and calibrated to determine the feed rate during the extrusion process, which was kept constant at 1 g/min. The process parameters for HME are listed in Table 13. The extrudates were then cooled to room temperature and

subsequently cryo-milled by ball milling using the MM400 (Retsch GmbH, Haan, Germany) 30 Hz 2 times each in 15 second cycle. The resultant extrudates were sieved through the *355*-µm mesh to standardize the particle size for different characterization studies.

Table 13: HME process parameters of binary and ternary mixtures containing LOR, A15 and SSB 55 in different ratios

Mixture Composition	Barrel temperature[°C]	Screw speed (rpm)	Torque (Nm)	Feed rate (g/min)
LOR- A15 20/80	65/110/110/110/110	100	7.0	1.0
LOR- SSB 55 20/80	50/80/90/90/90	100	4.5	1.0
LOR- A15 - SSB 55 20/75/5	65/105/105/105/105	100	5.6	1.0
LOR- A15 - SSB 55 20/70/10	65/105/105/105/105	100	4.3	1.0
LOR- A15 – SSB 55 20/60/20	65/105/105/105/105	100	4.1	1.0
LOR- A15 – SSB 55 20/50/30	65/105/105/105/105	100	3.8	1.0
LOR- A15 – SSB 55 20/40/40	65/105/105/105/105	100	3.1	1.0

c) Generation of remaining crystallinity using HME

The ratio of LOR-A15-SSB 55 (20/70/10) was prepared and mixed as detailed under 7.3.4. HME was performed at lower temperatures (Table 14) to obtain ASDs with remaining crystals, due to temperature dependent LOR dissolution within the polymeric matrix. After extrusion, the samples were collected and cryo-ball milled. The torque was higher in case of lower temperature, which is attributed to high melt viscosity of A15. However, with an increase in extrusion temperature, the melt viscosity decreased with reduced torque load.

Table 14: HME process parameters for Induced crystallinity at different temperatures

Mixture Composition	Barrel temperature[°C]	Screw speed (rpm)	Torque (Nm)	Feed rate (g/min)
LOR- A15 – SSB 55 20/70/10	55/55/55/55/55	100	6.8	1.0
LOR- A15 – SSB 55 20/70/10	60/60/60/60/60	100	5.5	1.0
LOR- A15 – SSB 55 20/70/10	70/70/70/70/70	100	4.8	1.0
LOR- A15 – SSB 55 20/70/10	80/80/80/80/80	100	4.9	1.0

d) HME mixture for IND based ASDs

HME was performed using a 12 mm twin-screw extruder (Three Tec, Seon, Switzerland) having a functional length of 25:1 L/D. The extruder barrel was composed of five individually adjustable heating zones to ensure a desirable melting and distribution of the respective mixture mentioned in Table 15. The process temperature was set up at 85 °C and above depending on the mixture in the high shear regions of the extruder screws (zone1: 30°-, 60 °; zone 2: 60°- and 90°-4-disc-kneading elements, zone 5: terminal zone consisted conveying elements [25,29] and equipped with a 2 mm die. 50 g of the powder mixtures of binary IND - SSB 55 (20/80), IND - EFS (20/80), IND - A15 (20/80), and ternary samples IND-SSB 55-A15 (20/70/10) were prepared in a Turbula Mixer (Willy A. Bachofen AG – Maschinenfabrik, Muttenz, Switzerland) for 10 min at 22 rpm. The binary and ternary mixture blends were transferred separately into the volumetric dosing feeder system ZD9 (Three-Tec GmbH, Seon, Switzerland) which was used to enable a constant feed rate (Table 15), and calibrated to determine the feed rate during the extrusion process, which was kept constant at 1 g/min. The process parameters for HME are listed in Table 15. The extrudates were then cooled to room temperature and subsequently, cryo-ball milled using the MM400 ball mill (Retsch GmbH, Haan, Germany) at 30 Hz for 2 times in 15 seconds cycle each. The resultant extrudates were sieved through the *355*-µm mesh to standardize the particle size for different characterization studies.

Table 15: HME parameters and composition of various mixtures of Indomethacin

Mixture Composition	Barrel temperature [°C]	Screw speed [rpm]	Torque [Nm]	Feed rate [g/min]
IND – SSB 55 (20/80)	55/85/85/85/85	100	3.2	1.0
IND – EFS (20/80)	65/100/100/100/100	100	6.5	1.0
IND – A15 HME (20/80)	110/110/110/110/110	100	7.2	1.0
IND-SSB 55-A15 (20/70/10)	110/110/110/110/110	100	5.5	1.0

7.3.6 Assay by HPLC

LOR was analyzed as per Ph Eur 6.0 liquid chromatography method on Waters HPLC system 2695 equipped with UV detector. The column used was C18 Multohigh 100 RP (125 × 4 mm, 5µ) from CS Chromatographie, Langerwehe, Germany maintained at a temperature of 50°C. The mobile phase consisted of methanol: 0.05 M potassium dihydrogen phosphate buffer pH 2.8 (adjusted with phosphoric acid): acetonitrile (30: 35: 40 v/v) it was filtered and degassed with ultrasonicator(Bandelin Electronic, Berlin, Germany) run at a flow rate of 1.0 ml/min. The detection was carried out at 220 nm, LOR was eluting at 8.00 min. The solid dispersion containing LOR equivalent to 20.0 mg was dissolved in 2 ml of methanol and diluted with the mobile phase up to 10.0 ml. All the samples were filtered through a 0.22 polyethersulfone filter before injection.

7.3.7 Solid-state characterization

7.3.7.1 X-ray powder diffraction (XRPD)

XRPD analyses were performed using a X'Pert MRD Pro (PANalytical, Almelo, The Netherlands) with an X'Celerator and nickel filtered Cu Kα radiation (k= 1.5409 A°) at 45 kV and 40 mA. The samples were placed in an aluminum sample port, and the reflection mode of X-rays was measured in the range of 5° to 45° (2θ) at increments of 0.04°/s. The data were analyzed using X'Pert High score plus software (PANalytical, Almelo, The Netherlands) and plotted in Origin Pro 8G software (Origin Lab Corporation, Massachusetts, USA).

To calculate the percentage of residual crystallinity, various mixtures of crystalline LOR (% w/w) with A15 and SSB 55 were prepared (30/35/35, 20/40/40, 15/42.5/42.5, 10/45/45, 5/47.5/47.5, 2/49/49). All diffractograms were background corrected (background is related to an amorphous fraction). Further, the area under the reflection peak in the range of 5° to 45° (2θ) was calculated and plotted against the crystalline fraction to obtain a calibration curve. The percentage of crystallinity was given in (% w/w) and referred to the LOR recrystallized [16].

7.3.7.2 Differential scanning calorimetry (DSC)

DSC measurements were carried out using a DSC 2 from Mettler Toledo (Gießen, Germany) equipped with a nitrogen cooling system and nitrogen as purge gas (30 ml/min). The calibration of temperature was done using indium as standard. 10 to 15 mg samples from each mixture were placed in an aluminum crucible pans with a pierced lid. The melting point of the neat compound was measured using conventional DSC mode. The samples were held isothermally at 25 °C for 2 min and then heated in a range of 25 °C to 160 °C at a heating rate of 10 °C /min for recording the melting temperature. Glass transition temperature (Tg) was measured using TOPEM- mode (DSC-measurements with multi-frequency temperature modulation), in which samples were held isothermally at -20 °C for 2 min and then heated in range of -20 °C to 160 °C with a heating rate of 2 °C/min.

7.3.7.3 Thermogravimetric analysis (TGA)

The TGA was used to investigate the thermal stability of polymers using Perkin-Elmer Thermogravimetric Analyzer TGA 7 (Waltham, MA, USA). The percentage weight loss was determined by heating the samples in platinum crucibles using a temperature gradient from 25 °C to 350 °C with a heating rate of 10 k/min and nitrogen purge of 20 ml/min.

7.3.7.4 Attenuated total reflectance infrared spectroscopy (ATR-IR)

Molecular interactions between LOR and polymers/excipient were studied by an ATR–IR spectrometer (Bruker Optik GmbH, Ettlingen). 5 to 10 mg powdered sample of neat and

ASDs was inserted in the ATR cell, the pressure was exerted by raising pressure arm downwards and scanned (averaged 27 scans) in the range of 4,000 to 400 cm^{-1}.

7.3.8 Dissolution Studies

The dissolution profile of LOR and ASD formulations was studied over 180 min under non-sink conditions, to measure and quantify the supersaturation performance of our various ASD formulations using USP apparatus type I (AT7 smart, Sotax AG, Allschwil, Switzerland) at 37^{o}C and 150 rpm using small volume vessels (max. 250 ml). The spray-dried powder and ball milled hot melt extrudates were sieved through a 355 µm sieve to standardize the particle size before placing into the baskets and subsequently introducing them into the dissolution vessels. The quantity equivalent to 10 mg of LOR from ASDs was taken and added to dissolution vessels containing 250 ml of phosphate buffer pH 6.8. The sample absorbance was recorded at an interval of 10 min using 10 mm flow-through multiple cell cuvette using an UV/VIS DAD spectrophotometer (Agilent 8454, Agilent Technologies GmbH, Waldbronn, Germany). Each sample was filtered online with glass micro-fiber filters (GE Healthcare, Buckinghamshire, UK). The detection wavelength was 281 nm for pH 6.8. The first derivative spectra were used to avoid interference of excipient's absorption. Drug release was calculated in terms of percentage of drug dissolved with respect to the dose of the drug (100 % dissolved amount is equivalent to 0.04 mg/ml). Dissolution experiments were performed in triplicate and results are expressed as percentage dissolved at the given sampling timepoint.

While, IND based SDs dissolution was carried out for 7 h under non-sink conditions using USP apparatus type II (AT7 smart, Sotax AG, Allschwil, Switzerland) at 37 ± 1 °C and 100 rpm. The melt extrudates containing indomethacin and the neat equivalent to a concentration of 83.3 µg/ml of API were separately placed in each dissolution vessel [141]. The dissolution was carried out in 500 ml of aqueous media at pH 1.2 (0.1 N HCl) for 30 minutes. Subsequently, the pH was adjusted to pH 5.5 using 38.4 ml of concentrated buffer solution. After monitoring for 90 min, the medium was readjusted to pH 6.8 using 8 ml of concentrated buffer. The dissolution rate was further monitored

for 120 min. Finally, the medium was readjusted to pH 7.4 using 2 ml of concentrated buffer and the recording continued for 180 min. The sample absorbance was recorded at an interval of 10 min using 1 mm flow-through multiple cell cuvettes in an UV/VIS spectrometer (Agilent 8454, Agilent Technologies GmbH, Waldbronn, Germany). Dissolution experiments were performed in triplicate and results are expressed as percentage of drug dissolved at the given sampling timepoint.

7.3.8.1 Solubility factor

Solubility factor (SF) was defined as the improvement of solubility for ASD relative to the solubility of the crystalline drug.

$$SF = \frac{Cs, sample}{Cs, crystalline}$$

where, SF is the solubility factor, $C_{s,\ sample}$ is the solubility of the ASD sample and $C_{s,\ crystalline}$ is the solubility of crystalline LOR

7.4 Stability studies

ASDs of LOR-A15-SB 55 20/70/10 prepared through SD and HME were stored in snap capped glass vials (closed) under ambient conditions (25°C, 60% RH) in stability chamber KBF 720 (Binder GmbH, Tuttlingen, Germany) and under accelerated conditions (40°C/75 % RH) in desiccator with over saturated (sodium chloride) solution in a hot air oven UM 400 (Memmert GmbH, Schwabach, Germany) for periods of 1, 2 and 4 weeks. The Activ® vials (closed with desiccant) samples, however, were studied only under the accelerated conditions in desiccators containing saturated salt solution. The studies were conducted to assess the stability performance of ASDs in different packaging material. SDs of IND-SSB 55-A15 20/70/10 prepared through HME were stored in Activ® vials (closed with desiccant) under accelerated conditions (40 °C/75 % RH).

8. Publications

Parts of this work are already published or submitted as:

Articles:

- Kapote, D.N., Wagner K.G. Influence of shellac on the improvement of solubility and supersaturation of loratadine amorphous solid dispersion using a new grade of HPMC. J Drug Del Sci Tech. 2021, https://doi.org/10.1016/j.jddst.2020.102116

- Kapote, D.N., Wagner K.G. Shellac a natural carrier for colon targeting of indomethacin using Hot melt extrusion. Drug Dev Ind Pharm. (submitted)

Abstracts/Posters (Conference participation):

- Kapote, Dnyaneshwar., Wagner K.G.; Colon targeting of indomethacin using shellac and Eudragit FS 100 via Hot melt extrusion- A comparison; 18th International symposium on Advances in technology and business potential of New drug delivery systems organized by Controlled Release Society- Indian Chapter, Mumbai, February 2020.

- Kapote, Dnyaneshwar., Wagner K.G.; Natural excipient- as a new matrix in development of amorphous solid dispersion via spray drying; 11th PBP World Meeting, Granada, Spain, March 2018.

9 References

[1] L. Z. Benet, 'The Role of BCS (Biopharmaceutics Classification System) and BDDCS (Biopharmaceutics Drug Disposition Classification System) in Drug Development', *J. Pharm. Sci.*, vol. 102, no. 1, pp. 34–42, Jan. 2013, doi: 10.1002/jps.23359.

[2] D. E. Zecevic and K. G. Wagner, 'Rational Development of Solid Dispersions via Hot-Melt Extrusion Using Screening, Material Characterization, and Numeric Simulation Tools', *J. Pharm. Sci.*, vol. 102, no. 7, pp. 2297–2310, Jul. 2013, doi: 10.1002/jps.23592.

[3] G. Van den Mooter, I. Weuts, T. De Ridder, and N. Blaton, 'Evaluation of Inutec SP1 as a new carrier in the formulation of solid dispersions for poorly soluble drugs', *Int. J. Pharm.*, vol. 316, no. 1–2, pp. 1–6, Jun. 2006, doi: 10.1016/j.ijpharm.2006.02.025.

[4] W. L. Chiou and S. Riegelman, 'Pharmaceutical Applications of Solid Dispersion Systems', *J. Pharm. Sci.*, vol. 60, no. 9, pp. 1281–1302, Sep. 1971, doi: 10.1002/jps.2600600902.

[5] S. Huang, K. P. O'Donnell, J. M. Keen, M. A. Rickard, J. W. McGinity, and R. O. Williams, 'A New Extrudable Form of Hypromellose: AFFINISOL™ HPMC HME', *AAPS PharmSciTech*, vol. 17, no. 1, pp. 106–119, Feb. 2016, doi: 10.1208/s12249-015-0395-9.

[6] K. Wlodarski, F. Zhang, T. Liu, W. Sawicki, and T. Kipping, 'Synergistic Effect of Polyvinyl Alcohol and Copovidone in Itraconazole Amorphous Solid Dispersions', *Pharm. Res.*, vol. 35, no. 1, p. 16, Jan. 2018, doi: 10.1007/s11095-017-2313-1.

[7] Kumar, D., Lewis, S., Udupa, N, 'Solid dispersions: A review'. Pakistan Journal of Pharmaceutical Sciences. 22, 234-246.

[8] Sekiguchi, K, Obi, N, 'Studies on absorption of eutetic mixture. I. A comparison of the behavior of eutetic mixture of sulfathiazole and that of ordinary sulfathiazole in man', *Chem. Pharm. Bull. 9: 866-872*.

[9] A. Madgulkar, M. Bandivadekar, T. Shid, and S. Rao, 'Sugars as solid dispersion carrier to improve solubility and dissolution of the BCS class II drug: clotrimazole', *Drug Dev. Ind. Pharm.*, vol. 42, no. 1, pp. 28–38, Jan. 2016, doi: 10.3109/03639045.2015.1024683.

[10] Moriyama M, Inoue A, Isoya M, Tanaka M, Hanano M., 'Dissolution properties and gastrointestinal absorption of chloramphenicol from hydrophilic high molecular compound coprecipitates', *Yakugaku Zasshi. 1978 Aug;98(8):1012-8*.

[11] Meng, F., Gala, U. & Chauhan, H, 'Classification of solid dispersions: correlation to (i) stability and solubility (ii) preparation and characterization techniques', *Drug Dev. Ind. Pharm. 41, 1401–1415 (2015)*.

[12] Leuner C, Dressman J, 'Improving drug solubility for oral delivery using solid dispersions', *Eur J Pharm Biopharm. 2000 Jul;50(1):47-60*.

[13] P. Srinarong, S. Hämäläinen, M. R. Visser, W. L. J. Hinrichs, J. Ketolainen, and H. W. Frijlink, 'Surface-Active Derivative of Inulin (Inutec® SP1) Is a Superior Carrier for Solid Dispersions with a High Drug Load', *J. Pharm. Sci.*, vol. 100, no. 6, pp. 2333–2342, Jun. 2011, doi: 10.1002/jps.22471.

[14] S. Janssens and G. Van den Mooter, 'Review: physical chemistry of solid dispersions', *J. Pharm. Pharmacol.*, vol. 61, no. 12, pp. 1571–1586, Dec. 2009, doi: 10.1211/jpp.61.12.0001.

[15] Y. Shibata *et al.*, 'Effect of storage conditions on the recrystallization of drugs in solid dispersions with crospovidone', *Pharm. Dev. Technol.*, vol. 19, no. 4, pp. 468–474, Jun. 2014, doi: 10.3109/10837450.2013.795168.

[16] H. Al-Obaidi and G. Buckton, 'Evaluation of Griseofulvin Binary and Ternary Solid Dispersions with HPMCAS', *AAPS PharmSciTech*, vol. 10, no. 4, p. 1172, Dec. 2009, doi: 10.1208/s12249-009-9319-x.

[17] D. Q. M. Craig, 'The mechanisms of drug release from solid dispersions in water-soluble polymers', *Int. J. Pharm.*, vol. 231, no. 2, pp. 131–144, Jan. 2002, doi: 10.1016/S0378-5173(01)00891-2.

[18] D. D. Sun and P. I. Lee, 'Probing the mechanisms of drug release from amorphous solid dispersions in medium-soluble and medium-insoluble carriers', *J. Controlled Release*, vol. 211, pp. 85–93, Aug. 2015, doi: 10.1016/j.jconrel.2015.06.004.

[19] C. L.-N. Vo, C. Park, and B.-J. Lee, 'Current trends and future perspectives of solid dispersions containing poorly water-soluble drugs', *Eur. J. Pharm. Biopharm.*, vol. 85, no. 3, pp. 799–813, Nov. 2013, doi: 10.1016/j.ejpb.2013.09.007.

[20] Bruno C. Hancock, B.C., Shamblin, S.L. & Zografi, G., 'Molecular mobility of amorphous pharmaceutical solids below their glass transition temperatures', *Pharm Res (1995) 12: 799*.

[21] Y. Aso, S. Yoshioka, and S. Kojima, 'Explanation of the Crystallization Rate of Amorphous Nifedipine and Phenobarbital from Their Molecular Mobility as Measured by 13C Nuclear Magnetic Resonance Relaxation Time and the Relaxation Time Obtained from the Heating Rate Dependence of the Glass Transition Temperature', *J. Pharm. Sci.*, vol. 90, no. 6, pp. 798–806, Jun. 2001, doi: 10.1002/jps.1033.

[22] G. Van den Mooter *et al.*, 'Physical stabilisation of amorphous ketoconazole in solid dispersions with polyvinylpyrrolidone K25', *Eur. J. Pharm. Sci.*, vol. 12, no. 3, pp. 261–269, Jan. 2001, doi: 10.1016/S0928-0987(00)00173-1.

[23] D. Zhou, G. G. Z. Zhang, D. Law, D. J. W. Grant, and E. A. Schmitt, 'Physical Stability of Amorphous Pharmaceuticals: Importance of Configurational Thermodynamic Quantities and Molecular Mobility', *J. Pharm. Sci.*, vol. 91, no. 8, pp. 1863–1872, Aug. 2002, doi: 10.1002/jps.10169.

[24] J. A. Baird, D. Santiago-Quinonez, C. Rinaldi, and L. S. Taylor, 'Role of Viscosity in Influencing the Glass-Forming Ability of Organic Molecules from the Undercooled Melt State', *Pharm. Res.*, vol. 29, no. 1, pp. 271–284, Jan. 2012, doi: 10.1007/s11095-011-0540-4.

[25] K. Kothari, V. Ragoonanan, and R. Suryanarayanan, 'The Role of Polymer Concentration on the Molecular Mobility and Physical Stability of Nifedipine Solid Dispersions', *Mol. Pharm.*, vol. 12, no. 5, pp. 1477–1484, May 2015, doi: 10.1021/mp500800c.

[26] Y. Tian, D. S. Jones, and G. P. Andrews, 'An Investigation into the Role of Polymeric Carriers on Crystal Growth within Amorphous Solid Dispersion Systems', *Mol. Pharm.*, vol. 12, no. 4, pp. 1180–1192, Apr. 2015, doi: 10.1021/mp500702s.

[27] P. J. Marsac, H. Konno, and L. S. Taylor, 'A Comparison of the Physical Stability of Amorphous Felodipine and Nifedipine Systems', *Pharm. Res.*, vol. 23, no. 10, pp. 2306–2316, Oct. 2006, doi: 10.1007/s11095-006-9047-9.

[28] F. Qian, J. Huang, and M. A. Hussain, 'Drug–Polymer Solubility and Miscibility: Stability Consideration and Practical Challenges in Amorphous Solid Dispersion Development', *J. Pharm. Sci.*, vol. 99, no. 7, pp. 2941–2947, Jul. 2010, doi: 10.1002/jps.22074.

[29] M. Yoshioka, B. C. Hancock, and G. Zografi, 'Inhibition of indomethacin crystallization in poly(vinylpyrrolidone) coprecipitates', *J. Pharm. Sci.*, vol. 84, no. 8, pp. 983–986, Aug. 1995, doi: 10.1002/jps.2600840814.

[30] F. Meng, V. Dave, and H. Chauhan, 'Qualitative and quantitative methods to determine miscibility in amorphous drug–polymer systems', *Eur. J. Pharm. Sci.*, vol. 77, pp. 106–111, Sep. 2015, doi: 10.1016/j.ejps.2015.05.018.

[31] J. A. Baird and L. S. Taylor, 'Evaluation of amorphous solid dispersion properties using thermal analysis techniques', *Adv. Drug Deliv. Rev.*, vol. 64, no. 5, pp. 396–421, Apr. 2012, doi: 10.1016/j.addr.2011.07.009.

[32] Hansen,C.M, *Hansen solubility parameters: a users's handbook*. CRC Press, 2007.

[33] C. M. Hansen, 'The Universality of the Solubility Parameter', *Ind. Eng. Chem. Prod. Res. Dev.*, vol. 8, no. 1, pp. 2–11, Mar. 1969, doi: 10.1021/i360029a002.

[34] C. M. Hansen, '50 Years with solubility parameters—past and future', *Prog. Org. Coat.*, vol. 51, no. 1, pp. 77–84, Oct. 2004, doi: 10.1016/j.porgcoat.2004.05.004.

[35] S. Just, F. Sievert, M. Thommes, and J. Breitkreutz, 'Improved group contribution parameter set for the application of solubility parameters to melt extrusion', *Eur. J. Pharm. Biopharm.*, vol. 85, no. 3, pp. 1191–1199, Nov. 2013, doi: 10.1016/j.ejpb.2013.04.006.

[36] J. Gupta, C. Nunes, S. Vyas, and S. Jonnalagadda, 'Prediction of Solubility Parameters and Miscibility of Pharmaceutical Compounds by Molecular Dynamics Simulations', *J. Phys. Chem. B*, vol. 115, no. 9, pp. 2014–2023, Mar. 2011, doi: 10.1021/jp108540n.

[37] E. Stefanis and C. Panayiotou, 'A new expanded solubility parameter approach', *Int. J. Pharm.*, vol. 426, no. 1–2, pp. 29–43, Apr. 2012, doi: 10.1016/j.ijpharm.2012.01.001.

[38] A. Prudic, Y. Ji, and G. Sadowski, 'Thermodynamic Phase Behavior of API/Polymer Solid Dispersions', *Mol. Pharm.*, vol. 11, no. 7, pp. 2294–2304, Jul. 2014, doi: 10.1021/mp400729x.

[39] A. Forster, J. Hempenstall, I. Tucker, and T. Rades, 'Selection of excipients for melt extrusion with two poorly water-soluble drugs by solubility parameter calculation and thermal analysis', *Int. J. Pharm.*, vol. 226, no. 1–2, pp. 147–161, Sep. 2001, doi: 10.1016/S0378-5173(01)00801-8.

[40] Flory, P.J, *Principles of polymer chemistry*. Cornell Univ. press.

[41] D. W. van Krevelen and K. te Nijenhuis, *Properties of polymers: their correlation with chemical structure: their numerical estimation and prediction from additive group contributions*, 4th, completely rev. ed ed. Amsterdam: Elsevier, 2009.

[42] J. Djuris, I. Nikolakakis, S. Ibric, Z. Djuric, and K. Kachrimanis, 'Preparation of carbamazepine–Soluplus® solid dispersions by hot-melt extrusion, and prediction of

drug–polymer miscibility by thermodynamic model fitting', *Eur. J. Pharm. Biopharm.*, vol. 84, no. 1, pp. 228–237, May 2013, doi: 10.1016/j.ejpb.2012.12.018.

[43] T. Lindvig, M. L. Michelsen, and G. M. Kontogeorgis, 'A Flory–Huggins model based on the Hansen solubility parameters', *Fluid Phase Equilibria*, vol. 203, no. 1–2, pp. 247–260, Dec. 2002, doi: 10.1016/S0378-3812(02)00184-X.

[44] P. J. Marsac, T. Li, and L. S. Taylor, 'Estimation of Drug–Polymer Miscibility and Solubility in Amorphous Solid Dispersions Using Experimentally Determined Interaction Parameters', *Pharm. Res.*, vol. 26, no. 1, pp. 139–151, Jan. 2009, doi: 10.1007/s11095-008-9721-1.

[45] P. J. Marsac, S. L. Shamblin, and L. S. Taylor, 'Theoretical and Practical Approaches for Prediction of Drug–Polymer Miscibility and Solubility', *Pharm. Res.*, vol. 23, no. 10, pp. 2417–2426, Oct. 2006, doi: 10.1007/s11095-006-9063-9.

[46] M. Maus, K. G. Wagner, A. Kornherr, and G. Zifferer, 'Molecular dynamics simulations for drug dosage form development: thermal and solubility characteristics for hot-melt extrusion', *Mol. Simul.*, vol. 34, no. 10–15, pp. 1197–1207, Sep. 2008, doi: 10.1080/08927020802411695.

[47] M. Maniruzzaman, M. J. Snowden, M. S. Bradely, and D. Douroumis, 'Studies of intermolecular interactions in solid dispersions using advanced surface chemical analysis', *RSC Adv.*, vol. 5, no. 91, pp. 74212–74219, 2015, doi: 10.1039/C5RA13176F.

[48] R. A. Bellantone *et al.*, 'A Method to Predict the Equilibrium Solubility of Drugs in Solid Polymers near Room Temperature Using Thermal Analysis', *J. Pharm. Sci.*, vol. 101, no. 12, pp. 4549–4558, Dec. 2012, doi: 10.1002/jps.23319.

[49] C. Donnelly, Y. Tian, C. Potter, D. S. Jones, and G. P. Andrews, 'Probing the Effects of Experimental Conditions on the Character of Drug-Polymer Phase Diagrams Constructed Using Flory-Huggins Theory', *Pharm. Res.*, vol. 32, no. 1, pp. 167–179, Jan. 2015, doi: 10.1007/s11095-014-1453-9.

[50] Y. Zhao, P. Inbar, H. P. Chokshi, A. W. Malick, and D. S. Choi, 'Prediction of the Thermal Phase Diagram of Amorphous Solid Dispersions by Flory–Huggins Theory', *J. Pharm. Sci.*, vol. 100, no. 8, pp. 3196–3207, Aug. 2011, doi: 10.1002/jps.22541.

[51] K. Bansal, U. S. Baghel, and S. Thakral, 'Construction and Validation of Binary Phase Diagram for Amorphous Solid Dispersion Using Flory–Huggins Theory', *AAPS PharmSciTech*, vol. 17, no. 2, pp. 318–327, Apr. 2016, doi: 10.1208/s12249-015-0343-8.

[52] A. L. Sarode, H. Sandhu, N. Shah, W. Malick, and H. Zia, 'Hot melt extrusion (HME) for amorphous solid dispersions: Predictive tools for processing and impact of drug–polymer interactions on supersaturation', *Eur. J. Pharm. Sci.*, vol. 48, no. 3, pp. 371–384, Feb. 2013, doi: 10.1016/j.ejps.2012.12.012.

[53] M. Vasanthavada, W.-Q. (Tony) Tong, Y. Joshi, and M. S. Kislalioglu, 'Phase Behavior of Amorphous Molecular Dispersions II: Role of Hydrogen Bonding in Solid Solubility and Phase Separation Kinetics', *Pharm. Res.*, vol. 22, no. 3, pp. 440–448, Mar. 2005, doi: 10.1007/s11095-004-1882-y.

[54] M. Yang, P. Wang, H. Suwardie, and C. Gogos, 'Determination of acetaminophen's solubility in poly(ethylene oxide) by rheological, thermal and microscopic methods',

Int. J. Pharm., vol. 403, no. 1–2, pp. 83–89, Jan. 2011, doi: 10.1016/j.ijpharm.2010.10.026.

[55] S. Thakral and N. K. Thakral, 'Prediction of Drug–Polymer Miscibility through the use of Solubility Parameter based Flory–Huggins Interaction Parameter and the Experimental Validation: PEG as Model Polymer', *J. Pharm. Sci.*, vol. 102, no. 7, pp. 2254–2263, Jul. 2013, doi: 10.1002/jps.23583.

[56] S. O. Kyerematen, M. Pudlas, and G. H. Woehrle, 'A Fast and Reliable Empirical Approach for Estimating Solubility of Crystalline Drugs in Polymers for Hot Melt Extrusion Formulations', *J. Pharm. Sci.*, vol. 103, no. 9, pp. 2847–2858, Sep. 2014, doi: 10.1002/jps.23941.

[57] A. Mahieu, J.-F. Willart, E. Dudognon, F. Danède, and M. Descamps, 'A New Protocol To Determine the Solubility of Drugs into Polymer Matrixes', *Mol. Pharm.*, vol. 10, no. 2, pp. 560–566, Feb. 2013, doi: 10.1021/mp3002254.

[58] M. Maniruzzaman, D. J. Morgan, A. P. Mendham, J. Pang, M. J. Snowden, and D. Douroumis, 'Drug–polymer intermolecular interactions in hot-melt extruded solid dispersions', *Int. J. Pharm.*, vol. 443, no. 1–2, pp. 199–208, Feb. 2013, doi: 10.1016/j.ijpharm.2012.11.048.

[59] P. Mistry, S. Mohapatra, T. Gopinath, F. G. Vogt, and R. Suryanarayanan, 'Role of the Strength of Drug–Polymer Interactions on the Molecular Mobility and Crystallization Inhibition in Ketoconazole Solid Dispersions', *Mol. Pharm.*, vol. 12, no. 9, pp. 3339–3350, Sep. 2015, doi: 10.1021/acs.molpharmaceut.5b00333.

[60] Taylor, L.S. & Zografi, G., 'Spectroscopic Characterization of Interactions Between PVP and Indomethacin in Amorphous Molecular Dispersions', *Pharm Res (1997) 14: 1691*.

[61] H. Liu, X. Zhang, H. Suwardie, P. Wang, and C. G. Gogos, 'Miscibility Studies of Indomethacin and Eudragit® E PO by Thermal, Rheological, and Spectroscopic Analysis', *J. Pharm. Sci.*, vol. 101, no. 6, pp. 2204–2212, Jun. 2012, doi: 10.1002/jps.23075.

[62] M. Kinoshita *et al.*, 'Improvement of solubility and oral bioavailability of a poorly water-soluble drug, TAS-301, by its melt-adsorption on a porous calcium silicate', *J. Pharm. Sci.*, vol. 91, no. 2, pp. 362–370, Feb. 2002, doi: 10.1002/jps.10026.

[63] Matsumoto, T. & Zografi, G., 'Physical Properties of Solid Molecular Dispersions of Indomethacin with Poly(vinylpyrrolidone) and Poly(vinylpyrrolidone-co-vinyl-acetate) in Relation to Indomethacin Crystallization', *Pharm Res (1999) 16: 1722*.

[64] F. Meng, A. Trivino, D. Prasad, and H. Chauhan, 'Investigation and correlation of drug polymer miscibility and molecular interactions by various approaches for the preparation of amorphous solid dispersions', *Eur. J. Pharm. Sci.*, vol. 71, pp. 12–24, Apr. 2015, doi: 10.1016/j.ejps.2015.02.003.

[65] M. Maniruzzaman, J. Pang, D. J. Morgan, and D. Douroumis, 'Molecular Modeling as a Predictive Tool for the Development of Solid Dispersions', *Mol. Pharm.*, vol. 12, no. 4, pp. 1040–1049, Apr. 2015, doi: 10.1021/mp500510m.

[66] K. Khougaz and S.-D. Clas, 'Crystallization inhibition in solid dispersions of MK-0591 and poly(vinylpyrrolidone) polymers', *J. Pharm. Sci.*, vol. 89, no. 10, p. 10, 2000.

[67] W. L. J. Hinrichs, M. G. Prinsen, and H. W. Frijlink, 'Inulin glasses for the stabilization of therapeutic proteins', *Int. J. Pharm.*, vol. 215, no. 1–2, pp. 163–174, Mar. 2001, doi: 10.1016/S0378-5173(00)00677-3.

[68] M. Stanković *et al.*, 'Low temperature extruded implants based on novel hydrophilic multiblock copolymer for long-term protein delivery', *Eur. J. Pharm. Sci.*, vol. 49, no. 4, pp. 578–587, Jul. 2013, doi: 10.1016/j.ejps.2013.05.011.

[69] M. R. Visser *et al.*, 'Inulin solid dispersion technology to improve the absorption of the BCS Class IV drug TMC240', *Eur. J. Pharm. Biopharm.*, vol. 74, no. 2, pp. 233–238, Feb. 2010, doi: 10.1016/j.ejpb.2009.10.004.

[70] Orlando, Floreani, Padrini, and Palatini, 'Determination of inulin clearance by bolus intravenous injection in healthy subjects and ascitic patients: equivalence of systemic and renal clearances as glomerular filtration markers: Short report', *Br. J. Clin. Pharmacol.*, vol. 46, no. 6, pp. 605–609, Jan. 2002, doi: 10.1046/j.1365-2125.1998.00824.x.

[71] S. Imran, R. B. Gillis, S. M. Kok, S. E. Harding, and G. G. Adams, 'Application and use of Inulin as a tool for therapeutic drug delivery', *Biotechnol. Genet. Eng. Rev.*, vol. 28, no. 1, pp. 33–46, Jan. 2012, doi: 10.5661/bger-28-33.

[72] H. Uchiyama, Y. Tozuka, M. Imono, and H. Takeuchi, 'Improvement of dissolution and absorption properties of poorly water-soluble drug by preparing spray-dried powders with α-glucosyl hesperidin', *Int. J. Pharm.*, vol. 392, no. 1–2, pp. 101–106, Jun. 2010, doi: 10.1016/j.ijpharm.2010.03.037.

[73] H. Uchiyama, Y. Tozuka, M. Imono, and H. Takeuchi, 'Transglycosylated stevia and hesperidin as pharmaceutical excipients: Dramatic improvement in drug dissolution and bioavailability', *Eur. J. Pharm. Biopharm.*, vol. 76, no. 2, pp. 238–244, Oct. 2010, doi: 10.1016/j.ejpb.2010.07.006.

[74] T. Vasconcelos, S. Marques, J. das Neves, and B. Sarmento, 'Amorphous solid dispersions: Rational selection of a manufacturing process', *Adv. Drug Deliv. Rev.*, vol. 100, pp. 85–101, May 2016, doi: 10.1016/j.addr.2016.01.012.

[75] Y. He and C. Ho, 'Amorphous Solid Dispersions: Utilization and Challenges in Drug Discovery and Development', *J. Pharm. Sci.*, vol. 104, no. 10, pp. 3237–3258, Oct. 2015, doi: 10.1002/jps.24541.

[76] S. V. Jermain, C. Brough, and R. O. Williams, 'Amorphous solid dispersions and nanocrystal technologies for poorly water-soluble drug delivery – An update', *Int. J. Pharm.*, vol. 535, no. 1–2, pp. 379–392, Jan. 2018, doi: 10.1016/j.ijpharm.2017.10.051.

[77] M. M. Crowley *et al.*, 'Pharmaceutical Applications of Hot-Melt Extrusion: Part I', *Drug Dev. Ind. Pharm.*, vol. 33, no. 9, pp. 909–926, Jan. 2007, doi: 10.1080/03639040701498759.

[78] M. Lu *et al.*, 'Application of Hot Melt Extrusion for Poorly Water-Soluble Drugs: Limitations, Advances and Future Prospects', *Curr. Pharm. Des.*, vol. 20, no. 3, pp. 369–387, Jan. 2014, doi: 10.2174/13816128113199990402.

[79] J. S. LaFountaine, J. W. McGinity, and R. O. Williams, 'Challenges and Strategies in Thermal Processing of Amorphous Solid Dispersions: A Review', *AAPS PharmSciTech*, vol. 17, no. 1, pp. 43–55, Feb. 2016, doi: 10.1208/s12249-015-0393-y.

[80] H. Patil, R. V. Tiwari, and M. A. Repka, 'Hot-Melt Extrusion: from Theory to Application in Pharmaceutical Formulation', *AAPS PharmSciTech*, vol. 17, no. 1, pp. 20–42, Feb. 2016, doi: 10.1208/s12249-015-0360-7.

[81] R. V. Tiwari, H. Patil, and M. A. Repka, 'Contribution of hot-melt extrusion technology to advance drug delivery in the 21st century', *Expert Opin. Drug Deliv.*, vol. 13, no. 3, pp. 451–464, Mar. 2016, doi: 10.1517/17425247.2016.1126246.

[82] A. Newman, G. Knipp, and G. Zografi, 'Assessing the performance of amorphous solid dispersions', *J. Pharm. Sci.*, vol. 101, no. 4, pp. 1355–1377, Apr. 2012, doi: 10.1002/jps.23031.

[83] B. Démuth *et al.*, 'Downstream processing of polymer-based amorphous solid dispersions to generate tablet formulations', *Int. J. Pharm.*, vol. 486, no. 1–2, pp. 268–286, May 2015, doi: 10.1016/j.ijpharm.2015.03.053.

[84] S. Baghel, H. Cathcart, and N. J. O'Reilly, 'Polymeric Amorphous Solid Dispersions: A Review of Amorphization, Crystallization, Stabilization, Solid-State Characterization, and Aqueous Solubilization of Biopharmaceutical Classification System Class II Drugs', *J. Pharm. Sci.*, vol. 105, no. 9, pp. 2527–2544, Sep. 2016, doi: 10.1016/j.xphs.2015.10.008.

[85] K. Sollohub and K. Cal, 'Spray Drying Technique: II. Current Applications in Pharmaceutical Technology', *J. Pharm. Sci.*, vol. 99, no. 2, pp. 587–597, Feb. 2010, doi: 10.1002/jps.21963.

[86] N. Bolourchian, M. M. Mahboobian, and S. Dadashzadeh, 'The Effect of PEG Molecular Weights on Dissolution Behavior of Simvastatin in Solid Dispersions', p. 10, 2013.

[87] J. Brouwers, M. E. Brewster, and P. Augustijns, 'Supersaturating Drug Delivery Systems: The Answer to Solubility-Limited Oral Bioavailability?', *J. Pharm. Sci.*, vol. 98, no. 8, pp. 2549–2572, Aug. 2009, doi: 10.1002/jps.21650.

[88] C. Liu *et al.*, 'Improving Oral Bioavailability of Sorafenib by Optimizing the "Spring" and "Parachute" Based on Molecular Interaction Mechanisms', *Mol. Pharm.*, vol. 13, no. 2, pp. 599–608, Feb. 2016, doi: 10.1021/acs.molpharmaceut.5b00837.

[89] G. A. Ilevbare, H. Liu, K. J. Edgar, and L. S. Taylor, 'Maintaining Supersaturation in Aqueous Drug Solutions: Impact of Different Polymers on Induction Times', *Cryst. Growth Des.*, vol. 13, no. 2, pp. 740–751, Feb. 2013, doi: 10.1021/cg301447d.

[90] C. DeMerlis, J. Goldring, R. Velagaleti, W. Brock, and R. Osterberg, 'Regulatory Update: The IPEC Novel Excipient Safety Evaluation Procedure', p. 6.

[91] T. Imai, Y. Saito, H. Matsumoto, T. Satoh, and M. Otagiri, 'Influence of egg albumin on dissolution of several drugs', *Int. J. Pharm.*, vol. 53, no. 1, pp. 7–12, Jul. 1989, doi: 10.1016/0378-5173(89)90355-4.

[92] T. Pas, B. Vergauwen, and G. Van den Mooter, 'Exploring the feasibility of the use of biopolymers as a carrier in the formulation of amorphous solid dispersions – Part I: Gelatin', *Int. J. Pharm.*, vol. 535, no. 1–2, pp. 47–58, Jan. 2018, doi: 10.1016/j.ijpharm.2017.10.050.

[93] M. A. Hull, S. H. Gardner, and G. Hawcroft, 'Activity of the non-steroidal anti-inflammatory drug indomethacin against colorectal cancer', *Cancer Treat. Rev.*, vol. 29, no. 4, pp. 309–320, Aug. 2003, doi: 10.1016/S0305-7372(03)00014-8.

[94] A. V. Ewing, G. S. Clarke, and S. G. Kazarian, 'Stability of indomethacin with relevance to the release from amorphous solid dispersions studied with ATR-FTIR spectroscopic imaging', *Eur. J. Pharm. Sci.*, vol. 60, pp. 64–71, Aug. 2014, doi: 10.1016/j.ejps.2014.05.001.

[95] Y.-L. Hsieh, G. A. Ilevbare, B. Van Eerdenbrugh, K. J. Box, M. V. Sanchez-Felix, and L. S. Taylor, 'pH-Induced Precipitation Behavior of Weakly Basic Compounds: Determination of Extent and Duration of Supersaturation Using Potentiometric Titration and Correlation to Solid State Properties', *Pharm. Res.*, vol. 29, no. 10, pp. 2738–2753, Oct. 2012, doi: 10.1007/s11095-012-0759-8.

[96] M. Monschke, K. Kayser, and K. G. Wagner, 'Processing of Polyvinyl Acetate Phthalate in Hot-Melt Extrusion—Preparation of Amorphous Solid Dispersions', *Pharmaceutics*, vol. 12, no. 4, p. 337, Apr. 2020, doi: 10.3390/pharmaceutics12040337.

[97] A. Paudel, Z. A. Worku, J. Meeus, S. Guns, and G. Van den Mooter, 'Manufacturing of solid dispersions of poorly water soluble drugs by spray drying: Formulation and process considerations', *Int. J. Pharm.*, vol. 453, no. 1, pp. 253–284, Aug. 2013, doi: 10.1016/j.ijpharm.2012.07.015.

[98] A. C. F. Rumondor and L. S. Taylor, 'Effect of Polymer Hygroscopicity on the Phase Behavior of Amorphous Solid Dispersions in the Presence of Moisture', *Mol. Pharm.*, vol. 7, no. 2, pp. 477–490, Apr. 2010, doi: 10.1021/mp9002283.

[99] A. C. F. Rumondor, H. Wikström, B. Van Eerdenbrugh, and L. S. Taylor, 'Understanding the Tendency of Amorphous Solid Dispersions to Undergo Amorphous–Amorphous Phase Separation in the Presence of Absorbed Moisture', *AAPS PharmSciTech*, vol. 12, no. 4, pp. 1209–1219, Dec. 2011, doi: 10.1208/s12249-011-9686-y.

[100] M. S. Ku and W. Dulin, 'A biopharmaceutical classification-based Right-First-Time formulation approach to reduce human pharmacokinetic variability and project cycle time from First-In-Human to clinical Proof-Of-Concept', *Pharm. Dev. Technol.*, vol. 17, no. 3, pp. 285–302, Jun. 2012, doi: 10.3109/10837450.2010.535826.

[101] G. L. Amidon, H. Lennernäs, V. P. Shah, and J. R. Crison, 'A theoretical basis for a biopharmaceutic drug classification:The correlation of in Vitro drug product dissolution and in Vivo biovailability', *Pharm Res*, vol. 12, no. 3, pp. 413–420, 1995.

[102] K. Vollmann, R. Qurishi, J. Hockemeyer, and C. Müller, 'Synthesis and Properties of a New Water-Soluble Prodrug of the Adenosine A2A Receptor Antagonist MSX-2', *Molecules*, vol. 13, no. 2, pp. 348–359, Feb. 2008, doi: 10.3390/molecules13020348.

[103] S. E. David, P. Timmins, and B. R. Conway, 'Impact of the counterion on the solubility and physicochemical properties of salts of carboxylic acid drugs', *Drug Dev. Ind. Pharm.*, vol. 38, no. 1, pp. 93–103, Jan. 2012, doi: 10.3109/03639045.2011.592530.

[104] A. J. Smith, P. Kavuru, L. Wojtas, M. J. Zaworotko, and R. D. Shytle, 'Cocrystals of Quercetin with Improved Solubility and Oral Bioavailability', *Mol. Pharm.*, vol. 8, no. 5, pp. 1867–1876, Oct. 2011, doi: 10.1021/mp200209j.

[105] S. Baghel, H. Cathcart, and N. J. O'Reilly, 'Investigation into the Solid-State Properties and Dissolution Profile of Spray-Dried Ternary Amorphous Solid Dispersions: A Rational Step toward the Design and Development of a

Multicomponent Amorphous System', *Mol. Pharm.*, vol. 15, no. 9, pp. 3796–3812, Sep. 2018, doi: 10.1021/acs.molpharmaceut.8b00306.

[106] D. E. Zecevic, R. Meier, R. Daniels, and K.-G. Wagner, 'Site specific solubility improvement using solid dispersions of HPMC-AS/HPC SSL – Mixtures', *Eur. J. Pharm. Biopharm.*, vol. 87, no. 2, pp. 264–270, Jul. 2014, doi: 10.1016/j.ejpb.2014.03.018.

[107] S. K. Sharma, S. K. Shukla, and D. N. Vaid, 'Shellac-Structure, Characteristics & Modification', *Def. Sci. J.*, vol. 33, no. 3, pp. 261–271, Feb. 1983, doi: 10.14429/dsj.33.6181.

[108] K. Buch, M. Penning, E. Wächtersbach, M. Maskos, and P. Langguth, 'Investigation of various shellac grades: additional analysis for identity', *Drug Dev. Ind. Pharm.*, vol. 35, no. 6, pp. 694–703, Jan. 2009, doi: 10.1080/03639040802563253.

[109] S. Srivastava and N. Thombare, 'Safety Assessment of Shellac as Food Additive through Long Term Toxicity Study', p. 9, 2017.

[110] Y. Farag and C. S. Leopold, 'Physicochemical Properties of Various Shellac Types', *Dissolution Technol.*, vol. 16, no. 2, pp. 33–39, 2009, doi: 10.14227/DT160209P33.

[111] N. Pearnchob, A. Dashevsky, and R. Bodmeier, 'Improvement in the disintegration of shellac-coated soft gelatin capsules in simulated intestinal fluid', *J. Controlled Release*, vol. 94, no. 2–3, pp. 313–321, Feb. 2004, doi: 10.1016/j.jconrel.2003.10.004.

[112] S. S. Gupta, N. Solanki, and A. T. M. Serajuddin, 'Investigation of Thermal and Viscoelastic Properties of Polymers Relevant to Hot Melt Extrusion, IV: Affinisol™ HPMC HME Polymers', *AAPS PharmSciTech*, vol. 17, no. 1, pp. 148–157, Feb. 2016, doi: 10.1208/s12249-015-0426-6.

[113] L. A. Ramos and É. T. G. Cavalheiro, 'Thermal behavior of loratadine', *J. Therm. Anal. Calorim.*, vol. 87, no. 3, pp. 831–834, Mar. 2007, doi: 10.1007/s10973-006-7752-6.

[114] S. Hengsawas Surasarang, J. M. Keen, S. Huang, F. Zhang, J. W. McGinity, and R. O. Williams, 'Hot melt extrusion versus spray drying: hot melt extrusion degrades albendazole', *Drug Dev. Ind. Pharm.*, vol. 43, no. 5, pp. 797–811, May 2017, doi: 10.1080/03639045.2016.1220577.

[115] R. Censi, M. Gigliobianco, C. Casadidio, and P. Di Martino, 'Hot Melt Extrusion: Highlighting Physicochemical Factors to Be Investigated While Designing and Optimizing a Hot Melt Extrusion Process', *Pharmaceutics*, vol. 10, no. 3, p. 89, Jul. 2018, doi: 10.3390/pharmaceutics10030089.

[116] A. L. Sarode, S. Obara, F. K. Tanno, H. Sandhu, R. Iyer, and N. Shah, 'Stability assessment of hypromellose acetate succinate (HPMCAS) NF for application in hot melt extrusion (HME)', *Carbohydr. Polym.*, vol. 101, pp. 146–153, Jan. 2014, doi: 10.1016/j.carbpol.2013.09.017.

[117] Kaushik, Ritu, K. P. O'Donnell, and Singh, Gopeshkumar, 'Impact of Extrusion Process Parameters on Drug Recovery and Dissolution Performance of Solid Dispersions of Ritonavir and AFFINISOL TM HPMC HME'. DOW Technical Bulletin, 2016.

[118] X. Lin *et al.*, 'Physical Stability of Amorphous Solid Dispersions: a Physicochemical Perspective with Thermodynamic, Kinetic and Environmental Aspects', *Pharm. Res.*, vol. 35, no. 6, p. 125, Jun. 2018, doi: 10.1007/s11095-018-2408-3.

[119] B. Tian, L. Zhang, Z. Pan, J. Gou, Y. Zhang, and X. Tang, 'A comparison of the effect of temperature and moisture on the solid dispersions: Aging and crystallization', *Int. J. Pharm.*, vol. 475, no. 1–2, pp. 385–392, Nov. 2014, doi: 10.1016/j.ijpharm.2014.09.010.

[120] P. Kanaujia *et al.*, 'Investigating the effect of moisture protection on solid-state stability and dissolution of fenofibrate and ketoconazole solid dispersions using PXRD, HSDSC and Raman microscopy', *Drug Dev. Ind. Pharm.*, vol. 37, no. 9, pp. 1026–1035, Sep. 2011, doi: 10.3109/03639045.2011.558091.

[121] P. Kanaujia *et al.*, 'Investigating the effect of moisture protection on solid-state stability and dissolution of fenofibrate and ketoconazole solid dispersions using PXRD, HSDSC and Raman microscopy', *Drug Dev. Ind. Pharm.*, vol. 37, no. 9, pp. 1026–1035, Sep. 2011, doi: 10.3109/03639045.2011.558091.

[122] S. Verheyen, N. Blaton, R. Kinget, and G. Van den Mooter, 'Mechanism of increased dissolution of diazepam and temazepam from polyethylene glycol 6000 solid dispersions', *Int. J. Pharm.*, vol. 249, no. 1–2, pp. 45–58, Dec. 2002, doi: 10.1016/S0378-5173(02)00532-X.

[123] S.-Y. Lin, C.-H. Hsu, and M.-T. Sheu, 'Curve-fitting FTIR studies of loratadine/hydroxypropyl-β-cyclodextrin inclusion complex induced by co-grinding process', *J. Pharm. Biomed. Anal.*, vol. 53, no. 3, pp. 799–803, Nov. 2010, doi: 10.1016/j.jpba.2010.06.010.

[124] F. Frizon, J. de O. Eloy, C. M. Donaduzzi, M. L. Mitsui, and J. M. Marchetti, 'Dissolution rate enhancement of loratadine in polyvinylpyrrolidone K-30 solid dispersions by solvent methods', *Powder Technol.*, vol. 235, pp. 532–539, Feb. 2013, doi: 10.1016/j.powtec.2012.10.019.

[125] H. Akinosho, S. Hawkins, and L. Wicker, 'Hydroxypropyl methylcellulose substituent analysis and rheological properties', *Carbohydr. Polym.*, vol. 98, no. 1, pp. 276–281, Oct. 2013, doi: 10.1016/j.carbpol.2013.05.081.

[126] D. Prasad, H. Chauhan, and E. Atef, 'Amorphous Stabilization and Dissolution Enhancement of Amorphous Ternary Solid Dispersions: Combination of Polymers Showing Drug–Polymer Interaction for Synergistic Effects', *J. Pharm. Sci.*, vol. 103, no. 11, pp. 3511–3523, Nov. 2014, doi: 10.1002/jps.24137.

[127] A. M. Agrawal, M. S. Dudhedia, and E. Zimny, 'Hot Melt Extrusion: Development of an Amorphous Solid Dispersion for an Insoluble Drug from Mini-scale to Clinical Scale', *AAPS PharmSciTech*, vol. 17, no. 1, pp. 133–147, Feb. 2016, doi: 10.1208/s12249-015-0425-7.

[128] M. Rahman, A. Coelho, J. Tarabokija, S. Ahmad, K. Radgman, and E. Bilgili, 'Synergistic and antagonistic effects of various amphiphilic polymer combinations in enhancing griseofulvin release from ternary amorphous solid dispersions', *Eur. J. Pharm. Sci.*, vol. 150, p. 105354, Jul. 2020, doi: 10.1016/j.ejps.2020.105354.

[129] X. Liu, X. Feng, R. O. Williams, and F. Zhang, 'Characterization of amorphous solid dispersions', *J. Pharm. Investig.*, vol. 48, no. 1, pp. 19–41, Jan. 2018, doi: 10.1007/s40005-017-0361-5.

[130] F. Vogt, 'Solid state characterization of amorphous solid dispersions', in *Pharm Amorph Solid Dispers*, 2015.

[131] J. J. Granados-Romero *et al.*, 'Colorectal cancer: a review', *Int. J. Res. Med. Sci.*, vol. 5, no. 11, p. 4667, Oct. 2017, doi: 10.18203/2320-6012.ijrms20174914.

[132] U. H. Gala, D. A. Miller, and R. O. Williams, 'Harnessing the therapeutic potential of anticancer drugs through amorphous solid dispersions', *Biochim. Biophys. Acta BBA - Rev. Cancer*, vol. 1873, no. 1, p. 188319, Jan. 2020, doi: 10.1016/j.bbcan.2019.188319.

[133] S. C. Gupta, B. Sung, S. Prasad, L. J. Webb, and B. B. Aggarwal, 'Cancer drug discovery by repurposing: teaching new tricks to old dogs', *Trends Pharmacol. Sci.*, vol. 34, no. 9, pp. 508–517, Sep. 2013, doi: 10.1016/j.tips.2013.06.005.

[134] H.-M. Wang, 'Indomethacin suppresses growth of colon cancer via inhibition of angiogenesis *in vivo*', *World J. Gastroenterol.*, vol. 11, no. 3, p. 340, 2005, doi: 10.3748/wjg.v11.i3.340.

[135] K. Lundholm, J. Gelin, A. Hyltander, and C. Lã, 'Anti-inflammatory Treatment May Prolong Survival in Undernourished Patients', p. 6.

[136] A. Akhgari, F. Sadeghi, and H. Garekani, 'Combination of time-dependent and pH-dependent polymethacrylates as a single coating formulation for colonic delivery of indomethacin pellets', *Int. J. Pharm.*, vol. 320, no. 1–2, pp. 137–142, Aug. 2006, doi: 10.1016/j.ijpharm.2006.05.011.

[137] Y. S. R. Krishnaiah, S. Satyanarayana, and Y. V. Rama Prasad, 'Studies of Guar Gum Compression-Coated 5-Aminosalicylic Acid Tablets for Colon-Specific Drug Delivery', *Drug Dev. Ind. Pharm.*, vol. 25, no. 5, pp. 651–657, Jan. 1999, doi: 10.1081/DDC-100102221.

[138] A. Akhgari *et al.*, 'Indomethacin electrospun nanofibers for colonic drug delivery: In vitro dissolution studies', *Colloids Surf. B Biointerfaces*, vol. 152, pp. 29–35, Apr. 2017, doi: 10.1016/j.colsurfb.2016.12.035.

[139] L. D. Bruce, N. H. Shah, A. Waseem Malick, M. H. Infeld, and J. W. McGinity, 'Properties of hot-melt extruded tablet formulations for the colonic delivery of 5-aminosalicylic acid', *Eur. J. Pharm. Biopharm.*, vol. 59, no. 1, pp. 85–97, Jan. 2005, doi: 10.1016/j.ejpb.2004.06.007.

[140] K. Edueng, D. Mahlin, P. Larsson, and C. A. S. Bergström, 'Mechanism-based selection of stabilization strategy for amorphous formulations: Insights into crystallization pathways', *J. Controlled Release*, vol. 256, pp. 193–202, Jun. 2017, doi: 10.1016/j.jconrel.2017.04.015.

[141] R. Kinget, W. Kalala, L. Vervoort, and G. van den Mooter, 'Colonic Drug Targeting', *J. Drug Target.*, vol. 6, no. 2, pp. 129–149, Jan. 1998, doi: 10.3109/10611869808997888.

[142] F. Zhang, 'Melt-Extruded Eudragit® FS-Based Granules for Colonic Drug Delivery', *AAPS PharmSciTech*, vol. 17, no. 1, pp. 56–67, Feb. 2016, doi: 10.1208/s12249-015-0357-2.

[143] S. Amidon, J. E. Brown, and V. S. Dave, 'Colon-Targeted Oral Drug Delivery Systems: Design Trends and Approaches', *AAPS PharmSciTech*, vol. 16, no. 4, pp. 731–741, Aug. 2015, doi: 10.1208/s12249-015-0350-9.

[144] A. Balogh *et al.*, 'Controlled-release solid dispersions of Eudragit® FS 100 and poorly soluble spironolactone prepared by electrospinning and melt extrusion', *Eur. Polym. J.*, vol. 95, pp. 406–417, Oct. 2017, doi: 10.1016/j.eurpolymj.2017.08.032.

[145] D. D. Sun and P. I. Lee, 'Probing the mechanisms of drug release from amorphous solid dispersions in medium-soluble and medium-insoluble carriers', *J. Controlled Release*, vol. 211, pp. 85–93, Aug. 2015, doi: 10.1016/j.jconrel.2015.06.004.

[146] Goodman GA (Name) and Goodman LS, *Analgesics-antipyretics; pharmacotherapy of gout.* New York: Mcgraw Hill, 2006.

[147] L. F. A. Asghar, C. B. Chure, and S. Chandran, 'Colon Specific Delivery of Indomethacin: Effect of Incorporating pH Sensitive Polymers in Xanthan Gum Matrix Bases', *AAPS PharmSciTech*, vol. 10, no. 2, pp. 418–429, Jun. 2009, doi: 10.1208/s12249-009-9223-4.

[148] Tang XLC, Pikal MJ, and L. S. Taylor, 'The effect of temperature on hydrogen bonding in crystalline and amorphous phases in dihydropyrine calcium channel blockers', *Pharm. Res.*, vol. 19, pp. 484–490, 2002.